

# Size Regulation and Stability of Charged Lipid Vesicles

Promotor     prof. dr. M. A. Cohen Stuart  
                  hoogleraar fysische chemie  
                  met bijzondere aandacht voor de kolloïdchemie

Copromotor   dr. ir. F. A. M. Leermakers  
                  universitair hoofddocent  
                  bij de leerstoelgroep fysische chemie en kolloïdkunde

                  dr. ir. F. A. Hoekstra  
                  universitair hoofddocent  
                  bij de leerstoelgroep plantenfysiologie

#### Samenstelling promotiecommissie

Prof. dr. A. M. Dogterom	Universiteit Leiden en AMOLF
Prof. dr. J. A. Killian	Universiteit Utrecht
Prof. dr. B. M. Mulder	Wageningen Universiteit en AMOLF
Prof. dr. G. Thiel	TU Darmstadt

# Size Regulation and Stability of Charged Lipid Vesicles

M.M.A.E. Claessens

Proefschrift  
ter verkrijging van de graad van doctor  
op gezag van de rector magnificus  
van Wageningen Universiteit  
prof. dr. ir. L. Speelman  
in het openbaar te verdedigen  
op woensdag 19 november 2003  
des namiddags te 16.00 in de Aula

ISBN 90-5808-927-4

# Contents

<b>1</b>	<b>Introduction</b>	<b>1</b>
1.1	Imbibitional damage . . . . .	2
1.2	Model membranes . . . . .	6
1.3	Aim of the thesis . . . . .	11
1.4	Outline . . . . .	12
<b>2</b>	<b>Charged Lipid Vesicles</b>	<b>15</b>
2.1	Introduction . . . . .	16
2.2	Materials and methods . . . . .	19
2.2.1	Experiments . . . . .	19
2.2.2	Self consistent field calculations . . . . .	20
2.2.3	Parameters . . . . .	23
2.3	Results . . . . .	24
2.3.1	Evolution of vesicle size in time . . . . .	25
2.3.2	Concentration dependence of vesicle radius . . . . .	26
2.3.3	Salt dependence of the equilibrium vesicle radius . . . . .	27
2.4	Discussion and conclusions . . . . .	34
<b>3</b>	<b>Entropic stabilization of vesicles</b>	<b>39</b>
3.1	Introduction . . . . .	40
3.2	Materials and Methods . . . . .	42
3.2.1	Experiments . . . . .	42
3.2.2	Self consistent field calculations . . . . .	43
3.3	Results . . . . .	43
3.3.1	DOPC phase diagram . . . . .	43
3.3.2	Curvature energy . . . . .	46
3.4	Discussion . . . . .	50
<b>4</b>	<b>Effect of cations on vesicle stability</b>	<b>55</b>
4.1	Introduction . . . . .	56
4.2	Materials and Methods . . . . .	58
4.2.1	Experiments . . . . .	58
4.2.2	Calculations . . . . .	59
4.3	Results . . . . .	60
4.3.1	Experiments . . . . .	60

## CONTENTS

4.3.2	Calculations . . . . .	62
4.4	Discussion . . . . .	65
4.5	Conclusions . . . . .	68
4.6	Appendix . . . . .	69
<b>5</b>	<b>Lipid- and surfactant-lipid mixtures</b>	<b>71</b>
5.1	Introduction . . . . .	72
5.2	Materials and Methods . . . . .	73
5.2.1	Experiments . . . . .	73
5.2.2	Self-consistent-field calculations . . . . .	74
5.3	Results . . . . .	76
5.3.1	Experiments . . . . .	76
5.3.2	Calculations . . . . .	77
5.4	Discussion . . . . .	83
5.5	Summary . . . . .	86
<b>6</b>	<b>Vesicle fusion</b>	<b>89</b>
6.1	Introduction . . . . .	90
6.2	Materials and Methods . . . . .	92
6.2.1	Parameters . . . . .	92
6.3	Results . . . . .	93
6.4	Discussion . . . . .	98
6.5	Conclusions . . . . .	103
<b>7</b>	<b>Osmotic shrinkage of giant vesicles</b>	<b>105</b>
7.1	Introduction . . . . .	106
7.2	Materials and Methods . . . . .	107
7.3	Results and Analysis . . . . .	108
7.4	Discussion . . . . .	113
	<b>Summary</b>	<b>125</b>
	<b>Samenvatting</b>	<b>131</b>
	<b>Dankwoord</b>	<b>137</b>
	<b>Levensloop</b>	<b>139</b>

# Chapter 1

## Introduction

## 1.1 Imbibitional damage

### 1.1 Imbibitional damage

Desiccation-tolerant organisms, such as seed and pollen, are capable of surviving the removal of the major part of their cellular water. Cells of these organisms often dry from 30 to 95 wt% dry matter without loss of viability. The loss of water involves enormous changes in the surface area to volume ratio. The cell meets with these changes by extensive cell wall folding (Ópik, 1980), (Ópik, 1985), (Platt et al., 1994), (Thomson and Platt, 1997). In the dry state, the plasma membrane is still attached to the cell wall. This means that it has to follow the cell wall during drying; it can do this in two ways: the membrane can get rid of the excess surface area either by folding, or by vesiculation (Fig. 1.1) (Chabot and Leopold, 1982), (Bliss et al., 1984). Both phenomena are observed in desiccation tolerance.

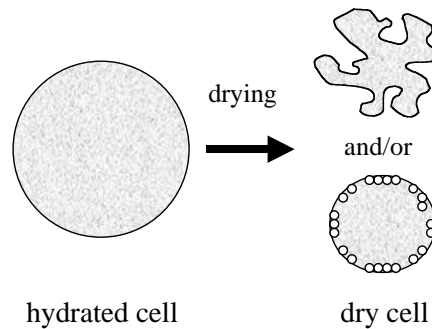


Figure 1.1: Schematic representation of a drying cell. The drying cell can cope with changes in the surface area to volume ratio by plasma membrane folding and/or vesiculation.

Although the structural integrity of the cells is preserved in the dry state, problems sometimes arise during rehydration. When dry cells take up water too quickly, they may suffer imbibitional injury. This kind of damage is especially common in seeds of (sub)tropical crops, and it is particularly severe at very low water content, or temperature. On a cellular level, imbibitional damage manifests itself by the permanent loss of membrane integrity, enormous leakage of endogenous substances, and disorganization of internal structures (Hobbs and Obendorf, 1972), (Hoekstra and Van der Wal, 1988). In seeds, this can result in a complete lack of germination, or lead to the formation of abnormal, partially deformed seedlings. Although it has been known for a long time that the plasma membrane is the main target of the rehydration stress, the exact cause of the damage to the membrane is still unknown.

The prevailing hypothesis for the mechanism of imbibitional damage is based on the observation that liposomal membranes become transiently leaky during a thermotropic phase transition from the gel to the liquid-crystalline



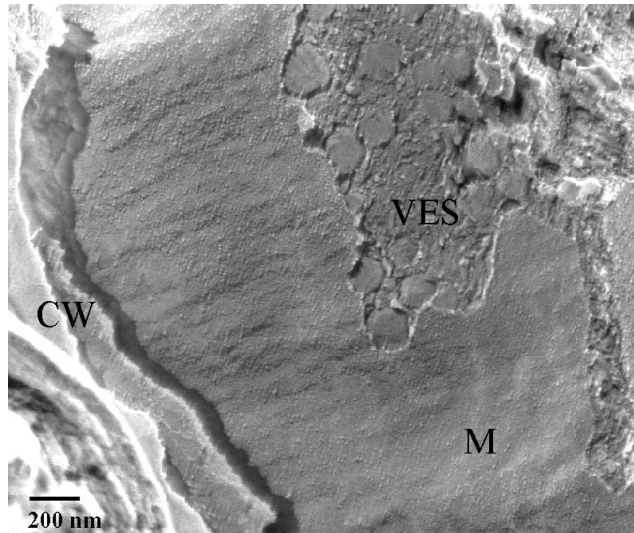


Figure 1.2: Protoplasmic face (PF) of a dry freeze-fractured cowpea embryo cell. ( $\sim 3\%$  RH). CW=cell wall, M=plasma membrane, VES=vesicles.

phase (Hammoudah et al., 1981). It assumes that structural defects at the boundary between coexisting gel and liquid-crystalline domains, in the rehydrating membrane, are responsible for the leakage of endogenous material. It has been shown that a phase transition, from gel to liquid crystalline takes place in the membranes of de- and rehydrating pollen (Hoekstra et al., 1992). This phase transitions indeed coincides with solute leakage from and reduced viability of pollen. The fact that two treatments that both lead to a membrane phase transition before the actual imbibition prevent imbibitional injury, supports the phase transition hypothesis. Pre-humidification of the the dry organism in humid air and imbibition at elevated temperatures reduce the leakage and preserve viability.

Although this theory can probably explain the transient loss of material during imbibition, it can not account for the permanent leakiness of the membranes observed when organisms are suffering from imbibitional damage (Hoekstra et al., 1999). The nature of this damage is probably related to the way the plasma membrane surface area is conserved in the dry state. Figure 1.2 shows a scanning electron microscope (SEM) picture of a dry cowpea embryo cell. The plasma membrane is undulated but intact, it shows a bilayer structure and the intra membrane particles (IMPs) are equally distributed over the plasma membrane. In spite of the fact that the membranes are probably in the gel state, no lateral phase separation was ever observed. In the dry state, the plasmodesmata are also intact (data not shown) and present in large amounts. Under the membrane surface a layer of closely packed vesicle-like structures is visible. These vesicles have a radius of approximately 50-100 nm and seem to be free of IMPs.

Cowpea seeds are sensitive to imbibitional damage. Figure 1.3 shows a

## 1.1 Imbibitional damage

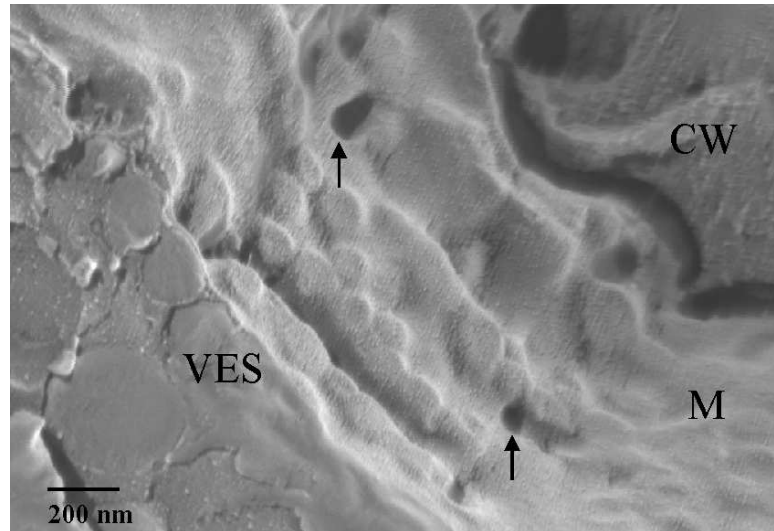


Figure 1.3: PF side of a freeze-fractured cowpea embryo cell. Cowpea was imbibed at 0°C for 10 minutes. M=plasma membrane, VES=vesicles, CW=cell wall. The arrows indicate holes in the plasma membrane.

SEM picture of the plasma membrane of a cell at the periphery of an embryo after imbibition for 10 minutes at 0°C. Upon cold imbibition, the vesicles are pressed against the plasma membrane, and its imprints are visible through the membrane. Although the membrane seems to retain its bilayer structure and random distribution of IMPs, it is no longer intact. With cold imbibition holes appear; it seems that the dry cell does not have access to enough membrane material to envelop the hydrating cell.

During rehydration, membrane unfolding and surface area expansion are probably required to accommodate the expanding cellular matrix. As suggested earlier (Chabot and Leopold, 1982), vesicles might serve as a membrane pool for the expanding cell by fusing with the plasma membrane. Fusion was indeed observed in cowpea embryo cells rehydrated at 30°C for 10 minutes (Fig. 1.4 and 1.5). The horseshoe and bubble like structures strongly resemble those observed during endo- and exocytosis of vesicles (Staehein and Chapman, 1987), (Emons et al., 1992). This indicates that the vesicles under the plasma membrane surface are fusing with the membrane; their surface area is needed to accommodate the hydrated cell. This idea is supported by a study on the IMP density on the plasma membrane of dry and hydrated cowpea radicles (Bliss et al., 1984). Membrane area expansion is needed to explain the decrease in IMP density on the PF side of membranes of water-imbibed cowpea radicle cells. The IMP-free vesicles under the plasma membrane surface are most likely the source of this lipid material.

Imbibitional damage is probably related to the difference in timescale at which the protoplast expands, and the plasma membrane unfolds and recruits material from the vesicles. At very low water content and temperature, the

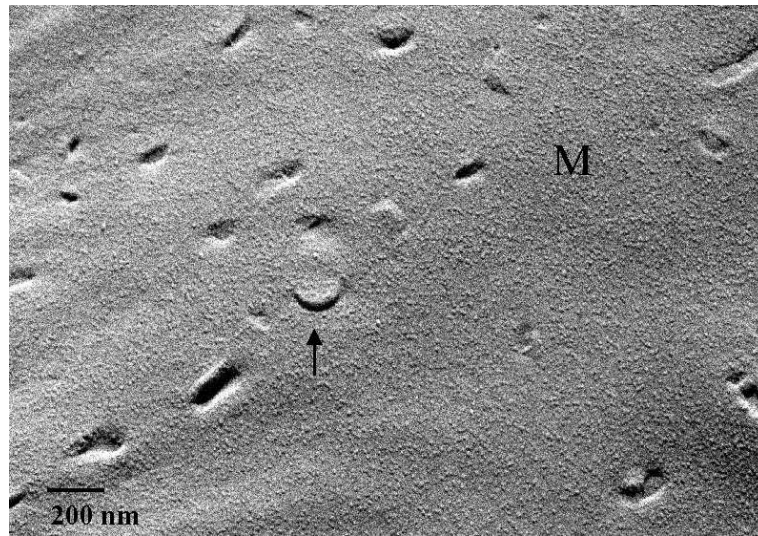


Figure 1.4: PF side of a of cowpea embryo cell membrane, the embryos rehydrated at 30°C for 10 minutes. The arrow indicate a horse shoe like structure that is typical for fusing vesicles.

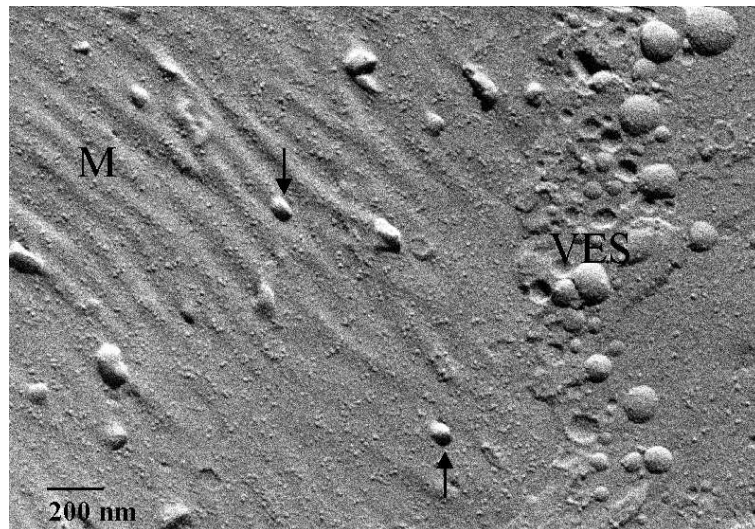


Figure 1.5: EF side of a of cowpea embryo cell membrane, the embryos rehydrated at 30°C for 10 minutes. The layer of vesicles close to the membrane is indicated (VES), and the arrows on the membrane surface show vesicles that are fusing with the plasma membrane.

## 1.2 Model membranes

timescale of membrane reorganization might be much slower than the increase in volume, possibly due to the low mobility of membrane components. The cold may hinder the reorganization of membranes, or the necessary incorporation of new lipids into the plasma membrane during the increase in size. (Chabot and Leopold, 1982). Under these conditions the membrane will rupture. The holes in the membrane are then somehow stabilized against sealing, as suggested by Hoekstra (Hoekstra et al., 1999) organelles probably fuse with the perforated membrane at higher water content. This fusion subsequently results in permanent leakage from the damaged cells, and eventually to cell death.

To understand the folding, vesiculation, and fusion behavior of the plasma membrane during de- and rehydration, a more detailed knowledge, of the thermodynamic and mechanical properties of the membrane, is required. A better understanding of membrane properties will also make it easier to suggest measures to prevent imbibitional damage.

## 1.2 Model membranes

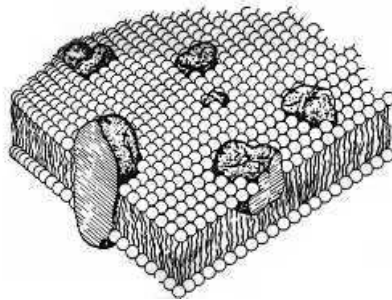


Figure 1.6: The fluid-mosaic model of a biological membrane consisting of phospholipids and proteins as it has been presented by Singer and Nicholson (Singer and Nicholson, 1972).

The simplest and most convenient model for a biological membrane is the lipid vesicle. All biological membranes are composed of two types of molecules; lipids and proteins (Fig. 1.6).

Although the weight proportion of proteins exceeds that of lipids in most bio-membranes, lipids play a unique role. This is reflected by the fact that lipids self-organize into a cell-like structure upon dispersion in excess water.

Membrane lipids, such as phospholipids, are amphiphiles; they have a polar headgroup and usually two long apolar tails (Fig. 1.7). The unfavorable interactions between water and the hydrophobic phospholipid tails will drive the phospholipids to self-association at already very low lipid concentrations. Typical critical micelle concentrations are in the order of  $10^{-12} - 10^{-8}$  M. Most phospholipids self-assemble into bilayers. In excess water, these bilayer spontaneously form the closed shells called vesicles (Fig. 1.8).

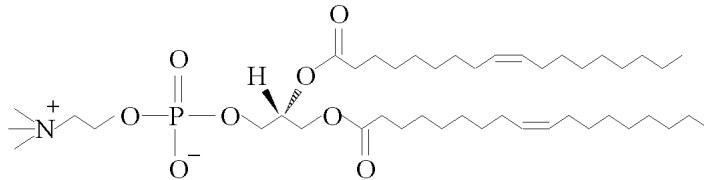


Figure 1.7: The phospholipid dioleoylphosphatidylcholine (DOPC) is an example of a phospholipid. It has a zwitterionic headgroup and two  $C_{18}$  tails that each contain one unsaturated bond. Phosphatidylcholines are abundant in bio-membranes.

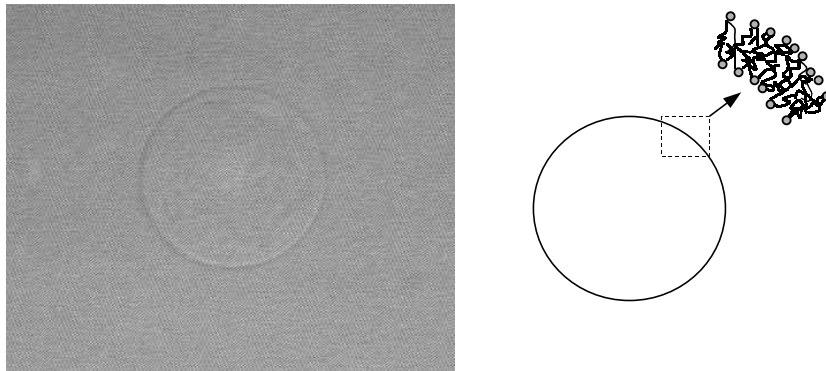


Figure 1.8: The picture on the left shows a giant vesicle ( $R = 62\mu\text{m}$ ) consisting of the anionic phospholipid DOPG in 5 mM NaBr. As can be seen in the schematic representation on the right hand side the vesicle is bounded by a bilayer consisting of phospholipids.

## 1.2 Model membranes

In many ways, the behavior of vesicles is similar to that of cell membranes. The vesicles' reaction to osmotic stress seems comparable to that of cells during drying and rehydration. Giant vesicles, made of plasma membrane lipid extracts of rye leaves that were not adjusted to cold, split off vesicles during freeze-induced osmotic contraction. Upon subsequent expansion, the vesicle lyses before gaining its original size (Steponkus and Lynch, 1989). Vesicles formed from lipids of cold-acclimated rye behave differently. Upon dehydration, they form tubular or vesicular extrusions that remain continuous with the original vesicle. During osmotic expansion, the extrusions are reincorporated in the membrane, and the vesicle regains its original size (Steponkus and Lynch, 1989). Although the lipid composition seems to play an important role in the behavior of the membrane upon osmotic stress, even simple vesicles show this behavior. Giant egg-lecithin vesicles split off daughter vesicles that seem to remain attached to the mother vesicles (Boroske et al., 1981). Mixtures of egg phosphatidylcholine, dicetyl phosphate and cholesterol were seen to form raspberry like structures within the mother vesicle upon osmotic contraction. The size of the daughter vesicles depended on the membrane composition and the size distribution became more monodisperse with the addition of cholesterol (Bernard et al., 2002). All these examples suggest that although processes like fission and fusion are probably catalyzed by proteins in biological systems, it is conceivable that the thermodynamic and mechanical properties of the phospholipid bilayer determine these phenomena.

Much of the current understanding of the morphology (changes) and stability of vesicles is based on the phenomenological model introduced by Helfrich (Helfrich, 1973). In this model the surface of the bilayer membrane is locally characterized by two radii of curvature  $R_1$  and  $R_2$ , which determine the mean curvature  $J$  ( $J = \frac{1}{R_1} + \frac{1}{R_2}$ ) and the Gaussian curvature  $K$  ( $K = \frac{1}{R_1 R_2}$ ) (Fig. 1.9). The surface tension,  $\gamma$ , of the bilayer is subsequently described as a second order expansion in the mean and Gaussian curvatures

$$\gamma = -k_c J_0 J + \frac{1}{2} k_c J^2 + \bar{k} K$$

This phenomenological description of  $\gamma(J, K)$ , gives access to some important properties of the bilayer membrane, the mean bending modulus  $k_c$ , the saddle-splay modulus  $\bar{k}$ , and the spontaneous curvature  $J_0$ .

The rigidity of a bilayer is determined by its mean bending modulus  $k_c$ . The sign of  $k_c$  is positive for membranes as any deviation from the equilibrium state increases the free energy. Great effort has been devoted to the determination of  $k_c$  of a phospholipid bilayer. The values reported vary somewhat depending on the measurement technique used, but are all in the order of 10-40  $k_B T$  (Seifert and Lipowsky, 1995). Up till now mainly phosphatidylcholine membranes have been studied. And there are only a few examples of studies in which parameters, other than the temperature are systematically varied. One study reports that the value of  $k_c$  of phosphatidylcholine bilayers increases with phospholipid chain length and decreases with increasing carbon tail saturation. In a series of

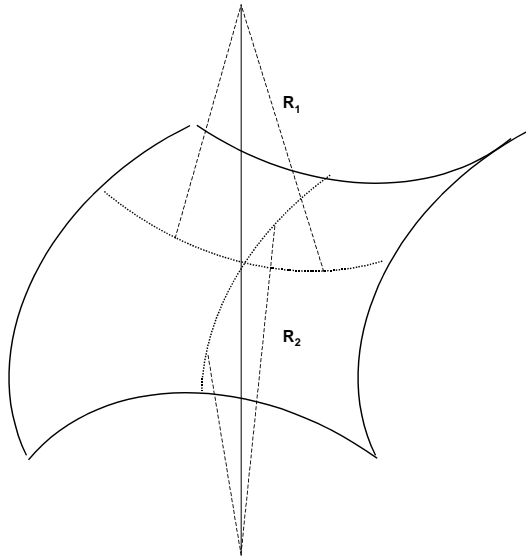


Figure 1.9: A two dimensional surface can be locally characterized by two radii of curvature  $R_1$  and  $R_2$ . For the saddle surface shown in this picture,  $R_1$  and  $R_2$  are opposite in sign. For a sphere  $R_1 = R_2$ , while for a cylinder  $R_1 = R$  and  $R_2 = \infty$ .

phosphatidylcholines  $k_c$  is related to the membrane thickness (Rawicz et al., 2000). Others report that with increasing amounts of dilauroylphosphatidic acid (DLPA), and therefore charge density, the  $k_c$  of DLPC bilayer vesicles increases (Meleard et al., 1998). Although there is already some information on  $k_c$  available, much more data and research are needed to make any predictions on the behavior of  $k_c$  in membranes, as function of salt, composition, and surface charge.

The saddle-splay, or Gaussian bending modulus,  $\bar{k}$  determines the topology of the interface rather than the bilayer rigidity. The sign of  $\bar{k}$  is not determined a priori. For negative values of  $\bar{k}$  the bilayer will prefer spherical deformations ( $\frac{1}{R_1 R_2} > 0$ ). For positive values of  $\bar{k}$ , the bilayer can only lower its free energy by the formation of saddle surfaces ( $\frac{1}{R_1 R_2} < 0$ ). This makes  $\bar{k}$  a very interesting parameter, as saddle surfaces always play a role in the shape transformations, budding, and fusion of vesicles. Unfortunately  $\bar{k}$  is difficult to measure, and no experimental data that we know of is available. Although there is some disagreement on this point (Lasic, 1990), (Lasic et al., 2001), it is usually assumed that  $k_c$  and  $-\bar{k}$  are of the same order of magnitude. At this time, realistic molecular model calculations seem to be the only means to obtain some insight into the behavior of  $\bar{k}$  in membranes.

The spontaneous curvature  $J_0$  is thought to be the curvature that minimizes the free energy. For bilayers consisting of a single phospholipid species  $J_0 = 0$ . For reasons of symmetry, it can not have a  $J_0 \neq 0$ . Since the bilayer consists of combined convex and concave monolayers of identical composition,

## 1.2 Model membranes

no monolayer can reach its preferred curvature without forcing a very unfavorable curvature upon the opposite monolayer. In bilayers of mixed composition, however, the membrane might develop a certain asymmetry in monolayer composition that gives rise to a  $J_0 \neq 0$  (Safran et al., 1990), (Safran et al., 1991). There is also no direct method to measure  $J_0$ ; its existence is usually derived from the spontaneous formation of vesicles. Mixtures of cationic and anionic surfactants are reported to spontaneously form equilibrium vesicles, which are stabilized by spontaneous curvature (Kaler et al., 1989). Recently this conclusion has been subsided, and some of the catanionic surfactant vesicles are most likely stabilized by entropy (Jung et al., 2001).

The Helfrichs' equation has also given insight into the thermodynamic stability of unilamellar vesicles. Vesicles can be stabilized against adhesion, fusion, and the formation of a multilamellar phase, by either a spontaneous curvature  $J_0 \neq 0$ , or by entropy. The first case is discussed above, non-ideal amphiphile mixing can give rise to a significant composition difference between the inner and outer monolayer, leading to spontaneous bilayer curvature and, therefore, vesicles of a particular size. In the case of entropic stabilization, the energy needed to curve a bilayer into a closed vesicle has to be compensated by entropy. For a bilayer without a spontaneous curvature, this curvature free energy,  $E_{ves}$ , equals  $4\pi(2k_c + \bar{k})$ . This means that the stability of vesicles is determined by the value of  $k_c$  and  $\bar{k}$ . If, for phospholipid bilayers,  $\bar{k}$  is indeed small and positive, as some people suggest (Lasic, 1990), (Lasic et al., 2001), and  $k_c$  is in the order of  $10\text{-}40 k_B T$ , phospholipid vesicles cannot be thermodynamically stable. If on the other hand  $k_c$  and  $-\bar{k}$  are of the same order of magnitude, entropic contributions, such as undulations, translations, and polydispersity, might be able to compensate  $E_{ves}$ .

The view of entropic stabilization of vesicles, sketched above, is probably rather primitive. In this view, vesicles cannot be stable against fusion and the formation of lamellar sheets. With each fusion event the bilayer gains  $4\pi(2k_c + \bar{k})$  energy. This problem is associated with the fact that the bending moduli  $k_c$  and  $\bar{k}$  are treated as phenomenological constants. This is probably true for vesicles that are very small compared to the membrane persistence length  $\xi_p \propto l e^{\frac{4\pi k_c}{k_B T}}$ , where  $l$  is a length scale proportional to the size of the molecules. But at length scales larger than  $\xi_p$  the bilayer freely undulates, and as the vesicle radius comes in the same order of magnitude as  $\xi_p$ , the effective  $k_c$  (and  $\bar{k}$ ) will become zero. As a result it will cost no energy to bend a bilayer into a closed vesicle. The size of these entropically stabilized vesicles will be determined by  $\xi_p$ .

As already mentioned above, at this time, the only means to get some insight into the Gaussian bending modulus  $\bar{k}$ , are realistic molecular model calculations. In this thesis self-consistent field calculations of the bending moduli of self assembled bilayers of phospholipid-like molecules will be presented. In these self-consistent field calculations lipids are treated as linear chains composed of different segments. These segments are subsequently placed on a



three-dimensional lattice composed of lattice sites, which all have equal volume. The lattice sites are all filled with either solvent, ions, or lipid segments. Inhomogeneities are not allowed within the lattice layers, as a mean field approximation of the interaction energies is employed. As the lipid molecules self assemble in a (geometry constrained) association colloid, equilibrium with the bulk solution is guaranteed. The structure of the membrane is not dictated; parameters like the membrane thickness and head-group area are a result of the calculations. The physical and mechanical properties of the membrane are therefore determined by the lipid composition and the interaction parameters of segments/molecules in the system.

Although very nice results on bilayer membranes have been obtained using self consistent field calculations there are some disadvantages in the model we use. In our calculations the exact atomic structure of the phospholipid is not taken into account; lipids are treated as linear chain molecules. This linear chain consists of a hydrophilic block surrounded by two hydrophobic chains; specific properties of phospholipids such as headgroup orientation or chain unsaturation are not taken into account. Furthermore, in the calculations the lipid molecules are fully flexible chains, and as a result the thickness of the phospholipid bilayer is underestimated. The lower value calculated for the bilayer thickness is expected to result in an underestimation of the mean bending modulus  $k_c$ . This effect on  $k_c$  of the lipid bilayer may however be compensated by the fact that collective fluctuations of the membrane are totally ignored; the calculations only account for fluctuations on a single molecule level. This means that although a more detailed description of the lipid molecules can be (and has been (Meijer et al., 1999), (Rabinovich et al., 2003), (Leermakers et al., 2003)) used, this will not necessarily result in better predictions of the bending moduli of the bilayer, unless collective fluctuations are also incorporated.

### 1.3 Aim of the thesis

Some desiccation-tolerant organisms suffer from imbibitional injury. The target of this rehydration stress is the plasma membrane, which loses its structural integrity and becomes permanently leaky. Electron microscopy data suggests that the cause of this damage may be related to the way in which membranes are preserved in the dry state. Strong folding and vesiculation of the plasma membrane are used to deal with the changes in area to volume ratio during dehydration. At very low initial water content or temperature, the reorganization needed upon imbibition is not fast enough. Membranes do not unfold, vesicles are probably not able to fuse with the membranes, and as a result the expanding cell ruptures.

Model membranes, made of phospholipids, behave similarly upon osmotic contraction and expansion. The question is whether the membrane properties can be influenced in such a way that imbibitional damage can be prevented. To answer this question, we decided to turn to model membranes. It appeared,

## 1.4 Outline

however, that even these relatively simple systems, consisting of only phospholipid, salt, and water, are not yet well understood. There is still a controversy concerning the question whether phospholipid vesicles are thermodynamically stable structures. The role of spontaneous curvature in the stabilization of vesicles of mixed composition also still needs clarification. Moreover, in spite of many theoretical predictions on how the membrane properties that follow from the Helfrich equation should scale with surface charge density (Winterhalter and Helfrich, 1988), (Lekkerkerker, 1989), ionic strength (Lekkerkerker, 1989), and composition (Szeleifer et al., 1988), there is still not much experimental data to support or contradict these claims. The role of  $\bar{k}$  is particularly interesting, as it seems an important parameter in the fission and fusion behavior of membranes, but due to the fact that  $\bar{k}$  is not experimentally accessible, little attention has been paid to it. In this thesis we aim to clarify some of the before-mentioned issues. This knowledge can hopefully be used to predict and alter membrane properties in a controlled way.

## 1.4 Outline

In Chapter 2 and Chapter 3 we will consider the thermodynamic stability of phospholipid vesicles. Both experimental data and self-consistent-field calculations will be used to show that phospholipid vesicles are stabilized against the formation of multilamellar phases by entropy. The vesicle radius follows the predicted scaling relation with phospholipid concentration, provided both the translational entropy and bilayer undulations are taken into account. Besides entropy, surface charge plays an important role in the stabilization of phospholipid vesicles. Similarities between the calculated mean bending modulus,  $k_c$ , and the measured vesicle radius as a function of ionic strength suggest that the vesicle radius is mainly determined by  $k_c$ .

Chapter 4 deals with effects of cations on the equilibrium size of vesicles of the anionic phospholipid dioleoylphosphatidylcholine (DOPC). The effect of the cations on the equilibrium radius is more complicated than that of anions. Not only has the ion hydration to be taken into account, specific binding of the cation to the anionic headgroup also plays a role.

Mixtures of lipids or lipids and surfactants are discussed in Chapter 5. The equilibrium size of the mixed vesicle is a function of the composition and the surface charge density. The fact that there is a good agreement between the behavior of the calculated  $k_c$  and the measured radius as a function of composition, suggests that these vesicles are also stabilized by entropy. Although there is much debate in the literature on the stabilization of vesicles by a non-zero spontaneous curvature, the calculations and experiments presented in this chapter show that vesicles are generally stabilized by entropy. Stabilization of vesicles by a spontaneous curvature is predicted to be rare due to the narrow range of parameters in which bilayers can obtain a  $J_0 \neq 0$ .

Although  $\bar{k}$  is not experimentally accessible, self-consistent-field calcula-

## Introduction

tions can give insight into the behavior of  $\bar{k}$ . In Chapter 6 we will present data that is expected to be relevant for vesicle fusion and fission. Calculations show that when the lipid bilayer contains surfactants,  $\bar{k}$  becomes more negative. When on the other hand alkanes are added,  $\bar{k}$  becomes less negative. This indicates that, up on addition of alkanes, it becomes easier for the bilayer to form saddle surfaces and therefore the intra membrane connections that are important in fusion phenomena. These results will be discussed in relation to the literature data on the effects of surfactants and alkanes on vesicle fusion.

In chapter 7 the response to osmotic stress observed for giant DOPG vesicles containing different amounts of cholesterol is reported. When these vesicles are subjected to a hypertonic osmotic gradient they shrink in size. During this shrinkage they remain spherical, and split off small vesicles that reside inside the giant. The size of the small vesicles is independent of the osmotic gradient, and depends on the membrane composition. Daughter vesicles are very small in the case of pure DOPG giants, whereas the radius of the daughters increases with increasing cholesterol content. This brings us to the idea that, similarly to equilibrium vesicles, the size of the daughter vesicles is related to the mean bending modulus of the bilayer. The reversibility of the vesiculation process is also studied, and will be discussed in relation to area increase and lysis phenomena.

## 1.4 Outline

## Chapter 2

# Charged lipid vesicles: effects of salts on bending rigidity, stability, and size

### Abstract

We show that it is possible to prepare unilamellar vesicles dioleoylphosphatidylglycerol (DOPG) and dioleoylphosphatidylcholine (DOPC) phospholipid bilayers that are stable in salt solutions. The equilibrium size of these vesicles strongly depends on the ionic strength of the solution and only weakly on the lipid concentration. Molecularly realistic self-consistent field modeling shows that single component vesicles have no spontaneous curvature  $J_0$ . The predictions for the mean bending moduli  $k_c$  correlate well with the experimentally found trends in vesicle radii. This gives rise to the hypothesis that the vesicles are entropically stabilized.

## 2.1 Introduction

## 2.1 Introduction

Phospholipid vesicles are often used as a model system to study membrane fusion. Vesicle content and lipid mixing, leakage, adhesion, and fusion stimuli studies are helpful in the elucidation of the molecular mechanism of membrane fusion. But to understand why vesicles fuse, it is essential to know which fundamental membrane properties determine their fusogenic behavior. Not being in equilibrium might be necessary but not sufficient for vesicles to fuse. If this assumption is true, it is expected that vesicles will grow to their equilibrium size during fusion. On the other hand vesicle budding is expected for vesicles that are very large compared to their equilibrium size. The daughter vesicles that arise in this way, may be near their equilibrium size. To systematically study these processes it is important to find ways to efficiently generate equilibrium vesicles, and to understand which factors govern their size.

Each surface, or more specific the membrane bilayer, can be locally characterized by two radii of curvature  $R_1$  and  $R_2$  which determine the total curvature  $J = \frac{1}{R_1} + \frac{1}{R_2}$ , and the Gaussian curvature  $K = \frac{1}{R_1 R_2}$ , of the interface at every point. The key physical parameters in relation to membrane stability and fusion may be found in the phenomenological equation derived by Helfrich to describe the undulation of lipid bilayers (Helfrich, 1973). This equation describes the surface tension  $\gamma$  as a second order expansion in the two local curvatures  $J$  and  $K$ .

$$\gamma = \gamma_0 + \frac{1}{2}k_c(J - J_0)^2 + \bar{k}K \quad (2.1)$$

From the thermodynamics of small systems it follows that, if the translational entropy of the membrane is neglected, a flat equilibrium bilayer membrane is tensionless, i.e.  $\gamma = 0$ . Therefore equation 2.1 reduces to

$$\gamma = -k_c J_0 J + \frac{1}{2}k_c J^2 + \bar{k}K \quad (2.2)$$

The coefficients in equation 2.2 that are of particular interest are the bending modulus  $k_c$ , the spontaneous curvature  $J_0$ , and the saddle-splay modulus  $\bar{k}$ . These coefficients can be derived from the curvature dependence of the interfacial tension.  $J_0$  is thought to be the curvature that minimizes the surface free energy. The Gaussian bending modulus,  $\bar{k}$  determines the topology of the interface rather than its rigidity, which in turn, is determined by  $k_c$ . The mean bending modulus,  $k_c$  is supposed to be positive for a bilayer, as any deformation from the equilibrium state has to increase the free energy. The sign of  $\bar{k}$  is not determined a priori. For negative values of  $\bar{k}$  the bilayer will prefer spherical deformations ( $\frac{1}{R_1 R_2} > 0$ ). For positive values of  $\bar{k}$  the only way for the surface to lower its free energy is the formation of saddle surfaces ( $\frac{1}{R_1 R_2} < 0$ ). The Gaussian bending modulus  $\bar{k}$  might therefore be an important parameter in vesicle fusion, as the interlamellar attachment between fusing vesicles is expected to be a saddle shaped surface. Although not sufficient for full fusion, a

## Charged Lipid Vesicles

possible criterion for the start of vesicle fusion might be  $\bar{k} \approx 0$ . For complete fusion it is conceivable, as mentioned before, that the equilibrium structure of the bilayer has to be different from the actual state (e.g. vesicle vs flat bilayer).

Although vesicles form spontaneously *in vivo*, they are generally not believed to represent the equilibrium structure of a single phospholipid species in water (Lasic, 1990), (Lasic et al., 2001). The reasoning behind this assumption is that the curvature energy of a phase consisting of spherical one-component vesicles is never lower than that of a multilamellar phase. Since the bilayer can be seen as combined convex and concave monolayers of identical composition, the system is frustrated; no monolayer can reach its preferred spontaneous curvature without forcing a very unfavorable curvature upon the opposite monolayer. However in this argument several entropic contributions are ignored. More specifically, both the translational entropy and the shape fluctuations, on the vesicle and on the lamellar sheets in the multilamellar liquid-crystalline phase, should be accounted for. This can be done using a simple scaling argument. Shape fluctuations lead to a finite membrane persistence length,  $\xi_p$ . On distances smaller than  $\xi_p$  the membrane is stiff, whereas above this length the information on orientation is lost. This means that, in first order approximation,  $\xi_p$  sets the lower limit to the vesicle size,  $\bar{R}$

$$\bar{R} \propto \xi_p \propto e^{\frac{k_c}{k_B T}} \quad (2.3)$$

Translational entropy which increases when vesicles become smaller and more dilute, allows the radius to be slightly less than given by Equation 2.3. For stiff membranes ( $k_c \gg k_B T$ ) the radius will be large, even in very dilute solutions. Only at high volume fractions, when the membranes strongly interact, undulation fluctuations are suppressed and translation entropy is absent. In this case the stacked lamellar state is expected to be energetically favorable.

Several experimental techniques have been used in the past to obtain estimates of  $k_c$  for phosphatidylcholine (PC) bilayers. The relation between the thickness of PC lipid bilayers and  $k_c$  was, for example, studied using the micropipette pressurization approach (Rawicz et al., 2000). By analyzing the shape fluctuations of giant vesicles,  $k_c$  was determined as a function of temperature for several PC lipids and for lipid mixtures (Meleard et al., 1998). Although the values for  $k_c$  differ between different techniques they are all in the range of 10-40  $k_B T$  (Seifert and Lipowsky, 1995). This implies that at typical concentrations entropically stabilized PC vesicles are in the order of some micrometers in size; this is flat on an atomic scale. All these measurements were done in demineralized water, sucrose/glucose solutions, or  $\mu\text{M}$  solutions of salt. Yet, a dependence of  $k_c$  on salt concentration is predicted for charged monolayers in the theoretical literature (Winterhalter and Helfrich, 1988), (Lekkerkerker, 1989).

Realistic molecular model calculations are the only theoretical means to predict the mechanical parameters of a lipid bilayer. Recently, Oversteegen showed how these parameters can be determined unambiguously from self-consistent field (SCF) calculations (Oversteegen and Leermakers, 2000). It is

## 2.1 Introduction

the aim of this paper to present the results of the SCF calculations for the Helfrich mechanical parameters of charged lipid-like bilayers, and to compare these to a series of experimental observations on vesicles in the presence of added salt.

The paper is organized as follows; we will first show that a freeze-thaw cycling procedure gives, for DOPG and DOPC, rise to vesicles of a specific size that depends only on the lipid- and salt concentration but not on the initial conditions. Experiments in which the vesicles size was followed in time indicate that multi-lamellar vesicles of charged phospholipids spontaneously evolve to the same (salt dependent) size. Further, data of vesicle radii as a function of the ionic strength will be presented. For vesicles of charged phospholipids two regimes are visible in the dependence of the size on the salt concentration. At low ionic strength the vesicle radius decreases with increasing salt concentration, but at a certain ionic strength the vesicle radius starts to increase with ionic strength. The size, and the rate of size change strongly depend on the intrinsic charge on the phospholipid and on the kind of salt used. The results for DOPG and DOPC vesicles in NaBr solution will be discussed in relation to their headgroup charge. The radii of anionic DOPG vesicles will be presented as a function of the NaCl and NaBr and NaI concentrations. These result show that the hydration of the anion influences the vesicle size at high ionic strength.

The second part deals with the mechanical parameters of a charged bilayer, as determined from SCF calculations. The interaction parameters between the model phospholipid and the ions used in the calculations will be discussed and become more realistic as the changes in solvent quality and differences between ions are taken into account. Special attention will be paid to the mean bending modulus  $k_c$ . In the simplest parameter setting  $k_c$  is a decreasing function of the ionic strength. This finding agrees qualitatively with the results of authors considering both charged monolayers and bilayers. The qualitative disagreement can be ascribed to changes in lipid packing with increasing ionic strength that are not accounted for in the literature (Lekkerkerker, 1989), (Daicic et al., 1996), (Winterhalter and Helfrich, 1988), (Fogden et al., 1997). When we choose more realistic parameters for the interactions between water and ions, two regimes are visible. Initially  $k_c$  decreases as a function of salt concentration, but at a certain ionic strength  $k_c$  starts to increase. This increase is correlated with an increase in bilayer thickness, while the decrease can be attributed to the decrease in the electric double layer thickness  $\kappa^{-1}$  with increasing ionic strength. Hence,  $k_c$  seems to be related to the overall thickness of the lipid layer, that is the lipid bilayer plus its electric double layer.

In the final discussion we will compare the experimental results with the data from the calculations. The size of the vesicles in the experiments depends on the ionic strength in a similar way as  $k_c$  in the SCF analysis. A relation between  $k_c$  and vesicle size is expected for fluctuation-stabilized vesicles as can be seen from equation 2.3. This brings us to the assumption that, in spite of the high values measured for  $k_c$  of PC membranes in the literature, vesicles of



phospholipids in salt solution might well be entropically stabilized. Finally the effects of the ionic strength on the saddle splay modulus  $\bar{k}$ , and its possible relation to fusion phenomena, will be discussed.

## 2.2 Materials and methods

### 2.2.1 Experiments

The anionic phospholipid dioleoylphosphatidylglycerol (DOPG) was purchased as a sodium salt, and the zwitterionic phospholipid dioleoylphosphatidylcholine (DOPC) as a chloroform solution, from Avanti Polar Lipids (Birmingham, AL), both were used without further purification. Analytical grade NaCl and NaI were purchased from Merck (Darmstadt, Germany) and NaBr from J.T. Baker Chemicals (Deventer, Holland). Vesicles were made by drying the phospholipids from chloroform under a stream of nitrogen followed by at least 2 hours under vacuum to remove the last traces of solvent. The dry lipid film was rehydrated with a salt solution of the desired ionic strength to a concentration of 2 mg lipid/ml unless stated otherwise. Three different methods were used for the final vesicle production. The lipid film was (1) rehydrated overnight to produce giant vesicles, (2) vortexed with the salt solution, or (3) sonicated in salt solution in a round bath sonicator to produce small unilamellar vesicles (SUVs).

Multilayered vesicles of phospholipids are known to fragment into small vesicles when the electrolyte solution in which they are suspended is subjected to successive cycles of freezing and thawing (MacDonald et al., 1994). Dioleoyl derivatives are particularly susceptible to fragmentation, and were therefore used in this study. The freeze-thaw procedure was used in the hope that the sealing of the bilayer fragments would lead to equilibrium membrane structures. To test this hypothesis, both the giant vesicles and the SUVs were subjected to a freeze-thaw procedure, as follows. 1 ml of vesicle containing solution was immersed in liquid nitrogen until completely frozen. The samples were thawed in a water bath at approximately 313 K. During thawing the half-frozen solution was vortexed regularly. The size evolution of vortexed vesicles was also followed in time (without any freeze-thaw steps), in order to see if this would give rise to vesicle radii comparable to those found in the freeze thaw procedure.

Both DOPG and DOPC samples were checked by eye for the appearance of multi lamellar phases. If the samples phase separated into a vesicle rich and a multilamellar phase, the data were not used. The results shown all apply to solutions that only contain vesicles.

The size of the vesicles was determined using dynamic light scattering (DLS). The instrumental setup consisted of an ALV-5000 correlator and a scattering device with an ALV-125 goniometer and a multiline Lexel AR-laser source. The data were collected at a scattering angle of 90 degrees at a wavelength of 513 nm. During the measurements the temperature was kept constant

## 2.2 Materials and methods

at 298 K. Before each measurement the samples were diluted by adding electrolyte solution. A cumulant analysis was used to determine the average vesicle size.

### 2.2.2 Self consistent field calculations

The self-consistent field theory can be used to evaluate the distribution of surfactant molecules in association colloids, e.g. micelles, vesicles, or bilayers. As surfactant molecules can assume many different conformations, it is convenient to divide the surfactants into segments, and space into a set of discrete coordinates. The surfactant chains are then restricted to have their segments on these coordinates.

The set of restricted coordinates on which the surfactant segments can be placed is called the lattice. In this lattice one can either have flat, cylindrical, or spherical lattice layers. These layers are used to reduce the complexity of the calculations. Within the lattice layers, numbered  $z = 1, \dots, m$ , no density gradients occur (mean field approximation). Tangential to the layers, gradients may develop. The lattice layers are composed of  $L(z)$  indistinguishable lattice sites. An, in principle, 3-dimensional problem can in this way be reduced to a 1-dimensional problem. Surfactants are composed of a string of segments, each of the size of a “water molecule”. When the solvent molecules, ions, and the segments of the surfactant chains are placed on the lattice, they all occupy one lattice site. Thus, as all the lattice sites have the same volume, each segment has a fixed size. Differences between segments can be introduced by changing their interactions with surrounding segments; their chemical nature can be accounted for. It should be kept in mind that by placing the molecules in a certain geometry, the symmetry of the lattice imposes a certain aggregate structure; as a result aggregates are unable to seek their optimum geometry.

All chain segments and monomers in the system have interactions with surrounding segments. Therefore a potential energy  $u_x(z)$  is assigned to each type of segment  $x$  relative to the bulk solution  $\beta$ . This potential energy belongs to the segment, irrespective of the chain to which the segment belongs. The potential energy  $u_x(z)$  depends on all possible interactions of segment  $x$  with its environment. Physically this means that  $u_x(z)$  contains all the potential energy contributions needed to bring a segment  $x$  from the bulk (where  $u_x(\infty) = 0$ ) to position  $z$ . Taking into account excluded volume, nearest neighbor and electrostatic interactions,  $u_x(z)$  becomes

$$u_x(z) = u'(z) + k_B T \sum_y \chi_{xy} (\langle \varphi_y(z) \rangle - \varphi_y^\beta) + \nu_x e \psi(z) - \frac{1}{2} \varepsilon_0 \varepsilon_x E(z)^2 \quad (2.4)$$

Here  $\varphi_y$  is the volume fraction of all other segment types  $y$ , the superscript  $\beta$  refers to the bulk solution, and  $\chi$  is the Flory-Huggins exchange energy parameter. The  $u'(z)$  term is the excluded-volume potential and originates from

## Charged Lipid Vesicles

optimizing the partition function with an incompressibility constraint; in each coordinate  $z$  the sum of the volume fractions should be unity,  $\sum_x \varphi_x(z) = 1$ . This means that  $u'(x)$  is the (free) energy needed to generate a vacant site in layer  $z$  so that the segment can be inserted. The second term in equation 2.4 accounts for all short-range nearest-neighbor contact energies that a segment  $x$  has with all other segments in the system (again relative to the interactions it has in the bulk). The angular brackets indicate averaging of  $\varphi(z)$  over the neighboring cells of a site in layer  $z$ . This term contains information on the lattice symmetry, which can be flat, cylindrical or spherical. The Flory-Huggins parameter  $\chi_{xy}$  describes the interaction between segments of type  $x$  and type  $y$ . This dimensionless parameter has a positive value when the attractive interactions between  $xx$  and  $yy$  pairs are larger than those between two  $xy$  pairs. At negative  $\chi$ -parameters, it is the other way around, i.e. the attractive interactions between the  $xy$  pairs are larger than the average of  $xx$  and  $yy$  pairs. In the  $\nu_x e \psi(z)$  term the electrostatics are taken into account. The electrostatic potential in a certain layer  $\psi(z)$ , determines how much energy it costs to place a charge  $\nu_x$  on this lattice layer. The valence of segment  $x$  is given by  $\nu_x$ ,  $e$  is the elementary charge. The last term accounts for the fact that the segments can be polarized in the presence of an electric field. The polarization is a function of the electric field  $E = -\frac{\partial \psi}{\partial z}$ , and its polarizability given by dielectric permittivity  $\varepsilon_x$ . The energy gain due to this polarization is again proportional to  $E$ . It can be shown that the free energy gain is just half this value, i.e. there is a term  $-\frac{1}{2}\varepsilon_0\varepsilon_x E^2$  in the segment potential. The electrostatic potential  $\psi(z)$ , and thus  $E(z)$  follow from the total charge distribution as will be discussed below.

The distribution of a free segment over the layers  $z$ , is given by its Boltzmann factor  $G_x(z)$

$$G_x(z) = e^{\frac{-u_x(z)}{k_B T}} \quad (2.5)$$

Which is generalized to

$$G_i(z, s) = \sum_x G_x(z) \delta_{i,s}^x \quad (2.6)$$

where  $\delta_{i,s}^x$  is unity when segment  $s$  of molecule  $i$  is of type  $x$  and zero otherwise. To find the volume fraction profile  $\varphi_i(z, s)$  of a particular segment  $s$  in chains of type  $i$ , a more complicated procedure is needed. For this purpose the segment distribution functions  $G_i(z, s | 1)$  are introduced. These functions are evaluated by step-weighted walks along the contour of chains  $i$ , starting at segment 1 at all allowed positions and finishing after  $s - 1$  steps with segments  $s$  in layer  $z$ . The segment distribution function  $G_i(z, s | 1)$  can be obtained from the segment weighting factor  $G_i(z, s)$  by the recurrence relation,

$$G_i(z, s | 1) = G_i(z, s) \langle G_i(z, s - 1 | 1) \rangle \quad (2.7)$$

## 2.2 Materials and methods

which implies a first-order Markov approximation. In equation 2.7, the angular brackets again denote averaging over neighboring cells. If segment  $s$  is of type  $x$ , the weight of segment  $s$  in layer  $z$ ,  $G_i(z, s | s)$ , of course equals  $G_i(z, s)$ . A similar segments distribution function  $G_i(z, s | N)$ , can be obtained by starting at segment  $N$  at the end of the chain, instead of segment 1. Now,  $\varphi(z, s)$  can be calculated, taking into account that the segment  $s$  in chain  $i$  is connected to both segment  $s - 1$  and  $s + 1$ .

$$\varphi_i(z, s) = C_i \frac{G_i(z, s | 1)G_i(z, s | N)}{G_i(z, s)} \quad (2.8)$$

Since segment  $s$  appears in the segment distribution functions of both chain-ends, the division by  $G_i(z, s)$  is needed to correct for double counting. In the case one chooses to fix the bulk concentration, the normalization factor  $C_i$  is related to the equilibrium volume fraction  $\varphi_i^\beta$  in the bulk solution.

$$C_i = \frac{\varphi_i^\beta}{N_i} \quad (2.9)$$

When, on the other hand, the number of molecules of type  $i$ ,  $n_i$  is fixed the sum of the volume fractions over all layers will yield the total number of monomers  $\sum_z L(z)\varphi_i(z) = n_i N_i$ , and therefore  $C_i$  is given by

$$C_i = \frac{n_i}{\sum_z L(z)G_i(z, N | 1)} \quad (2.10)$$

The volume fractions of all moieties in the system can now be determined from the segment weighting factors, which follow from the potential energies  $u_x(z)$ . However the energies  $u_x(z)$ , in turn, determine the volume fractions as can be seen from equation 2.4. The total charge distribution  $q(z)$  follows from the densities of all charged components in the system.

$$q(z) = \sum_x \varphi_x(z) e \nu_x$$

In addition, the dielectric permittivity profile can be estimated by

$$\varepsilon(z) = \sum_x \varphi_x(z) \varepsilon_x \varepsilon_0$$

These quantities are then used in the Poisson equation generalized for dielectric permittivity gradients

$$\text{div}(\varepsilon \nabla \psi) = -q$$

Consequently the set of equations has to be solved iteratively until the segment potentials and volume fractions are consistent.

Once the self-consistent solution is found from the potential energies and the segment distribution functions, the equilibrium density profiles and the potential profiles are known. Moreover, the self-consistent solutions give access

to the thermodynamic quantities such as the free energy, chemical potential, and the grand potential in the system.

At the self-consistent field solution the bulk solution is in equilibrium with the inhomogeneous system. In the bulk solution the densities of all the components are known. From these bulk densities the chemical potentials, with respect to the pure amorphous reference state, can be calculated

$$\frac{\mu_i - \mu_i^*}{k_B T} = \ln \phi_i^\beta + 1 - N_i \sum_j \frac{\phi_j^\beta}{N_j} + \frac{N_i}{2} \sum_x \sum_y \chi_{xy} (\phi_{xi}^* - \phi_x^\beta) (\phi_y^\beta - \phi_{yi}^*) \quad (2.11)$$

The superscript \* denotes the reference state of the pure unmixed components. The grand potential is given by

$$\Omega = \frac{\gamma A}{k_B T} = - \sum \pi(z) \quad (2.12)$$

in which

$$\begin{aligned} \pi(z) = & \sum_i \frac{\varphi_i(z) - \varphi_i^\beta}{N_i} - \sum_x \varphi_x(z) u_x(z) \\ & - \frac{1}{2} \sum_{xy} \chi_{xy} [\varphi_x(z) (\langle \varphi_y(z) \rangle - \varphi_y^\beta) - \varphi_x^\beta (\varphi_y(z) - \varphi_y^\beta)] \quad (2.13) \end{aligned}$$

The volume fractions and electrostatic potentials are known everywhere in the system and therefore the interfacial tension  $\gamma$  can be calculated from the grand potential according to equation 2.12. The values obtained for the grand potential from the SCF calculations are unequivocal (Oversteegen and Leermakers, 2000) and therefore the Helfrich constants can be determined unambiguously. For the calculation of the Helfrich constants the curvature dependence of the interfacial tension  $\gamma$  is required. The curvature of a lipid bilayer can be varied in the calculations by changing the amount of lipids in the system of cylindrical or spherical geometry.

### 2.2.3 Parameters

Phospholipids were modeled as linear chains with segment sequence  $C_{18}X_2C_2X_2C_{18}$ . The two  $C_{18}$ -groups represent the hydrophobic tails, the  $X_2C_2X_2$  group stands for the hydrophilic headgroup. The X segments carry a charge. Water was modeled by a simple solvent monomer W. The ionic strength of the solution was determined by two monomer types, cation and anion, with valency +1 e and -1 e, respectively. The Flory-Huggins interaction parameter  $\chi_{C-W}$ ,  $\chi_{C-X}$  and  $\chi_{C-ion}$  are 1.6. The lipid headgroup was made soluble in water by choosing a  $\chi$  value of -2 for the interaction between the solvent W and the headgroup segment X. Of course the ions will differ in their interactions with water from the lipid molecules. To make the interaction between the water and the

## 2.3 Results

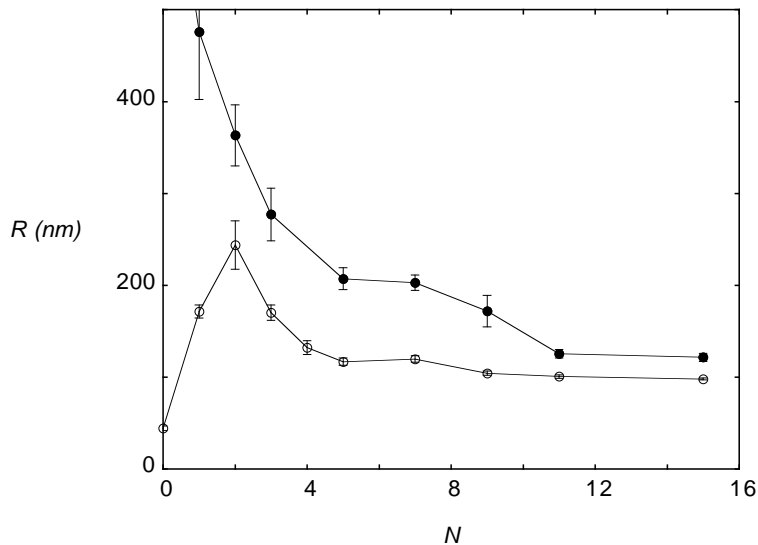


Figure 2.1: The radius of large multilamellar DOPG vesicles in 300 mM NaBr ( $\bullet$ ) and small sonicated DOPG vesicles in 200 mM NaBr ( $\circ$ ) as a function of the number of repeated freeze freeze-thaw cycles,  $N$ .

ions more realistic, the  $\chi$  values were varied, as will be discussed in the results. In all calculations the following dielectric constants were used  $\varepsilon_C=2$ ,  $\varepsilon_X=\varepsilon_{\text{cation}},=\varepsilon_{\text{anion}}=5$ ,  $\varepsilon_W=80$ .

## 2.3 Results

### Effect of the number of freeze thaw cycles on vesicle size

The effect of freezing and thawing on the size of phospholipid vesicles was investigated with dynamic light scattering. Figure 2.1 shows the radius of DOPG vesicles in 200 and 300 mM NaBr solutions as a function of the number of freeze-thaw cycles. Giant DOPG vesicles fragmented into smaller ones during freeze thawing. After 12 to 15 cycles their size seemed to stabilize. When small unilamellar DOPG vesicles (SUVs) were subjected to the same procedure, they grew in size. Again, after 12 to 15 freeze-thaw cycles their size did not change anymore. With increasing number of freeze-thaw cycles the standard deviation of the vesicle radii distribution became smaller, indicating an increase in homodispersity. The final radius of the DOPG vesicles did not depend on the starting size, but was determined only by the ionic strength of the salt solution.

## Charged Lipid Vesicles

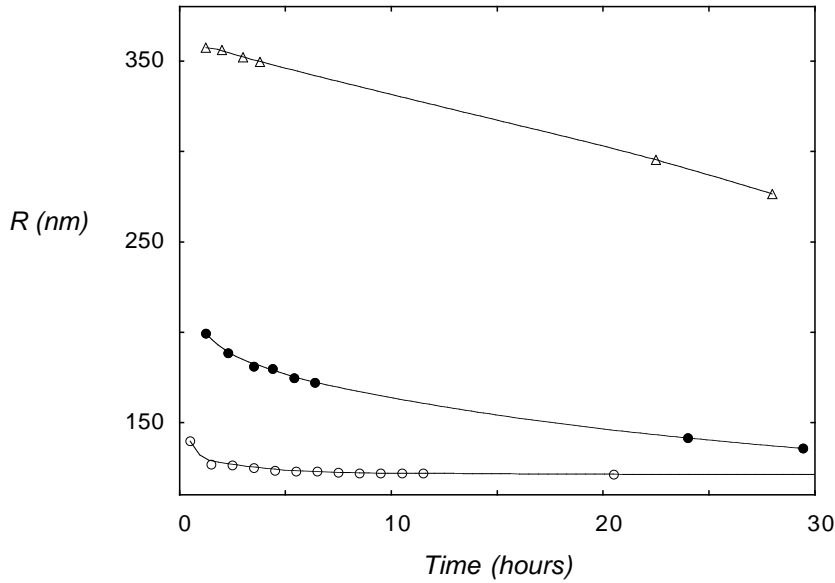


Figure 2.2: The size evolution of multilamellar DOPG vesicles was followed in time. Data are shown for DOPG vesicles in (o) demineralized water, (●) 25mM NaCl, and (Δ) 200mM NaCl. The higher the electrolyte concentration, the slower the vesicle size decreases. In demineralized water the radius evolves to the radius found after 15 freeze-thaw cycles.

### 2.3.1 Evolution of vesicle size in time

Though the starting size had no influence on the final vesicle size in the freeze-thaw experiment, it is not clear whether this size represents the equilibrium size of the vesicle, or is just a result of the preparation method. Therefore, the size evolution of vortexed vesicles was followed in time. These vesicles were not subjected to the freeze-thaw method. Figure 2.2 shows the results of the size evolution of DOPG vesicles in three different salt concentrations. At all salt concentrations the vesicle radius decreased with time, but the higher the ionic strength of the solution the slower the observed size decrease. The initial vesicle radius, as it was found after vortexing, was also significantly higher at higher salt strength. This is probably due to the increased screening of the charge on the phospholipid by the salt which renders the phospholipid less soluble, giving rise to larger aggregates and a slower exchange of lipid between them. Vesicles normally change in size by the diffusion of lipid monomers between the vesicles (Madani and Kaler, 1990), (Olsson and Wennerström, 2002). This is probably also true for phospholipid vesicles, as the size evolution of the vesicles was slowed down with increasing vesicle concentration (data not shown). Unfortunately, it is not possible to follow the vesicles longer than two days. Oxidation and hydrolysis products obscure the results at longer time scales. Only in the case of no added salt the exchange of material between vesicles is fast enough to reach a stable size. In demi water vortexed vesicles evolve to the same

## 2.3 Results

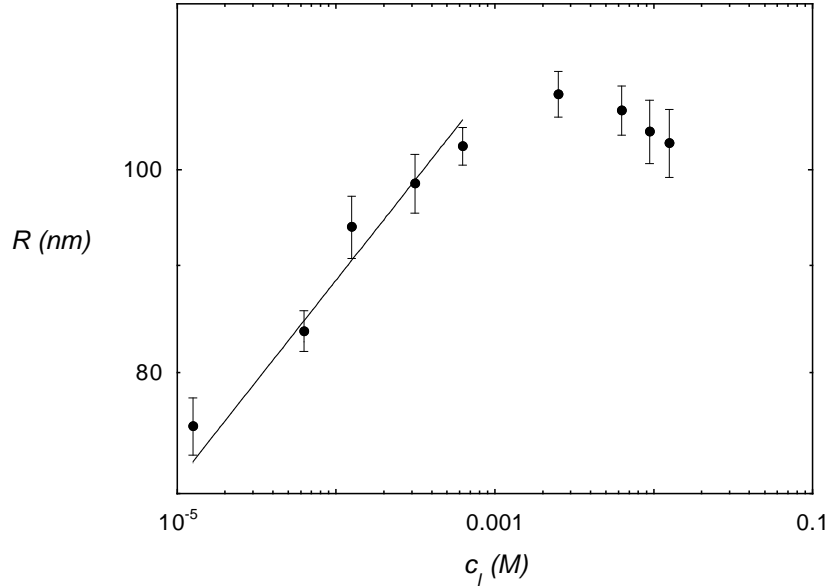


Figure 2.3: The vesicle size as a function of the concentration of DOPG. Data is shown for DOPG in 300mM NaCl.

radius as the ones obtained after the freeze thaw experiment. This result implies that the vesicles we observe probably represent the equilibrium structure of charged phospholipids. If the exchange of material between the aggregates can take place fast enough, completely different methods of vesicle preparation give rise to vesicles of the same size. Apparently, the freeze-thaw procedure just accelerates the exchange of lipid and the reconstruction of vesicles.

### 2.3.2 Concentration dependence of vesicle radius

Below we will argue that the vesicles, produced by the freeze-thaw method, are entropically stabilized. In this case one expects that there is an effect of dilution on size. Moreover, for membranes with a high bending modulus vesicles will only be stable in the very dilute regime. The values reported for the bending moduli of PC membranes are in the order of 10-40  $k_B T$  (Seifert and Lipowsky, 1995), (Meleard et al., 1998), (Rawicz et al., 2000), which is rather high. The dependence of the lipid concentration during production on the vesicle size therefore deserves attention.

Suspensions of  $10^{-3}$  to 10 mM DOPG were subjected to the freeze thaw procedure. Figure 2.3 shows the dependence of the vesicle radius, after 15 freeze thaw cycles, on the phospholipid concentration ( $c_{DOPG}$ ) in a 300 mM NaCl solution. At low lipid concentration the size of the vesicles increased with increasing  $c_{DOPG}$ , the data can be fitted with a power  $\sim 0.1$ .

In the case, the total curvature energy is lowered due to contributions of the translation entropy only,  $R$  is expected to scale  $\bar{R} \propto (\phi_{lipid})^{\frac{1}{4}}$  (Safran et al., 1991). When the undulational entropy is also taken into account by renormal-



ization of the bending modulus,  $R$  scales as  $\bar{R} \propto (c_{lipid})^{\frac{3}{20}}$  (Simons and Cates, 1992), (Herve et al., 1993). This value is very close to the experimentally found power law. It is therefore most likely that DOPG vesicles in salt solution prepared by the freeze-thaw method are stabilized by undulation entropy.

Around  $c_{DOPG} = 2$  mM the vesicle size stabilized, or decreased slightly with increasing  $c_{DOPG}$ . At these high lipid concentrations the packing of vesicles becomes more dense (volume fraction of vesicles,  $\phi_{vesicle} \approx 0.1$ ), excluded volume interactions can no longer be neglected, and the radius levels off (or decreases slightly) with increasing  $c_{DOPG}$ .

DOPC behaved slightly different from DOPG. We were able to produce vesicles of DOPC in NaBr by freeze-thawing, but not in NaCl. In NaCl multilamellar sheets were formed up to very high salt concentrations. At high concentrations of NaBr, a well defined vesicle size was obtained after freezing and thawing, for different starting conditions. But at low concentrations of salt the system phase-separated into a vesicle rich and a lamellar phase. Therefore it seemed interesting to have a look at the size of DOPG and DOPC vesicles in a range of salt concentrations.

### 2.3.3 Salt dependence of the equilibrium vesicle radius

The freeze-thaw procedure was applied to DOPG and DOPC vesicle suspensions in a range of NaBr concentrations. The effect of the ionic strength on the final (after 15 cycles) vesicle radius is shown in figure 2.4. In figure 2.4, two regimes are visible for DOPG vesicles. At low NaBr concentration, the vesicle radius decreased with increasing ionic strength. At low ionic strength the radius of the DOPG vesicles decreased fast with NaBr concentration. At high NaBr concentration a modest size increase was visible with increasing salt strength. The freeze-thaw method only gave stable DOPC vesicles at high NaBr concentration. The radius of these DOPC vesicles decreased slightly up to 150 mM NaBr, in even higher NaBr concentrations  $R$  increases with ionic strength. The slopes of the DOPG and DOPC curves at higher ionic strength were comparable, but here the less charged DOPC vesicles are always smaller. At concentrations higher than 400 mM salt the vesicles started to aggregate and the radius could no longer be determined by DLS.

It is known from literature that PC lipids in salt solutions behave in some ways as if they were slightly negatively charged (Tatulian, 1983). In spite of their zwitterionic nature, PC lipid vesicles in salt solution show electrophoretic mobility. The charging can be ascribed to binding of anions to the trimethylammonium group of the PC lipid. The net charge on the vesicle surface depends on the salt concentration and the kind of salt used. The order of effectiveness to increase the head-group charge is in agreement with the lyotropic series, in this respect  $I^-$  is more effective than  $Br^-$ , and  $Br^-$  is more effective than  $Cl^-$ . Comparing DOPG and DOPC vesicles in a certain salt solution is actually the same as comparing vesicles with a difference in surface charge density. Initially, a lower surface charge density gives rise to a slower size decrease.

## 2.3 Results

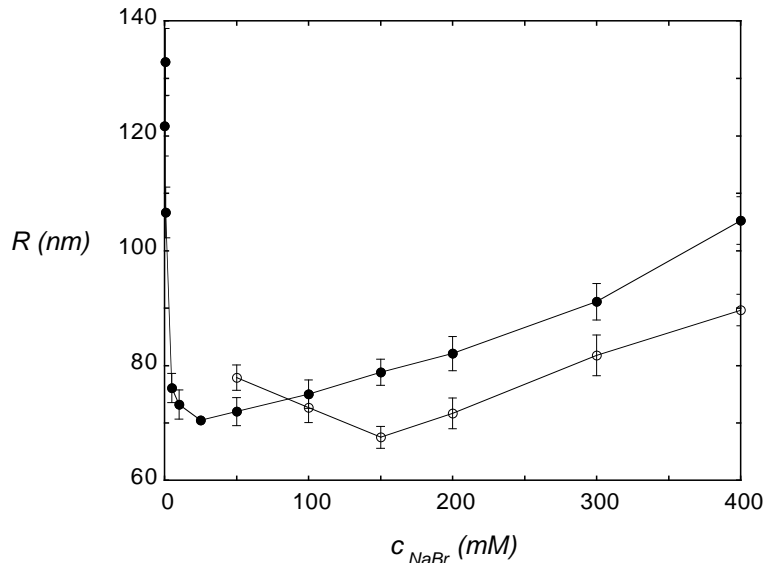


Figure 2.4: The size of DOPG ( $\bullet$ ) and DOPC ( $\circ$ ) vesicles in NaBr after 15 freeze-thaw cycles as a function of the ionic strength. The phospholipid concentration during freezing and thawing was 2 mg/ml. The  $R$  vs  $c_s$  curves can be divided into two regimes; at low ionic strength the vesicle radius decreases, while it increases at higher salt concentrations.

But at higher ionic strength the curves for high and low surface charge density cross (Fig. 2.4). Vesicles with a low surface charge density reach a smaller vesicle radius at high ionic strength.

Ions do not only influence the vesicle radius by specific binding. Variations in ion hydration can have a large influence on vesicle size. To test the role of ion hydration on the radius of DOPG vesicles, three different salts in the lyotropic series were tested. In this series the strength of hydration decreases in the order  $Cl^- > Br^- > I^-$ . Figure 2.5 presents the data obtained for DOPG in NaCl, NaBr and NaI solution. The initial size decrease with ionic strength was comparable for all salts used. However, at high ionic strength the size of vesicles in NaI was always smaller than that of vesicles in NaBr and these were in turn smaller than those in NaCl. The stronger the ion is hydrated, the more the bilayer membrane is dehydrated. Therefore the ionic strength at which the vesicle radius starts to increase is much lower for strongly hydrated ions. As a consequence vesicles reach smaller radii in solutions of weakly hydrated ions at high ionic strength.

### Self-consistent field calculations

The mechanical parameters from the Helfrich equation can be determined unambiguously from SCF calculations. They follow from the curvature dependence of the interfacial tension (Oversteegen and Leermakers, 2000). The cur-

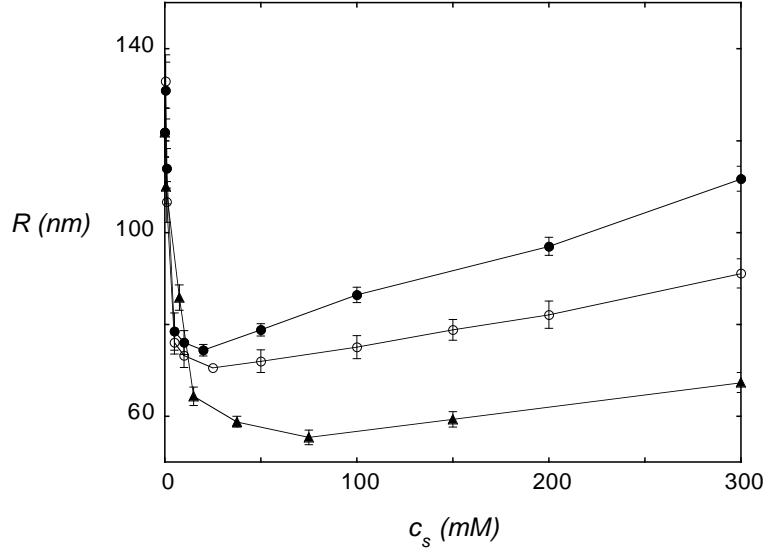


Figure 2.5: The radius  $R$  of DOPG vesicles as a function of ionic strength. Vesicles were prepared by freeze thawing DOPG vesicles 15 times in NaCl (●), NaBr (○), and NaI (▲).

vature of the bilayer can be varied, by changing the number of lipid molecules in the system. For a given number of lipid molecules the constrained (i.e., the geometry is an input constraint) equilibrium density profiles were calculated. From the resulting interfacial tensions of both a spherical and a cylindrical vesicle as a function of the vesicle radius, the Helfrich constants are calculated. For a cylindrical vesicle ( $K = 0$ ,  $J = \frac{1}{R}$  and  $A = 2\pi Rh$ , where  $h$  is the length of the cylinder) equation 2.2 can be written as

$$\gamma A = -2\pi k_c J_0 + \pi k_c J \quad (2.14)$$

and for a spherical vesicle ( $J^2 = 4K = \frac{4}{R^2}$ , and  $A = 4\pi R^2$ ) one has

$$\gamma A = -8\pi k_c J_0 R + 4\pi (2k_c + \bar{k}) \quad (2.15)$$

Thus,  $k_c$  was determined from a cylindrical interface, by varying the total curvature  $J$ . This  $k_c$  was subsequently used to derive  $\bar{k}$  from the data on the spherical geometry. Figure 2.6 shows the dependence of  $\gamma A$  on the mean curvature  $J$  for a bilayer composed of  $C_{18}X_2C_2X_2C_{18}$  in cylindrical lattice geometry. As predicted in equation 2.14,  $\gamma A$  depended linearly on  $J$ . By extrapolating the  $\gamma A$  vs  $J$  data,  $J_0$  can be calculated. For the one component systems studied here extrapolation of the  $\gamma$  vs  $J$  data to zero interfacial tension yielded a zero abscissa for all ionic strengths studied. This means that a bilayer composed of a single charged lipid species has no spontaneous curvature,  $J_0 = 0$ . The mean bending modulus  $k_c$  follows from the slope of the curve. Figure 2.7 gives the corresponding result for a spherical vesicle. The curve is in agreement with equation 2.15, provided that the vesicle does not have a spontaneous curvature.

## 2.3 Results

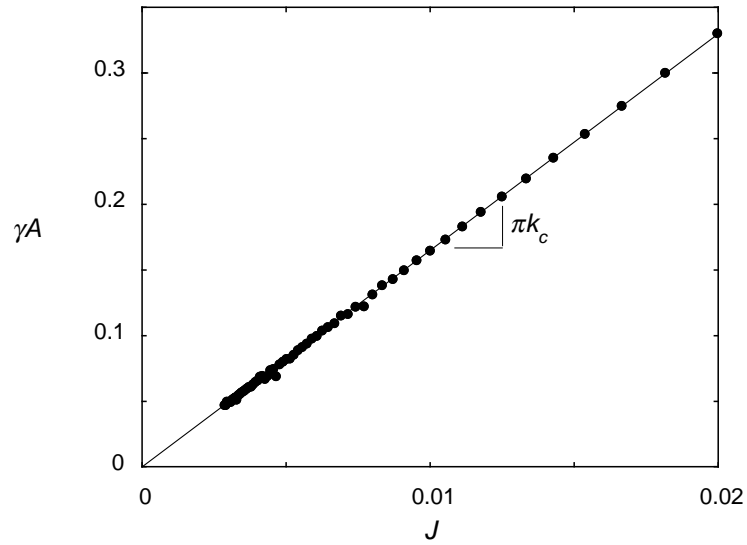


Figure 2.6:  $\gamma A$  as a function of the mean curvature  $J$  for a lipid bilayer in a cylindrical lattice geometry at a volume fraction of salt,  $\phi_s = 0.01$ .

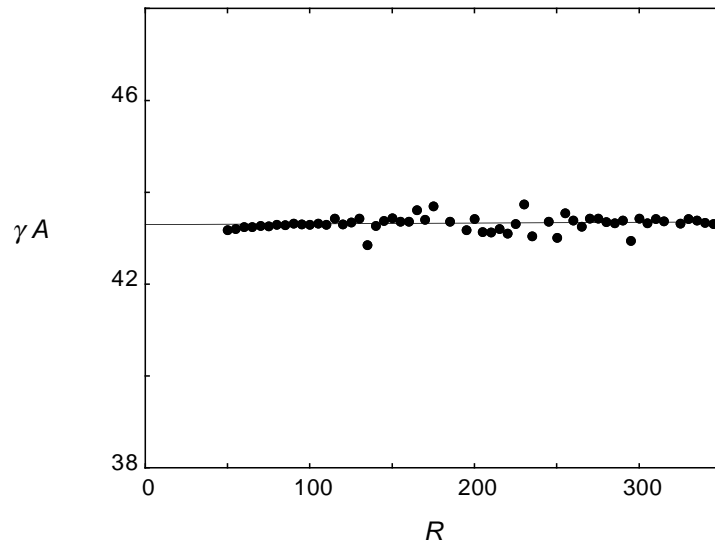


Figure 2.7:  $\gamma A$  as a function of the vesicle radius  $R$  (lattice layers) at  $\phi_s = 0.01$ . The calculations were performed in a spherical lattice geometry

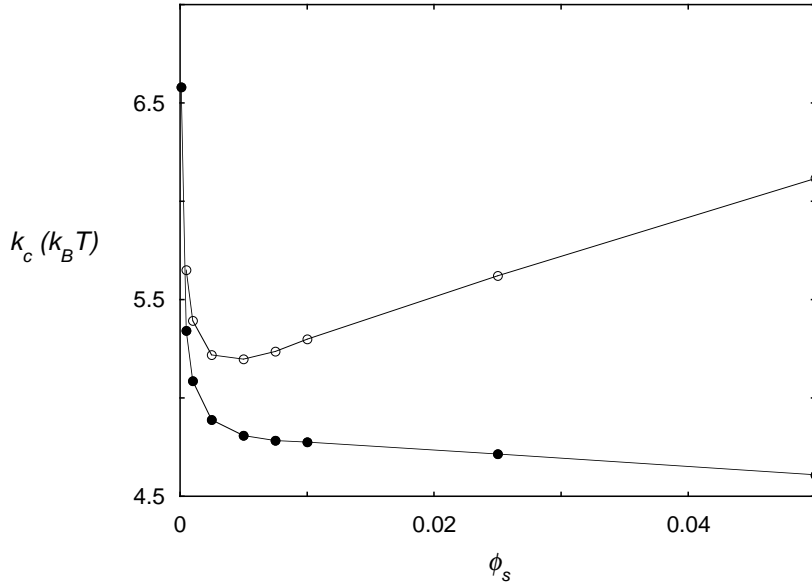


Figure 2.8: The mean bending modulus,  $k_c$ , of a charged  $C_{18}X_2C_2X_2C_{18}$  bilayer membrane as a function of the ionic strength. If ideal (athermal) interaction between water and ions is assumed ( $\chi_{W-ion} = 0$ ),  $k_c$  is decreasing (●), when ion hydration is taken into account ( $\chi_{W-ion} = -2$ ) two regimes become visible (○).

For small values of  $R$ ,  $\gamma A$  is no longer constant,  $k_c$  becomes a function of  $R$  as the inner monolayer starts to feel the inner monolayer on the opposite side.

Bilayer stability depends on the values of the bending moduli  $k_c$  and  $\bar{k}$ . Stable bilayers are only found if the total free energy of bending is positive. In a spherical geometry this means that  $2k_c + \bar{k} > 0$ . In our system the bilayers became unstable at very low ionic strength, but all the data shown pertain to stable vesicles. It should be kept in mind that the  $k_c$  found in the calculations represents an intrinsic instead of an effective  $k_c$ , as shape fluctuations are not taken into account in the SCF calculations.

To obtain  $k_c$  and  $\bar{k}$  for phospholipid-like bilayers, the calculations were first performed with the default choice of  $\chi$  parameters. This default choice can be made by assuming that, except for their charge, the electrolyte ions are identical to the solvent monomers in their interactions with water and the hydrophobic tails. The total charge on the headgroup was chosen to be  $-1$ , this corresponds to a valence of  $-\frac{1}{4}$  per  $X$ . With these assumptions  $k_c$  is found to decrease with ionic strength (Fig. 2.8). This decrease indicates that the bending is dominated by electrostatic effects. With increasing salt concentration the diffuse double layer around the negatively charged vesicle surface will become thinner and therefore  $k_c$  will decrease. However the bilayer itself will become thicker, as closer lipid packing is possible when the charges get screened at high salt concentrations. The increase in bilayer thickness is apparently not as effective as the decrease in diffuse double layer thickness.

## 2.3 Results

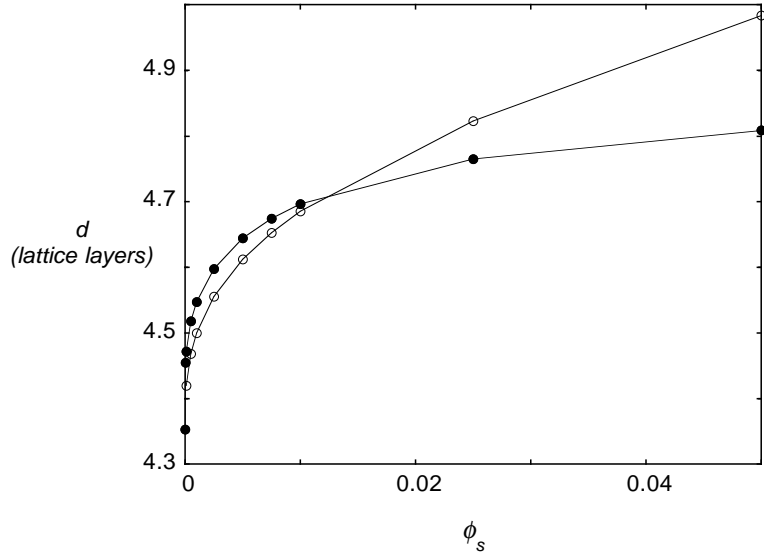


Figure 2.9: Half the bilayer thickness  $d$  in lattice layers, as a function of ionic strength for  $\chi_{W-ion} = -2$  (○) and  $\chi_{W-ion} = 0$  (●).

The result is a decrease in total thickness of the bilayer plus the electric double layer, and therefore a decrease in  $k_c$ .

The assumption that  $\chi_{W-ion} = 0$  is probably an oversimplification, as ions are hydrated. The introduction of a negative  $\chi$ -parameter for the interaction between the solvent  $W$  and the ions therefore seems justified. When a value of  $-2$  is chosen for  $\chi_{W-ion}$ , two regimes become visible in the  $k_c$  vs ionic strength plot (Fig. 2.8). In the low ionic strength regime,  $k_c$  decreases, while at higher ionic strengths it increases significantly with salt concentration. Apparently, the increase in bilayer thickness overrules the decrease in double layer thickness at high ionic strength. As the ionic strength increases, the dehydration effect becomes more important, and this is equivalent to the solvent quality becoming worse for the hydrophobic tails. Membrane dehydration will cause the lipids to pack into a more dense bilayer at high salt concentration (Fig. 2.9). The decrease in solvent quality causes the membrane to become thicker and thus  $k_c$  to increase; this effect is the dominating one at high ionic strength.

Our calculations can be further refined by making a difference in the affinity of cations and anions for the solvent  $W$ . Cations are known to be much smaller than anions; as a result their surface charge is more concentrated, and they are therefore more strongly hydrated. The difference in affinity of anions and cations for the solvent has been modeled by choosing a more negative value for  $\chi_{W-cation}$  than for  $\chi_{W-anion}$ .

Experimental results on the vesicle radius as a function of ionic strength were obtained for three different anions all with the same cation. The anions differ in their degree of hydration. The difference in hydration has been modeled in the calculations by choosing three different values for  $\chi_{W-anion}$  while

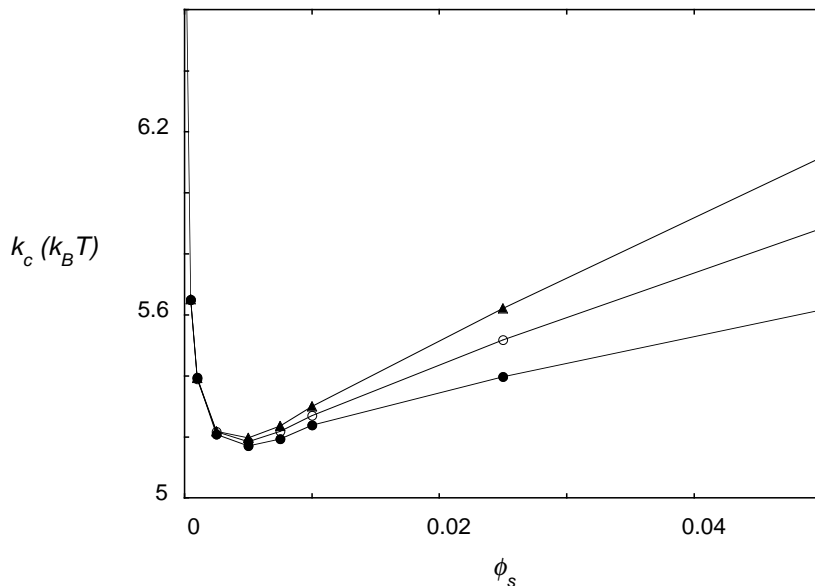


Figure 2.10: The mean bending modulus  $k_c$  vs ionic strength. Data are shown for  $\chi_{W-anion} = 0$  ( $\bullet$ ),  $\chi_{W-anion} = -1$  ( $\circ$ ),  $\chi_{W-anion} = -2$  ( $\blacktriangle$ ); in all cases  $\chi_{W-cation} = -2$ .

keeping  $\chi_{W-cation}$  constant (Fig. 2.10). With decreasing  $\chi_{W-anion}$  the bilayer becomes slightly more dehydrated. The initial decrease in  $k_c$  with ionic strength is the same for all  $\chi$ -parameters used; the differences can be found in the increase in  $k_c$  at higher ionic strength. The more negative the value for  $\chi_{W-anion}$ , the lower the ionic strength at which the increase in  $k_c$  starts. As a result lower  $k_c$  values are reached for lower values of  $\chi_{W-anion}$ . The increase in  $k_c$  at high ionic strength is much faster for a high value of  $\chi_{W-anion}$  than for lower values. Variations in the hydration of ions seem to be the main reason for the ion specific behavior of  $k_c$  with ionic strength.

DOPG is a negatively charged phospholipid, while DOPC is zwitterionic. Until now, we only dealt with lipids carrying a net charge. These lipids are probably not representative for DOPC lipids. Therefore the model-lipid was slightly modified by replacing one of the  $X_2$  segments by a segment  $Y_2$  ( $C_{18}X_2C_2Y_2C_{18}$ ), in which Y carries the same but opposite charge as X. Aggregates of these lipids behaved similar to vesicles of neutral lipids, as can be seen in figure 2.11. On the other hand, it is well known from the literature (Tatulian, 1983), that vesicles of PC lipids in salt solution have an electrophoretic mobility. This effect has been ascribed to the specific binding of ions to the PC membrane. Anions increase the surface charge of PC vesicles, by specific binding to the trimethylammonium group, in the order of the lyotropic series,  $Cl^- < Br^- < I^- < SCN^-$  (Tatulian, 1983). But although PC membranes are supposed to have a net negative charge, this charge will not be as large as the charge on the anionic PG bilayers. To gain insight into the effect of the

## 2.4 Discussion and conclusions

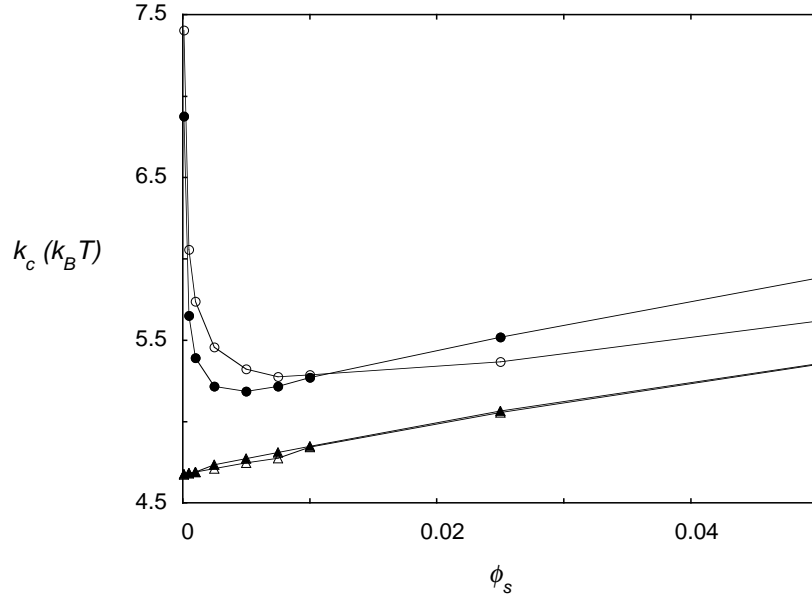


Figure 2.11: The mean bending modulus,  $k_c$ , of a bilayer membrane as a function of the ionic strength. The charges on the lipids' headgroup were  $-1$  ( $\bullet$ ), or  $-\frac{1}{2}$  ( $\circ$ ), or the headgroup was zwitterionic ( $\blacktriangle$ ), or not charged ( $\triangle$ ).

headgroup charge, calculations have been done for amphiphiles with a different headgroup charge. Figure 2.11 shows  $k_c$  as a function of ionic strength for two headgroup charges. Again two regimes can be distinguished. The decrease in  $k_c$  is faster for lipids with a higher headgroup charge. In the decreasing regime,  $k_c$  of the higher charged lipid is always smaller than that of the less charged one. In the regime where  $k_c$  increases as a function of the ionic strength, it is the other way around,  $k_c$  of the higher charged lipid is always larger.

In the introduction we argued that besides being off equilibrium, the value of  $\bar{k}$  might determine whether bilayers can fuse. To get more insight into the behavior of  $\bar{k}$  with ionic strength,  $\bar{k}$  was calculated for bilayers composed of lipids that differ in headgroup charge (Fig. 2.12). For all headgroup charges,  $\bar{k}$  becomes less negative with increasing ionic strength. This increase in  $\bar{k}$  with ionic strength is initially very fast for charged bilayers that initially have a more negative  $\bar{k}$ .

## 2.4 Discussion and conclusions

The experiments show that vesicles in salt solution made by freeze thaw experiments are very likely to be equilibrium vesicles. The initial size of the vesicles has no influence on their final size (Fig. 2.1). In addition, a complementary preparation method shows that vortexed vesicles tend to evolve to the same size, if the exchange of material is fast enough (Fig. 2.2). This size depends on



## Charged Lipid Vesicles

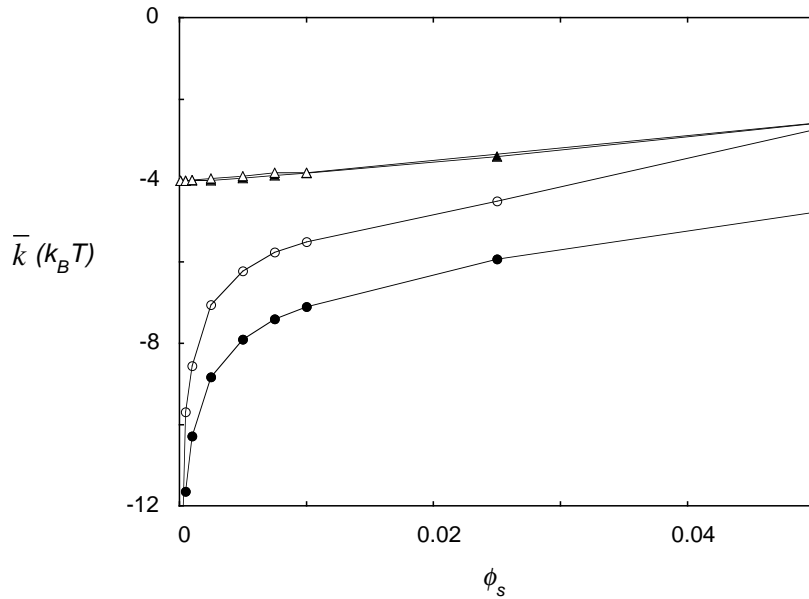


Figure 2.12: The Gaussian bending modulus,  $\bar{k}$ , of a bilayer membrane as a function of the ionic strength. The value of  $\bar{k}$  strongly depends on the charge on the headgroup. The less charge on the headgroup the closer the membrane is to  $\bar{k} = 0$ . The charges on the lipids' headgroup were  $-1$  ( $\bullet$ ), or  $-\frac{1}{2}$  ( $\circ$ ), or the headgroup was zwitterionic ( $\blacktriangle$ ), or not charged ( $\Delta$ ).

the kind of salt, the salt concentration and the lipid used. The fact that these vesicles do not form spontaneously upon addition of a salt solution is probably due to the very low solubility of the phospholipids. The critical micelle concentration of the lipids decreases dramatically as the ionic strength increases. The bulk concentration of lipid becomes very low and therefore the exchange of material between vesicles becomes slower with increasing ionic strength. Presumably, this is also the reason why phospholipid vesicles can be prepared in particular sizes and remain as such without fast re-equilibration. In this respect the freeze thaw procedure is very helpful; it seems to be a method for fast vesicle equilibration. The disruption of the vesicle membrane into small fragments apparently helps to exchange material between the vesicles. This lipid exchange is normally very low due to the limited solubility of charged phospholipids in salt solution.

The size of the phospholipid vesicles seems to be related to the mean bending modulus  $k_c$ . The trends seen in the  $k_c$ -curves (calculations, Fig. 2.11) as a function of ionic strength strongly resemble those of the vesicle size (experiments, Fig. 2.4) as a function of ionic strength. For vesicles of a single lipid species the spontaneous curvature  $J_0$  is expected to be zero, this was also found in the calculations. The equilibrium vesicles found for this system will therefore be fluctuation stabilized. For entropic stabilization a dependence of the radius on  $k_c$  is expected. If  $k_c$  and vesicle size are indeed related the initial

## 2.4 Discussion and conclusions

decrease in vesicle size can be attributed to the decreasing thickness of the diffuse double layer with increasing salt concentration. The size increase at high ionic strength is due to a thickening of the lipid bilayer. Calculations show that with increasing ionic strength the membrane dehydrates, which leads to closer lipid packing, a thicker membrane, and therefore a higher  $k_c$ .

A dependence of the vesicle radius on the lipid concentration is expected for entropically stabilized vesicles. Safran shows that in the limit where translational entropy plays a role, vesicles with  $k_c \gg 1$  are only stable at very low volume fractions of lipid (Safran et al., 1991). Here, two regimes are distinguished in the dependence of the vesicle radius,  $R$  on the DOPG concentration. As predicted by theory,  $R$  increases with the lipid concentration in the dilute regime. At higher lipid concentrations,  $R$  stays constant, or slightly decreases with increasing lipid concentrations. In these more concentrated systems the translational entropy does probably not really play a role. The vesicle size is mainly determined by the persistence length of the bilayer, and therefore by  $k_c$  in combination with the vesicle-vesicle interaction.

Highly charged lipids pack into significantly thinner bilayers than lipids that carry no charge, therefore  $k_c$  of these membranes is much lower. This is probably also the reason why DOPG vesicles are smaller than DOPC vesicles at low ionic strength, in spite of the presence of the electric double layer. Extrapolation of the  $k_c$  vs ionic strength data to zero salt, predicts very high  $k_c$  values for lipids carrying a low charge. This would explain the high values of the bending moduli of PC lipids measured in the literature (Rawicz et al., 2000). With (almost) no salt added, the flat bilayer is indeed the equilibrium structure for phosphatidylcholines. At higher salt concentration, fluctuation-stabilized vesicles apparently become favorable. The solubility of phospholipids is known to be low, and the CMC decreases with increasing ionic strength (Marsh, 1986). This means that with increasing salt concentration the equilibration to a certain vesicle size will become slower. Hence, equilibrium structures will form spontaneously only at sufficiently low salt concentrations.

To understand the effect of  $\text{Cl}^-$ ,  $\text{Br}^-$ , and  $\text{I}^-$  on the bilayer membrane, ion hydration has to be taken into account. According to the Hofmeister series, it will cost more energy to bring  $\text{Cl}^-$  into the hydrophobic phase, as this ion is more strongly hydrated than  $\text{Br}^-$  and  $\text{I}^-$ . Therefore ions dehydrate the membrane in the series  $\text{Cl}^- > \text{Br}^- > \text{I}^-$ . In the calculations this can be simulated by choosing different  $\chi$ -parameters for the interactions between the anions and the solvent. The more negative  $\chi$ -parameter will correspond to the more strongly hydrated anion. The cation  $\text{Na}^+$  is, due to its surface charge density, even more strongly hydrated than both anions and therefore its  $\chi$ -parameter is the most negative.

In the calculations, the most negative  $\chi_{\text{W-anion}}$  gives the highest  $k_c$  values. For entropically stabilized vesicles, higher vesicle radii are expected for higher  $k_c$  values. Compared to lower values, the increase in  $k_c$  with ionic strength is also faster for the lowest  $\chi_{\text{W-anion}}$ . Experiments on DOPG vesicles in NaCl, NaBr, and NaI indeed show that the vesicles in NaCl are always larger than

## Charged Lipid Vesicles

the ones in NaBr, and these are always larger than the ones in NaI. In the high ionic strength regime, the radii of the DOPG vesicles in NaCl also increase faster with ionic strength than similar vesicles in the other salt solutions. Also, for this situation,  $k_c$  from the calculations and the experimentally determined vesicle radius show the same trends in their behavior as a function of ionic strength (Fig. 2.10 and Fig. 2.5).

The mean bending modulus  $k_c$  is not the only interesting parameter that can be obtained from the SCF calculations. As mentioned before, the Gaussian bending modulus  $\bar{k}$  can also be determined and is probably of great importance in vesicle fusion. A first step in membrane fusion will be the formation of connections between opposed membranes. These connections will evolve into fusion pores. Some researchers have suggested that this process is very similar to the transition from the lamellar  $L_\alpha$  to the inverted hexagonal  $H_{II}$  or inverted cubic  $Q_{II}$  phase (Siegel, 1997), (Siegel, 1999). In both processes the formation of a saddle surface-like connection between opposing membranes is essential. The Gaussian bending modulus  $\bar{k}$ , may give insight in the formation of saddle surfaces. The value of  $\bar{k}$  is normally negative for a stable bilayer. However, for positive values of  $\bar{k}$  the bilayer can only lower its curvature energy by making the Gaussian curvature term,  $K$ , negative. This means that then the surface can be locally characterized by two radii of curvature of opposing sign, like the saddle-surface.

Two vesicles might be able to form an intermembrane connection as soon as  $\bar{k}$  approaches zero. Theoretical predictions of  $\bar{k}$  indicate that its value becomes less negative with increasing ionic strength (Lekkerkerker, 1989); our calculations show a similar behavior of  $\bar{k}$  (Fig. 2.12). The change of  $\bar{k}$  with ionic strength is rather interesting, as for each fusogenic cation there is a specific concentration at which fusion starts. This so-called fusion threshold may correspond to the ionic strength at which  $\bar{k} \approx 0$ .

Although the correlation seems nice, the  $\bar{k} \approx 0$  criterion is probably not enough for full vesicle fusion. The calculations show that the lower the net charge on the headgroup, the less negative  $\bar{k}$  (Fig. 2.12). In some (zwitterionic) PC vesicle systems inter-lamellar connections between vesicles have been observed (Kløggen and Helfrich, 1997) and ascribed to  $\bar{k} \approx 0$ , even though PC lipids are almost inert to fusion. The equilibrium size of the vesicle probably also plays a role. At very low salt concentrations DOPC prefers to form lamellar phases. With increasing ionic strength the membrane becomes charged and the formation of small vesicles is preferred. This means that upon addition of salt vesicles would like to become smaller instead of bigger, therefore the formation of intermembrane connections does not necessarily lead to vesicle fusion. The preferred size of highly charged phospholipids like, e.g., DOPG increases with increasing ionic strength, therefore we predict that the formation of an interlamellar attachment (ILA) does, in this system, lead to full fusion. The salt concentration at which the actual vesicle size is smaller than the preferred one, will be lower for SUVs compared to LUVs. SUVs will therefore, if the formation of ILAs is not limiting, have a lower threshold concentration for

## 2.4 Discussion and conclusions

fusion. It is interesting to note that SUV fusion often stops as the vesicles grow in size. Phosphatidylserine (PS) SUVs do fuse in the presence of  $Mg^{2+}$ , but this process ceases spontaneously after a few rounds of fusion, whereas at the same  $Mg^{2+}$  concentration PS LUVs do not fuse at all (Wilschut et al., 1985).

Although in biological systems vesicle budding and fusion phenomena are probably assisted by proteins, it is conceivable that the mechanical properties of the phospholipid bilayer play an important role in fusion and fission phenomena.

## Chapter 3

# Entropic stabilization of dioleoylphosphatidylcholine and dioleoylphosphatidylglycerol vesicles

### Abstract

The anionic phospholipid dioleoylphosphatidylglycerol (DOPG) forms entropically stabilized vesicles over a large range of phospholipid and salt concentrations. Membranes of the zwitterionic dioleoylphosphatidylcholine (DOPC) phase separate into a lamellar and a vesicular phase at high lipid concentration, both at low and high ionic strength. DOPC forms stable vesicles at intermediate ionic strength. This can in part be explained by specific binding of anions that gives rise to an effective surface charge on the DOPC membranes at intermediate ionic strength.

The size and size distribution of DOPG and DOPC vesicles result from the competition between the bending energy and translation and undulation entropy. A power-law concentration dependence of the vesicle radius is found except at very low phospholipid concentrations, there the vesicle radius no longer decreases with lipid concentration. Self consistent field calculations show that, for these small radii, the mechanical properties of the bilayer can no longer be described by a second order expansion of the surface tension in the curvatures and effectively  $k_c$  is increasing with decreasing vesicle radii.

### 3.1 Introduction

## 3.1 Introduction

Entropy can stabilize unilamellar vesicles of a single phospholipid species against the formation of infinite planar bilayers. The equilibrium size distribution of such a vesicle population is determined by a competition between curvature free energy and various sources of entropy, such as e.g. vesicle translation and bilayer undulation. The curvature energy per unit of area may, in good approximation, be described as a second order expansion of the surface tension,  $\gamma$ , in the mean curvature  $J = \frac{1}{R_1} + \frac{1}{R_2}$  and the Gaussian curvature  $K = \frac{1}{R_1 R_2}$ , where  $R_1$  and  $R_2$  are the two local curvatures (Helfrich, 1973). Assuming that the equilibrium membrane is tensionless, and that it has no spontaneous curvature, the equation originally proposed by Helfrich (Helfrich, 1973) reduces to

$$\gamma = \frac{1}{2}k_c J^2 + \bar{k}K \quad (3.1)$$

in which  $k_c$  and  $\bar{k}$  are the mean and Gaussian bending moduli, respectively. From equation 3.1, and the definitions of  $J$  and  $K$ , it follows that the energy needed to curve a flat bilayer into a closed vesicle,  $E_{ves} = \gamma A$ , ( $A = 4\pi R^2$ ), is independent of the vesicle radius  $R$  and can be written as

$$E_{ves} = 4\pi(2k_c + \bar{k}) \quad (3.2)$$

To make vesicle formation possible, the curvature energy costs must be compensated by entropy.

In contrast to vesicles stabilized by a spontaneous curvature, the average size of entropically stabilized vesicles must vary measurably with changes in the total phospholipid concentration. In the literature, there are a few attempts to obtain predictions on the size and size distribution of entropically stabilized vesicles as a function of the surfactant concentration,  $c$  (Safran et al., 1991), (Simons and Cates, 1992), (Herve et al., 1993), (Morse and Milner, 1995). Up till now, there is however no consensus on how to treat this problem. In principle, many entropic contributions that can compensate for the curvature (free) energy, can be taken into account, but it is unlikely that they are all equally important. In the simplest case, only the translational entropy is accounted for. Since vesicles have a finite size, they have an entropy of mixing that is much larger than that of the lamellar phase. In the dilute limit, where excluded-volume interactions can be neglected, this results in the prediction that the average vesicle radius  $\bar{R}$ , scales as  $\bar{R} \propto (c_{lipid})^{\frac{1}{4}}$  (Safran et al., 1991). However, translational entropy is probably not the only entropic factor of importance. Undulations might also play a role in lowering the curvature energy. The effect of undulations of the bilayer membrane can be understood by introducing a membrane persistence length  $\xi_p$ , in analogy with the persistence length of a polymer chain. The bilayer has no resistance to shape changes over length scales larger than  $\xi_p$ . This means, that the bending moduli of the membrane are no longer independent of the vesicle radius. To deal with this, Helfrich proposed a renormalization of the bending moduli in which  $k_c$  and  $\bar{k}$  are replaced

## Entropic stabilization of vesicles

by the effective bending moduli  $k_c^{eff}(R)$  and  $\bar{k}^{eff}(R)$

$$k_c^{eff}(R) = k_c - a \frac{k_B T}{4\pi} \ln \left[ \frac{R}{l} \right] \quad (3.3)$$

and

$$\bar{k}^{eff}(R) = \bar{k} - \bar{a} \frac{k_B T}{4\pi} \ln \left[ \frac{R}{l} \right] \quad (3.4)$$

where  $l$  is a length scale proportional to the size of the molecules. The membrane persistence length is related to the mean bending modulus  $k_c$  by  $\xi_p \propto l e^{\frac{4\pi k_c}{k_B T}}$ . The numerical constants  $a$  and  $\bar{a}$  are in the order unity and this results in  $R \approx l \rightarrow k_c^{eff}(R) = k_c$  and when  $R \approx \xi_p \rightarrow k_c^{eff}(R) = 0$ . The lowering of the bending moduli with increasing vesicle radii, leads to a decrease in the curvature energy 3.2.

When both entropy of mixing and undulations are taken into account,  $\bar{R}$  is predicted to scale as  $\bar{R} \propto (c_{lipid})^{\frac{3}{20}}$  (Simons and Cates, 1992), (Herve et al., 1993). Morse and Milner extended this approach, and took into account other entropic contributions as well (Morse and Milner, 1995). Collective degrees of freedom such as translations and polydispersity and a different treatment of the contributions to the undulation entropy result in the prediction that  $\bar{R}$  should scale as  $\bar{R} \propto (c_{lipid})^{\frac{3}{5}}$  (Morse and Milner, 1995).

The lipid concentration will not only influence the equilibrium size of entropically stabilized vesicles, it is also expected to have a profound effect on the phase behavior of phospholipid dispersions. The values reported for  $k_c$  of phospholipid membranes are all in the order of  $10 - 40k_B T$  (Seifert and Lipowsky, 1995), (Rawicz et al., 2000). When  $k_c$  is this high, vesicles can only be thermodynamically stable in the dilute regime. At high phospholipid concentrations the translational entropy is negligible, and lamellar phases are therefore expected to be favored.

The salt concentration will also affect the phase behavior of phospholipid dispersions. Vesicles of charged phospholipids are supposed to become unstable at very high ionic strength, when the surface charge is completely screened. For zwitterionic phospholipids a slightly different behavior is expected. Self consistent field calculations on DMPC show that bilayers composed of this phospholipid attract each other at very low ionic strength (Meijer et al., 1995). They also show that it is possible to find a regime of intermediate ionic strength at which stable membranes can be formed from zwitterionic phospholipids. In this regime an electric double layer develops on the periphery of the bilayer which gives rise to an electrostatic repulsion that is sufficiently long ranged and strong enough to overcome the Van der Waals attraction (Meijer et al., 1995). Measurements on the electrophoretic mobility of phosphatidylcholines show that specific binding of anions can also give rise to an effective surface charge at intermediate ionic strength (Tatulian, 1983), (Tatulian, 1987).

As shown before, the freeze-thaw method results in phospholipid vesicles that are thermodynamically stable (Chapter 2). Surfactant vesicles normally

## 3.2 Materials and Methods

age by diffusion of monomers between vesicles (Madani and Kaler, 1990), (Olsson and Wennerström, 2002). The low solubility of the phospholipids prevents fast rearrangements, and equilibration is typically very slow. However, charged lipids such as DOPG are still relatively soluble when no salt is added. They therefore form vesicles, that evolve to their equilibrium radius in demineralized water, but at higher ionic strength the solubility becomes worse (Marsh, 1986) and equilibration is slower. The freeze thaw method allows for rearrangements to take place on a faster timescale (Chapter 2).

In this article we will try to find the relation between phospholipid concentration and the size of thermodynamically stable vesicles, experimentally. For this study we used DOPG and DOPC which have an anionic and a zwitterionic headgroup, respectively.

## 3.2 Materials and Methods

### 3.2.1 Experiments

The anionic phospholipid dioleoylphosphatidylglycerol (DOPG) was purchased as a sodium salt, and the zwitterionic phospholipid dioleoylphosphatidylcholine (DOPC) as a chloroform solution, from Avanti Polar Lipids. Both phospholipids were used without any further purification. Analytical grade sodium bromide (NaBr) was obtained from J.T. Baker Chemicals.

Vesicles were made by drying the phospholipids in chloroform under a stream of nitrogen followed by at least 2 hours under vacuum to remove the last traces of solvent. The dry lipid film was rehydrated with a salt solution of the desired ionic strength. The resulting multilayered phospholipid vesicles were subjected to the freeze thaw method. 1 ml of vesicle containing solution was immersed in liquid nitrogen until it was completely frozen. The samples were thawed in a water bath at approximately 313 K. During thawing the half-frozen solution was vortexed regularly. The vesicles are known to fragment into small vesicles as a result of freezing and thawing (MacDonald et al., 1994). Dioleoyl derivatives are particularly susceptible to fragmentation, and were therefore used in this study (MacDonald et al., 1994).

The days after freeze thawing, both DOPG and DOPC samples were checked for the appearance of multi lamellar phases. At some salt and DOPC concentrations the samples indeed phase separated into a vesicle rich and a multilamellar phase. When phase separation took place, the opaque vesicle phase was carefully removed and the radius of vesicles in this phase was determined.

The size of the vesicles was determined using dynamic light scattering (DLS). The instrumental setup consisted of an ALV-5000 correlator and a scattering device with an ALV-125 goniometer and a multiline Lexel AR-laser source. The data was collected at a scattering angle of 90 degrees at a wavelength of 513 nm. During the measurements the temperature was kept constant at 293 K. Before each measurement the samples were diluted by adding



## Entropic stabilization of vesicles

electrolyte solution. A cumulant analysis was used to determine the average hydrodynamic vesicle radius from the intensity autocorrelation function.

Electrophoretic mobility measurements on DOPC vesicles were performed using a Malvern Zetasizer 3 (Malvern Instruments, U.K.). The DOPC vesicles used in this experiment were obtained by extrusion through a 100 nm polycarbonate filter, in this way vesicles with a radius of approximately 60 nm were obtained, regardless of the ionic strength of the NaBr solution.

### 3.2.2 Self consistent field calculations

The Self Consistent Field (SCF) theory can be used to evaluate the distribution of surfactant molecules in association colloids. These self assembled objects can be either micelles, vesicles, or bilayers. Structural, thermodynamic and mechanical parameters of a lipid bilayer can subsequently be predicted. Recently, Oversteegen showed how the mechanical parameters can be determined unambiguously from SCF calculations (Oversteegen and Leermakers, 2000), (Chapter 2).

In our SCF calculations phospholipid like molecules were modeled as linear chains with segment sequence  $C_{18}X_2C_2X_2C_{18}$ , in which the X segments carry a charge. The two  $C_{18}$ -groups represent the hydrophobic tails, the  $X_2C_2X_2$  group stands for the hydrophilic headgroup. Water was modeled by a simple solvent monomer W. The ionic strength of the solution was determined by two monomer types, cation and anion, with valency +1 e and -1 e, respectively. The hydration of ions was taken into account by the choice of the Flory-Huggins interaction parameters,  $\chi_{\text{cation-W}} = -2$  and  $\chi_{\text{anion-W}} = -1$ . The more negative value for  $\chi_{\text{anion-W}}$  reflects the stronger hydrogen bonding property of the cation. The surfactant headgroup was made soluble in water by choosing  $\chi_{\text{X-W}} = -2$ . In all calculations the following dielectric constants were used  $\varepsilon_C = 2$ ,  $\varepsilon_X = \varepsilon_{\text{cation}} = \varepsilon_{\text{anion}} = 5$ ,  $\varepsilon_W = 80$ .

## 3.3 Results

### 3.3.1 DOPC phase diagram

Figure 3.1 shows the phase diagram of DOPC in NaBr solution. A single phase of thermodynamically stable vesicles is formed at intermediate ionic strength. At both low and high NaBr concentrations the system phase separates into a vesicular and a lamellar phase which differ in phospholipid concentration. The dilute phase contains vesicles that are equal in size to the ones obtained just before crossing the binodal without changing the ionic strength, while the concentrated phase consists of multilamellar sheets. At high phospholipid concentrations the ionic strength region in which a single phase of stable vesicles exists becomes more narrow. The vesicular phase will probably disappear at even higher DOPC concentrations, when translational entropy of the vesicles

### 3.3 Results

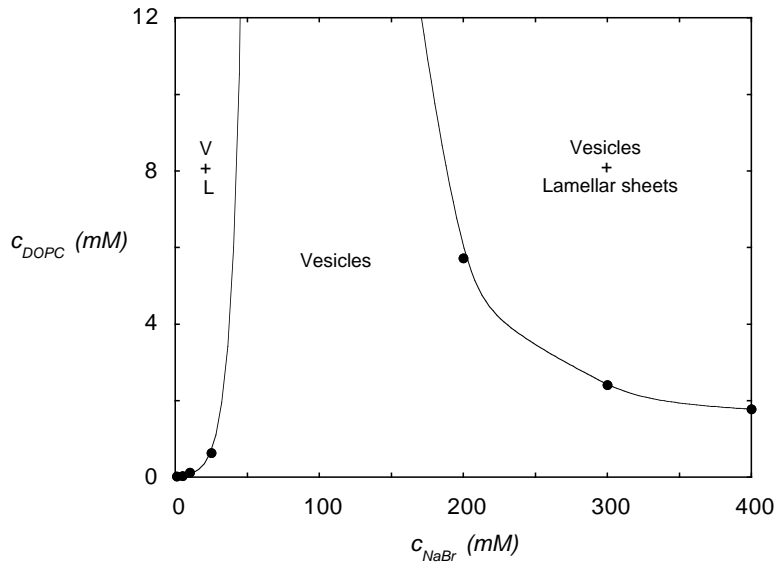


Figure 3.1: Phase diagram of the zwitterionic phospholipid DOPC in NaBr solution.

becomes very small.

DOPG vesicles are stable over a large range of phospholipid and salt concentrations. In the ionic strength and phospholipid concentration regime shown in figure 3.1, DOPG always forms stable unilamellar vesicles. Even up to concentrations as high as 160 mM DOPG at 250 mM NaBr no multilamellar sheets appear in the solution. When the volume fraction of vesicles approaches 0.1, the vesicles packing becomes so crowded that the translation entropy vanishes. At these concentrations of DOPG, the vesicle radius levels off, but vesicles still seem to be the preferred structure.

The size of the thermodynamically stable vesicles was found to be a function of the ionic strength. Figure 3.2 shows the equilibrium size of both DOPC and DOPG vesicles as a function of the NaBr concentration with  $c_{lipid} = 2mM$ . At low ionic strength the hydrodynamic vesicles radius decreases with increasing salt concentration, at high ionic strength a significant increase in size is visible. DOPC vesicles are always smaller than DOPG vesicles at high NaBr concentrations.

The vesicle radius does not only depend on the ionic strength, it is also a function of the phospholipid concentration. In the ionic strength regime where stable vesicles are found, DOPC and DOPG vesicle sizes have similar trends as a function of the lipid concentration (Fig. 3.3 and Fig. 3.4). At very low lipid concentrations the vesicle radius decreases with increasing  $c_{lipid}$  until a minimum radius is reached. This minimum radius is approximately 42 nm for DOPC vesicles in 150 mM NaBr, for DOPG vesicles, larger minimum radii were found. At 150 mM NaBr the minimum radius of DOPG vesicles was approximately 67 nm. The minimum radius depended on the ionic strength,

## Entropic stabilization of vesicles

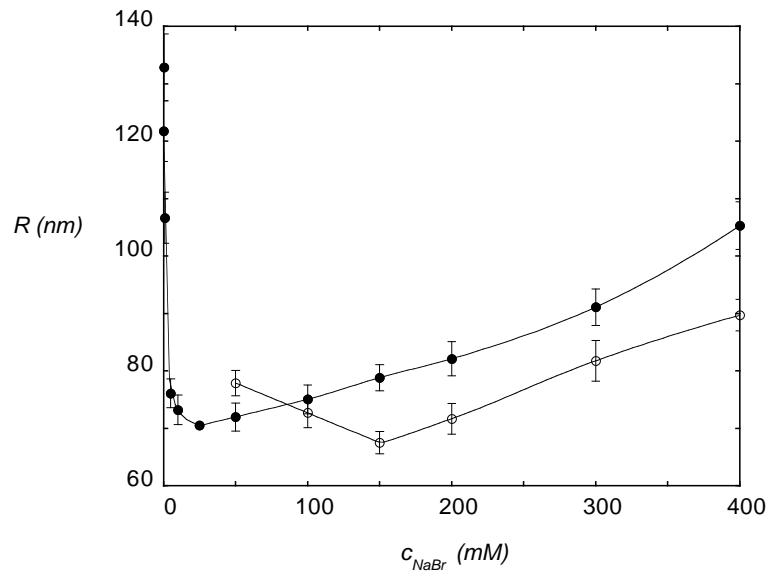


Figure 3.2: The radius of DOPG ( $\bullet$ ) and DOPC ( $\circ$ ) vesicles after 15 freeze-thaw cycles as a function of the NaBr concentration at  $c_{lipid} = 2mM$ .

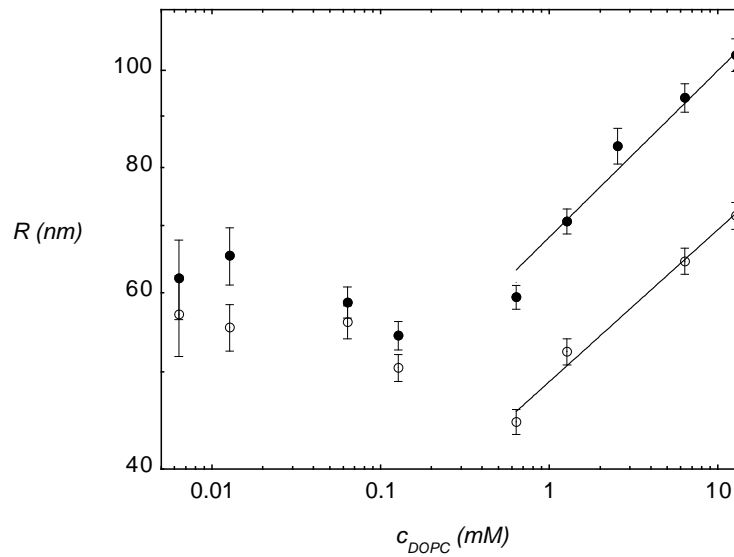


Figure 3.3: DOPC vesicles in 50 mM NaBr ( $\bullet$ ) and 150 mM NaBr( $\circ$ ). The vesicle radius after 15 freeze-thaw cycles is plotted as a function of the DOPC concentration.

### 3.3 Results

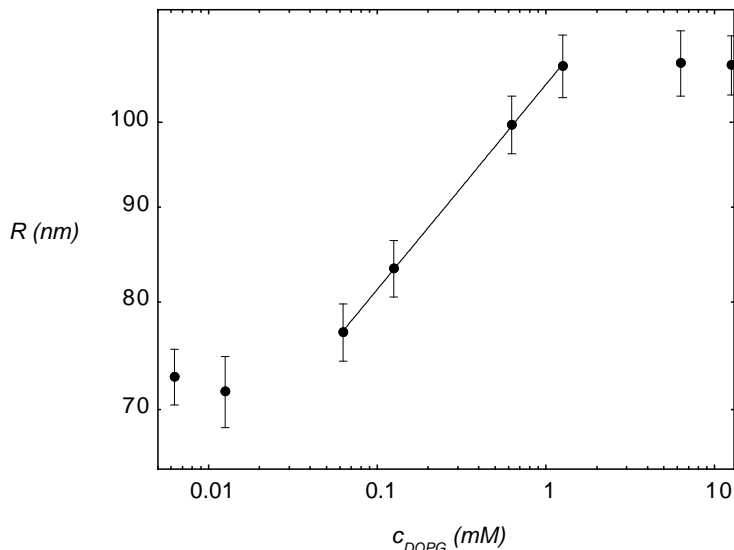


Figure 3.4: DOPG vesicles in 400 mM NaBr. The radius of the vesicles after 15 freeze-thaw cycles as a function of the DOPG concentration. The bars indicate the standard deviation on 200 measurements

going from 150 to 400 mM NaBr it increased by 10 nm.

Going to higher  $c_{lipid}$  the vesicles became larger in size. In this regime of vesicle size increase, the  $R$  versus  $c_{lipid}$  data of DOPC and DOPG vesicles at different NaBr concentrations could be fitted to a power-law,  $R \propto c_{lipid}^\alpha$ . The coefficient  $\alpha$  of this power-law was approximately  $0.15 \pm 0.01$  and  $0.13 \pm 0.03$  for DOPC and DOPG vesicles, respectively. Above approximately  $c_{lipid}=1$  mM DOPG and DOPC differ in their behavior. The size of the DOPG vesicles levels off as the vesicles get packed more close with increasing  $c_{DOPG}$  while DOPC prefers to form lamellar phases at high  $c_{DOPC}$ .

Vesicles composed of phospholipids with a zwitterionic headgroup, such as phosphatidylcholine, are often reported to carry a net negative charge (Tatulian, 1983), (Tatulian, 1987). The value of this charge is known to depend on the ionic strength and the salt used. Figure 3.5 shows the result of the measurements on the electrophoretic mobility  $u$  of DOPC vesicles in NaBr solution. The negative value of  $u$  is the result of a net negative charge on the bilayer membrane. This negative surface charge increases to a maximum at approximately 100 mM NaBr; further increase of the ionic strength leads to a decrease in  $u$ .

#### 3.3.2 Curvature energy

The mechanical parameters from the Helfrich equation follow from the curvature dependence of the interfacial tension, and mean field predictions of these parameters can be determined unambiguously from self-consistent-field (SCF) calculations (Oversteegen and Leermakers, 2000). In the calculations the cur-

## Entropic stabilization of vesicles

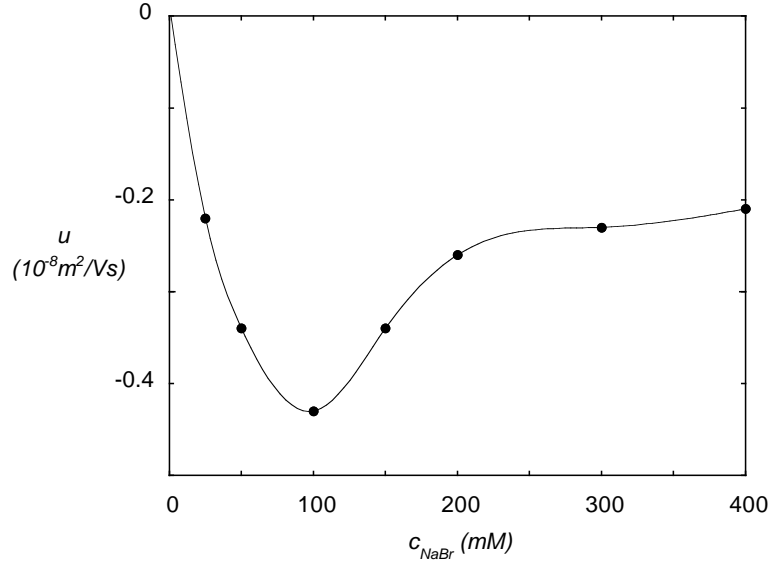


Figure 3.5: Electrophoretic mobility of extruded DOPC vesicles as a function of the NaBr concentration.

vature of the bilayer can be varied, by changing the number of lipid molecules in the system. For a given number of lipid molecules geometry-constrained equilibrium density profiles and the corresponding interfacial tensions can be determined. The interfacial tensions of both a spherical and a cylindrical vesicle as a function of the vesicle radius give access to the bending moduli and curvature energy. When calculations are performed in a cylindrical geometry, using  $K = 0$ ,  $J = \frac{1}{R}$ ,  $A = 2\pi Rh$ , and  $J_o = 0$ , equation 3.1 gives

$$\gamma A = \pi k_c J \quad (3.5)$$

In a spherical geometry ( $J^2 = 4K = \frac{4}{R^2}$ ,  $A = 4\pi R^2$ , and  $J_o = 0$ ) the result corresponds to 3.2

$$\gamma A = 4\pi(2k_c + \bar{k}) = E_{ves}$$

Thus,  $k_c$  can be determined from calculations in a cylindrical geometry, by varying the total curvature  $J$ . This  $k_c$  can be used to derive  $\bar{k}$  from the data obtained in the spherical geometry. The  $k_c$  calculated in this way is not renormalized, it represents an intrinsic instead of an effective  $k_c$ ; the SCF calculations do not take into account shape fluctuations and undulations.

In this way, the curvature energy of the  $C_{18}X_2C_2X_2C_{18}$  bilayer was calculated for different volume fractions of salt,  $\phi_s$ . Figure 3.6 shows the results of such calculations for three surfactants which differ only in headgroup charge. For the same situation,  $k_c$  can be determined from the calculations in the cylindrical geometry (Fig. 3.7). The results of this analysis show that the curvature energy is, at all salt concentrations, highest for an uncharged bilayer and decreases with increasing headgroup charge. For all lipids shown,  $E_{ves}$  increases

### 3.3 Results

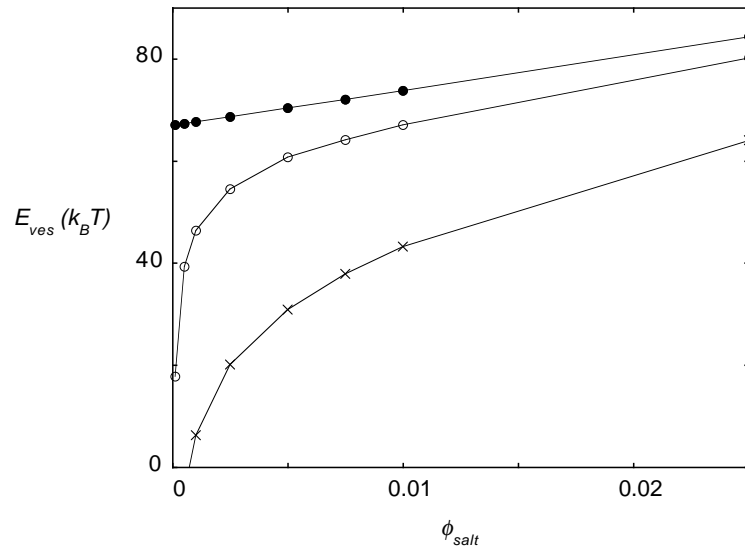


Figure 3.6: The curvature energy  $E_{ves}$  as a function of the ionic strength for bilayers that, carry no charge (●), a charge of  $-\frac{2}{5} e$  (○), and a charge of  $-1 e$  per lipid molecule (×).

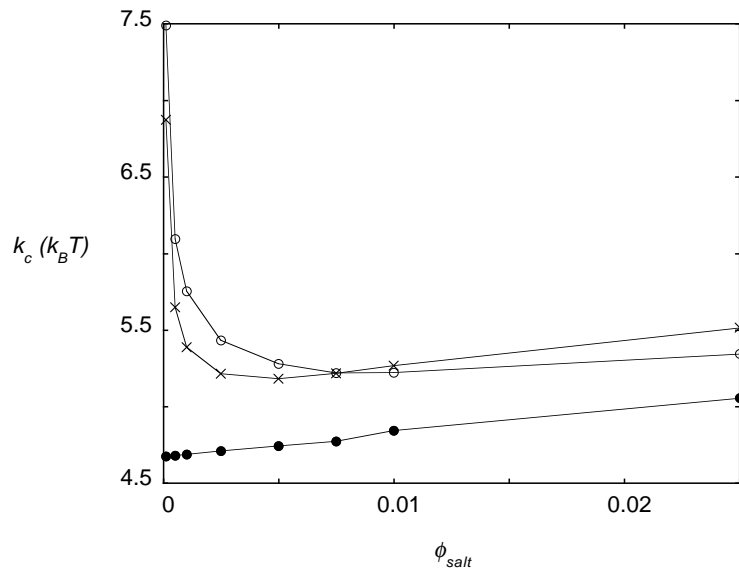


Figure 3.7: The mean bending modulus  $k_c$  of a bilayer membrane as a function of the ionic strength. The charges on the lipids' headgroup were 0 (●),  $-\frac{2}{5} e$  (○), and  $-1 e$  (×).

## Entropic stabilization of vesicles

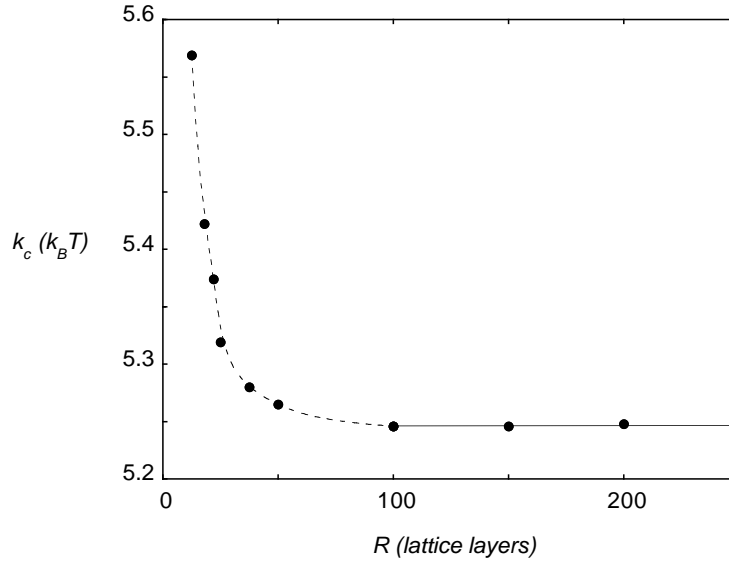


Figure 3.8: The mean bending modulus,  $k_c$  as determined from expanding the surface tension upto terms  $(\frac{1}{R})^2$ . At very low radii  $k_c$  is no longer independent of the vesicle radius.

with increasing  $\phi_s$ , but the very strong increase at low ionic strength is only predicted for the charged surfactants. The formation of bilayers becomes unfavorable and micellar structures are preferred when  $E_{ves}$  becomes negative. This happens at very low ionic strength. The ionic strength at which the micellization starts is higher for the more soluble charged surfactants than for the uncharged ones. This is in agreement with the fact that the critical micelle concentration is higher for phosphatidylglycerols than for that of phosphatidylcholines (Marsh, 1986).

The mean bending modulus  $k_c$  of a charged bilayer decreases with increasing ionic strength at low  $\phi_s$ , while it increases at higher ionic strength. This phenomenon has been described earlier (Chapter 2), and is due to a competition between the decrease in electric double layer thickness and an increase in the bilayer thickness. A sum of the contributions of the bilayer thickness and the double layer thickness determines the absolute value of  $k_c$ . The electric double layer thickness reduces with increasing ionic strength and this would in it self result in smaller values of  $k_c$ . On the other hand, the surfactant bilayer increases in thickness as a result of both denser packing of the lipids due to screening of the headgroup charges and dehydration of the membrane by ions. When the membrane is not charged, no electric double layer is present, and  $k_c$  only reflects the increase in bilayer thickness due to dehydration.

When the vesicle radius decreases beyond 100 lattice layers (equivalent to a radius of approximately 35 nm) a second order expansion is no longer sufficient to describe the behavior of the surface tension with the curvature, and higher order terms in the Helfrich equation are needed. Alternatively, one can invoke

### 3.4 Discussion

the ansatz to allow the mean bending modulus to be a function of  $R$ ,  $k_c(R)$ . In other words, at high curvature  $k_c$  is no longer independent of the vesicle radius. If equation 3.5 is fitted to the data  $k_c$  was observed to increase with decreasing vesicle radius (Fig. 3.8). Remember that the SCF calculations do not take into account entropic contributions. Note that the changes in  $k_c$  visible in Fig. 3.8 are not related to the  $R$  dependence of  $k_c^{eff}$  given in equation 3.3.

## 3.4 Discussion

In contrast to DOPG, DOPC only forms vesicles in a very limited range of phospholipid concentrations and ionic strengths (Fig. 3.1). This is in agreement with SCF calculations on PC membranes (Meijer et al., 1995). According to these predictions it is possible to find a regime of intermediate ionic strength in which an electric double layer develops at the periphery of the bilayer, which gives rise to an electrostatic repulsion strong enough to overcome the Van der Waals attraction between the PC bilayers. The charging of the bilayer is due to a net tilting of the choline moiety out of the membrane plane. Changing the salt concentration to both lower and higher ionic strength diminishes the repulsion between the bilayers; the reason for this behavior, however, is different for the two extremes. At low strength, the Debye length is large and therefore tilting of the charged choline moiety out of the membrane plane becomes difficult. As the cholines' orientation becomes perfectly parallel to the membrane surface with decreasing salt concentration, the surface potential diminishes and even becomes zero. At high ionic strength, the Debye length is small and the electrostatic repulsion between membranes becomes ineffective. DOPG membranes will become unstable at high ionic strength for the same reason, but because DOPG carries a permanent charge its bilayers are stable at low ionic strength.

The idea that DOPC bilayers obtain a small negative charge over a certain ionic strength region is supported by measurements of the electrophoretic mobility of DOPC vesicles (Fig. 3.5). The ionic strength region in which stable vesicles are found up to high DOPC concentrations corresponds to the region in which  $u$ , and therefore the charge on the vesicle surface, is high. The surface charge is, however, still very low, so that  $u$  of the DOPC vesicles is approximately ten times lower than  $u$  of similarly sized DOPG vesicles (Barchini et al., 2000). The net charge on the DOPC bilayer is probably not solely due to tilting of the choline moiety out of the bilayer plane, other work suggests that the observed electrophoretic mobility is due to the adsorption of anions to the phosphatidylcholine vesicles. The affinity of anions for the phosphatidylcholine surface was reported to increase in the order  $I^- > Br^- > Cl^-$  (Tatulian, 1983), (Tatulian, 1987). The fact that we were not able to obtain stable DOPC vesicles in NaCl solution whereas vesicles made in NaI solution are stable over a much larger ionic strength range, suggests that specific binding of ions to the headgroup indeed plays an important role in generating an effective sur-



## Entropic stabilization of vesicles

face charge on zwitterionic phospholipid membranes. It is, however, not clear whether the headgroup tilting plays no role at all, or perhaps facilitates the binding of the anions to the trimethylammonium group when the headgroup tilts out of the membrane plane at intermediate ionic strength. The results do show that electrostatics play an important role in the stability of phospholipid bilayers against adhesion and fusion.

When bilayers are stable it is usually more favorable to make closed spherical vesicles rather than planar membranes. In this way unfavorable edges are eliminated, and the system gains mixing entropy. In the absence of a spontaneous curvature, the energy needed to curve the flat bilayer into a closed vesicle will have to be compensated by entropy. If we assume that both the entropy of mixing and undulations play a role in the entropic stabilization of phospholipid vesicles, the lower limit to the vesicle radius is expected to be set by a persistence length  $\xi_p$  of the bilayer. The vesicle radius is therefore expected to scale as

$$R \propto \xi_p \propto e^{\frac{4\pi k_c}{k_B T}} \quad (3.6)$$

Changes in vesicle radii are in this way directly related to changes in  $k_c$ . When the shape of the calculated  $k_c$  versus  $\phi_s$  curve is compared to the experimentally determined  $R$  versus NaBr concentration plot, striking similarities are observed. Both variables decrease with ionic strength at low salt concentrations and increase at high ionic strength.

DOPG and DOPC vesicles increase in size over a certain range of phospholipid concentrations. This increase was predicted in the literature for vesicles stabilized by entropy (Safran et al., 1991), (Simons and Cates, 1992), (Herve et al., 1993), (Morse and Milner, 1995). The fact that all the data on vesicle size as a function of phospholipid concentration can be fitted with a power-law with coefficients of  $0.15 \pm 0.01$  or  $0.13 \pm 0.03$  points to stabilization by undulations and translational entropy. For this kind of stabilization it was predicted that the average vesicle radius should scale as  $\bar{R} \propto (c_{lipid})^{\frac{3}{20}}$  (Simons and Cates, 1992), (Herve et al., 1993). Other entropic contributions are apparently not needed to compensate for the cost of curving the phospholipid bilayer into a closed vesicle, or cancel against subtle effects that may have been ignored or that we are not aware of.

At low phospholipid concentrations the vesicle radius was observed to have a minimum. Lowering the phospholipid concentration beyond this concentration resulted in a slight increase in vesicle size. This result was not predicted in the literature, but the SCF calculations give results that are in agreement with this observation. When the bilayer is curved beyond a certain radius,  $k_c$  starts to increase. At high curvatures, the intrinsic  $k_c$  is no longer independent of the vesicle radius. Equivalently, higher order terms in the Helfrich equation become important in the description of the mechanical properties of the bilayer. Surprisingly, this already happens when the vesicles are still rather large. The increase in  $k_c$  favors larger vesicles, and this effect is apparently greater than the effect of lipid concentration on the vesicle size: Therefore, the vesicles increase

### 3.4 Discussion

slightly in size.

Although it seems that most experimental observations can be explained, the results of the calculations for the zwitterionic surfactant do not relate exactly to the data obtained for DOPC vesicles. In contrast to DOPC, the linear chain molecules used in the calculations cannot tilt their headgroup out of the membrane plane, and specific adsorption of ions is also not taken into account in our model. This means that possible mechanisms to charge the zwitterionic membrane are entirely neglected, while it is known that phosphatidylcholines do behave as slightly charged surfactants. In salt solutions they show electrophoretic mobility, depending on the salt and the ionic strength used (Tatulian, 1983). Here we show that DOPC vesicles in NaBr indeed have an electrophoretic mobility (Fig. 3.5). At intermediate NaBr concentrations, the electrophoretic mobility and therefore the surface charge are highest. At these NaBr concentrations, DOPC forms stable vesicles over a large range of phospholipid concentrations. At intermediate ionic strength, it is therefore probably more correct to compare the results of DOPC vesicles with calculations on surfactants that carry only a small amount of charge instead of no charge at all. Bilayers of surfactants that carry only fractional charge have a smaller  $k_c$  than those carrying a full charge. This is indeed similar to the behavior of the vesicle radius as a function of the NaBr concentration. The shape of the  $k_c$  versus  $\phi_s$  curves is the result of a competition between two parameters that strongly influence  $k_c$ . On the one hand, the bilayer tends to become thicker when the charged surfactants can pack into more dense bilayers due to screening of their headgroup charge. This gives rise to stiffer membranes, and hence  $k_c$  is expected to increase. Another factor that leads to thicker membranes, is the dehydration of the membrane due to the salt, which becomes especially important at high salt concentrations. On the other hand, the electric double layer thickness decreases with increasing ionic strength, and this results in lower values of  $k_c$ . At low ionic strength the decrease in double layer thickness dominates for the charged surfactants and a decrease in  $k_c$  is observed. At high ionic strength the increase in bilayer thickness results in a slight increase in  $k_c$  (Chapter 2).

The calculations show that the curvature energy  $E_{ves}$  of an uncharged membrane is high. The fact that the net uncharged DOPC at low ionic strength favors the formation of membrane sheets, supports the view that  $E_{ves}$  is too high to be overcome by entropy (Lasic, 1990). According to the SCF predictions the curvature energy for a charged bilayer is much lower. This agrees with the observations that entropically stabilized vesicles are only found in the regime where DOPC bilayers carry a net charge.

Micropipette pressurization measurements on DOPC membranes in a sucrose/glucose solution give a value of approximately  $21 k_B T$  for  $k_c$  (Rawicz et al., 2000). This is much higher than the  $k_c$  values predicted in the SCF calculations. Although the predicted trends in  $k_c$  with ionic strength are expected to be realistic, the absolute values calculated for  $k_c$  are less certain. In contrast to the real phospholipid chains the apolar chains in the SCF calculations are

## Entropic stabilization of vesicles

fully flexible, this results in relatively thin bilayers, and therefore  $k_c$  is possibly underestimated. On the other hand  $k_c$  may be overestimated because the SCF calculations only take into account fluctuations on the single-molecule level; collective fluctuations are totally ignored.

From the SCF calculations it follows that the  $k_c$  of a charged surfactant bilayer is much higher than that of a neutral one. This means that membranes made of DOPG are expected to be much stiffer than DOPC membranes. This illustrates again that it is not the value of  $k_c$ , but the curvature energy  $E_{ves}$  that determines whether or not entropic vesicle formation is possible. The values for  $\bar{k}$  of the charged membrane are much more negative, and as a result  $E_{ves}$  is small enough to be overcome by entropic contributions. According to the SCF calculations the curvature energy of highly charged surfactants might come close to zero at very low ionic strength. This would lead to stable vesicles without any involvement of entropy. However, due to the high value of  $k_c$  at low ionic strength, this would result in a very polydisperse population of giant vesicles. Close to  $E_{ves} = 0$ , the transition from vesicles to micelles might even compete with the formation of giants; this probably gives rise to huge polydispersity in size.

### 3.4 Discussion

# Chapter 4

## Effect of mono- and divalent cations on the equilibrium radius of negatively charged lipid vesicles

### Abstract

Bilayers of the negatively charged phospholipid dioleoylphosphatidylglycerol (DOPG) form vesicles of which the curvature energy can be compensated for by undulational and translational entropic contributions. The equilibrium radius  $R$  of these vesicles is, in first order, determined by the persistence length  $\xi_p$  and thus the mean bending modulus  $k_c$  of the membrane. Measurements on the equilibrium radius of DOPG vesicles produced by the freeze-thaw method in the presence of different alkali and earth alkali chlorides show that the cation has a large effect on  $R$ . The main trends in  $R$  as a function of ionic strength are the same for all salts tested. At low ionic strength,  $R$  decreases because of a reduced double layer thickness, whereas at high ionic strength  $R$  increases as a result of closer packing of the lipids in the bilayer. However large differences in absolute values of  $R$  were observed between the different cations tested; in 100 mM of alkali chloride solution, the vesicles radius increased in the order CsCl < LiCl < NaCl < RbCl < KCl. Self-consistent-field calculations on  $k_c$  show that this behavior can be explained when both the specific binding of cations to the PG-headgroup and cation hydration are taken into account. On the one hand, cations lower the surface charge on the vesicles by binding to the PG-headgroup, which causes  $k_c$  to decrease. On the other hand strong cation hydration leads to thicker membranes, which causes  $k_c$  to increase. Because the most strongly binding cations are also the most strongly hydrated, the largest value of  $k_c$  is reached for cations with an intermediate binding affinity and hydration. Therefore the DOPG vesicles produced by the freeze-thaw method are largest in the presence of KCl.

## 4.1 Introduction

### 4.1 Introduction

Biological membranes are typically negatively charged. This is mainly due to the fact that the bilayer consists for approximately 5-20 % of anionic phospholipids. The negative surface charge and the resulting negative membrane potential make the membrane very sensitive to interactions with cations. This is probably one of the reasons why cations are involved in so many membrane related processes. An increase in the intracellular concentration of  $\text{Ca}^{2+}$ , for example, is thought to be a requirement for intracellular fusion and a signal for exocytosis in many secretory cells (Arnold, 1995), (Mayer, 2002).

In order to obtain electro-neutrality in the solution close to the surface, the negative membrane potential  $\Psi_0$  is accompanied by a diffuse layer of cations in solution. As a result the electrostatic potential drops with the distance  $x$  from the surface. At low potentials ( $\frac{ze\psi}{k_B T} < 1$ ), the potential profile  $\Psi(x)$  can be written as:

$$\Psi(x) = \Psi_0 e^{-\kappa x} \quad (4.1)$$

in which  $\kappa^{-1}$  is the Debye length. This  $\kappa^{-1}$  is also called the double layer thickness and is given by:

$$\kappa^2 = 2Qcz^2 \quad (4.2)$$

In this equation  $c$  is the salt concentration,  $z$  the valency of the ions, and  $Q$  is the Bjerrum length. The Bjerrum length is defined as the length at which two unit charges feel each other with energy  $k_B T$ . The Bjerrum length  $Q$  is given by  $\frac{e^2}{4\pi\epsilon_0 k_B T}$ , in which  $e$  is the elementary charge and  $\epsilon\epsilon_0$  is the dielectric permittivity. From equations 4.1 and 4.2 it is clear that the double layer extends further into the bulk solutions at low salt concentration and low valency.

The surface charge and presence of the electric double layer will influence the mechanical properties of the membrane. The electrostatic part of the mean bending modulus  $k_c$  of the charged bilayer follows from the properties of the electric double layer that is associated with the membrane surface. Within a mean field approximation the electrostatic contribution to  $k_c$ ,  $k_c^{el}$  can be calculated on the basis of the Poisson-Boltzmann equation (Winterhalter and Helfrich, 1988), (Lekkerkerker, 1989). In this analysis the electrical free energy for a charged cylindrical surface is expanded in the inverse powers of the radius of curvature of the cylinder,  $R_1$ . The  $k_c^{el}$  can subsequently be obtained from the coefficient of the quadratic term in this expansion. For low surface charge densities this results in (Winterhalter and Helfrich, 1988), (Lekkerkerker, 1989):

$$k_c^{el} = \frac{3}{2}\pi k_B T \frac{Q\sigma^2}{\kappa^3 e^2} \quad (4.3)$$

in which  $\sigma$  is the surface charge density. From equation 4.3  $k_c$  is predicted to decrease with increasing salt concentration and valency. Indeed when the surface charge density is assumed to be fixed  $k_c^{el} \propto c_s^{-\frac{3}{2}}$ . Screening of the headgroup charges by the counter ions will however promote a closer packing of the phospholipids. This gives rise to an increase of  $\sigma$  and therefore an

## Effect of cations on vesicle stability

increase in  $k_c^{el}$ . Moreover, closer packing of the phospholipids leads to thicker bilayers and therefore to an increase of the overall (non-electrostatic)  $k_c$ . Both aspects thus counteract the  $\frac{1}{\kappa^3}$  effect.

There is yet another way in which cations can affect  $k_c^{el}$ . By binding to the negatively charged membrane cations decrease the surface charge density  $\sigma$ . According to equation 4.3 this results in a decrease in  $k_c^{el}$ . The binding of ions to model phospholipid bilayers has been studied extensively. It has been well established that cations bind to the phosphate group of the phospholipids. Although there is still no consensus on the exact values of the binding constants it is clear that divalent cations bind more strongly to the bilayer than monovalent ones. The effectiveness of cation binding decreases in the order  $\text{Ca}^{2+} > \text{Mg}^{2+} > \text{Li}^+ > \text{Na}^+ > \text{K}^+ > \text{Rb}^+ > \text{Cs}^+$  (Eisenberg et al., 1979), (Tatulian, 1983), (Tatulian, 1987), (Kraayenhof et al., 1996), (Cevc, 1990). These results indicate that the effective surface charge and thus  $k_c$  of a phospholipid bilayer will be influenced by the cation present in solution.

The dependence of  $k_c$  (and  $k_c^{el}$ ) on the concentration and type of cations is expected to influence the equilibrium radius of charged phospholipid vesicles. For entropic reasons, the preferred aggregate structure of a charged phospholipid bilayer is the vesicle. The radius  $R$  of entropically stabilized vesicles depends to a large extent on the persistence length of the bilayer  $\xi_p$ . This can be understood in the following way; the translational entropy will favor many small and thus strongly curved vesicles, but bending bilayers on a length scale much smaller than  $\xi_p$  will cost energy because the bilayer will lose undulation entropy (Chapter 2 and Chapter 3). As  $R$  follows  $\xi_p$  and  $\xi_p$  is an exponential function of  $k_c$ , it seems plausible that, in first order:

$$R \propto \xi_p \propto e^{\frac{k_c}{k_B T}} \quad (4.4)$$

A previous study, in which experiments on the radius of DOPG vesicles were correlated with self-consistent field predictions on  $k_c$  of a charged bilayer membrane, revealed that the experimentally found  $R$  and the corresponding theoretical predictions of  $k_c$  have very similar ionic strength dependences (Chapter 2).

Anions differ from cations in their interaction with negatively charged bilayers: anions are not expected to bind specifically to anionic phospholipids. As a result the influence of a series of anions on the equilibrium vesicle radius is relatively simple and can be understood from the hydration characteristics of the anions (Chapter 2). Strongly hydrated anions decrease the solvent quality for the lipid tails and therefore tend to dehydrate the membrane. This dehydration leads to thicker membranes with an increased  $k_c$ . Differences in the equilibrium radius of DOPG vesicles in NaCl, NaBr, and NaI solutions, could be attributed to differences in the hydration of  $\text{Cl}^-$ ,  $\text{Br}^-$ , and  $\text{I}^-$ . In the case of cations, hydration is therefore also expected to influence  $k_c$  and thus  $R$  of negatively charged phospholipid vesicles.

Here we will report on the effect of alkali and earth-alkali cations on the equilibrium radius of negatively charged dioleoylphosphatidylglycerol (DOPG)

## 4.2 Materials and Methods

vesicles. Because of ion hydration and specific binding to the PG headgroup, cations are, on top of the generic electrostatic screening effects, expected to influence the equilibrium radius of negatively charged vesicles in a non trivial way. As before, self-consistent field predictions will be used to help understand the experimental findings.

## 4.2 Materials and Methods

### 4.2.1 Experiments

The anionic phospholipid dioleoylphosphatidylglycerol (DOPG) was purchased as a sodium salt from Avanti Polar Lipids (Birmingham, AL), and used without further purification. Analytical grade NaCl, KCl, CsCl, CaCl<sub>2</sub> were obtained from Merck (Darmstadt, Germany), LiCl and MgCl<sub>2</sub> from J.T. Baker Chemicals (Deventer, Holland), and RbCl from Fluka.

The experimental procedure to obtain equilibrium vesicles has been described in detail elsewhere (Chapter 2, Chapter 3). Briefly, DOPG was dried from a chloroform solution under a stream of nitrogen. Traces of solvent were removed from the lipid film by storing it for at least 2 hours under vacuum. The dry lipid film was then rehydrated with a salt solution of the desired ionic strength to a concentration of 2 mg/ml lipid. This solution was subjected to repetitive cycles of freezing in liquid nitrogen and thawing. The freeze-thaw cycling results in fragmentation and resealing of the vesicles (MacDonald et al., 1994). After approximately fifteen freeze-thaw cycles, the vesicle radius did not change anymore with increasing number of cycles. Apparently, subsequent freeze-thaw cycles have no effect on the redistribution of material between the vesicles. At low ionic strength the lipids have a relatively high solubility in water, and the vesicles spontaneously evolve to this radius by a kind of Ostwald ripening (Chapter 2). Moreover, the dependence of the radius  $R$  on the lipid concentration agrees with what literature predicts for vesicles stabilized by undulations and translational entropy (Simons and Cates, 1992), (Herve et al., 1993), (Chapter 3). We therefore assume that the vesicles produced by the freeze-thaw method are close to thermodynamic equilibrium, so that their radius is a thermodynamically regulated quantity.

Electrophoretic mobility measurements were performed on a Malvern Zetasizer 3 (Malvern Instruments, U.K.). The vesicles that were used in these experiments were obtained by extrusion of a rehydrated DOPG solution of 20 mg/ml through a 100 nm polycarbonate filter. In this way a rather homodisperse solution of similarly sized vesicles was obtained for all salt solutions used. This made the comparison between the different cations more easy.

Vesicles radii were determined using dynamic light scattering. The instrumental setup consisted of an ALV-5000 correlator, a scattering device with a ALV-125 goniometer and a multiline Lexel AR-laser source. The data was collected at an angle of 90 degrees at a wavelength of 513 nm. During the mea-



measurements the temperature was kept constant at 293 K. Before each measurement the samples were diluted with electrolyte solution. A cumulant analysis was used to determine the average hydrodynamic vesicle radius from the intensity autocorrelation function. Minor differences in medium viscosity between the salts and changes in viscosity with ionic strength were not accounted for. Although this does weakly affect the evaluation of the absolute values of the hydrodynamic radii, it has no influence on the observed trends.

### 4.2.2 Calculations

The radius of vesicles that are stabilized by entropy is determined by the persistence length of the bilayer  $\xi_p$  and therefore by  $k_c$ . This mechanical parameter of the lipid bilayer can be obtained unambiguously from self consistent field (SCF) calculations and the Helfrich equation (Oversteegen and Leermakers, 2000). The Helfrich equation (Helfrich, 1973) describes the surface tension  $\gamma$  of a bilayer as a second order expansion in the mean curvature  $J = \frac{1}{R_1} + \frac{1}{R_2}$  and the Gaussian curvature  $K = \frac{1}{R_1 R_2}$ , in which  $R_1$  and  $R_2$  are the two radii of curvature that locally describe the bilayer.

$$\gamma = \gamma_0 + \frac{1}{2}k_c(J - J_0)^2 + \bar{k}K \quad (4.5)$$

It follows from the thermodynamics of small systems that, if the translational entropy is neglected, the flat equilibrium membrane is tensionless, i.e.  $\gamma = 0$ . As a consequence equation 4.5 reduces to

$$\gamma = -k_c J_0 J + \frac{1}{2}k_c J^2 + \bar{k}K \quad (4.6)$$

This equation gives access to some important thermodynamic and mechanical properties of the bilayer. The spontaneous curvature  $J_0$  is thought to be the curvature that minimizes the curvature free energy of a cylindrical vesicle. The Gaussian bending modulus  $\bar{k}$  determines the topology of the interface, whereas its rigidity is determined by the mean bending modulus  $k_c$ .

The SCF theory can be used to evaluate the distribution of surfactant molecules in self assembled objects such as lipid vesicles and bilayers. In the calculations the curvature of the bilayer can be varied by changing the number of lipid molecules in the system of a given geometry. When for each given number of lipid molecules the geometry-constrained equilibrium density profiles are calculated,  $k_c$  can subsequently be determined from the resulting interfacial tensions (equation 4.6). On a cylindrical interface  $K = 0$ ,  $J = \frac{1}{R}$ , and the surface area  $A = 2\pi R h$ , equation 4.6 can therefore be rewritten as

$$\gamma A = -2k_c J_0 + \pi k_c J \quad (4.7)$$

By varying the number of lipid molecules in the system the radius  $R$  and therefore the curvature  $J$  is automatically adjusted. Then,  $k_c$  can be obtained directly from the slope of the  $\gamma$  vs  $J$  plots.

## 4.3 Results

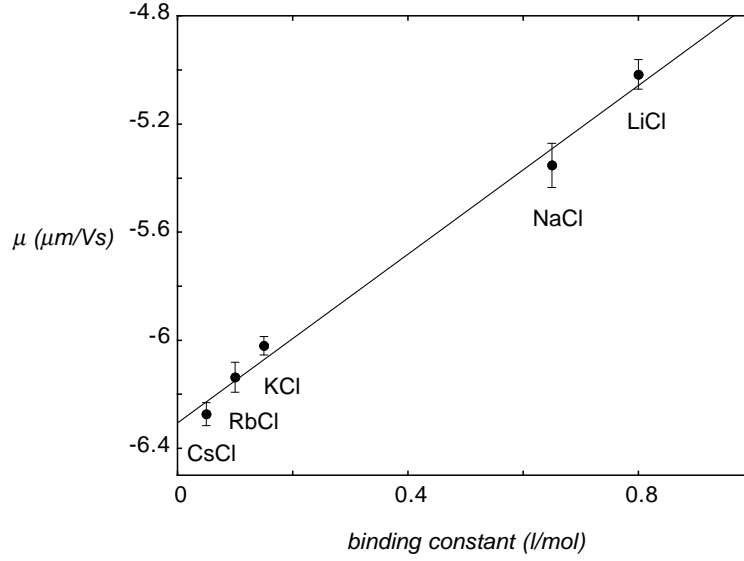


Figure 4.1: The electrophoretic mobility  $\mu$  of DOPG vesicles in 100mM of an alkali chloride as a function of the tabulated binding constant (Cevc, 1990) of the cation with the phosphatidylglycerol headgroup.

To obtain data on  $k_c$  of lipid-like bilayers in the presence of different cations, the lipid is modeled, as in previous studies, as a chain molecule  $C_{18} X_2 C_2 X_2 C_{18}$ . Here, the  $C_{18}$  fragments stand for the hydrophobic phospholipid tail, while the  $X_2 C_2 X_2$  represents the hydrophilic headgroup. Each segment  $X$  carries a charge of  $-\frac{1}{4} e$  making the total charge per lipid  $-1 e$ . The water molecules are modeled as a simple monomer solvent  $W$ . The system further contains monomeric cations and anions to account for the salt present. These monomers carry a charge of  $+1 e$  and  $-1 e$ , respectively. The hydration of ions was taken into account by the choice of the Flory-Huggins interaction parameters,  $\chi_{\text{anion-W}}$  and  $\chi_{\text{cation-W}}$ , where the stronger hydrogen bonding properties are represented by the more negative interaction parameters. The binding of cations to the anionic lipid headgroup was achieved by choosing negative values for  $\chi_{\text{cation-X}}$ . The headgroup of the lipid molecule was made more soluble in water by choosing  $\chi_{X-W} = -2$ . In all calculations the following segment-type dielectric constants were used  $\varepsilon_C = 2$ ,  $\varepsilon_X = \varepsilon_{\text{cation}} = \varepsilon_{\text{anion}} = 5$ ,  $\varepsilon_W = 80$ . The local dielectric constants were computed from a volume fraction weighted average.

## 4.3 Results

### 4.3.1 Experiments

By binding to a negatively charged DOPG bilayer, cations lower the surface charge on the DOPG vesicle. To check whether the surface charge on the vesicles is in agreement with the binding constants tabulated in the literature

## Effect of cations on vesicle stability

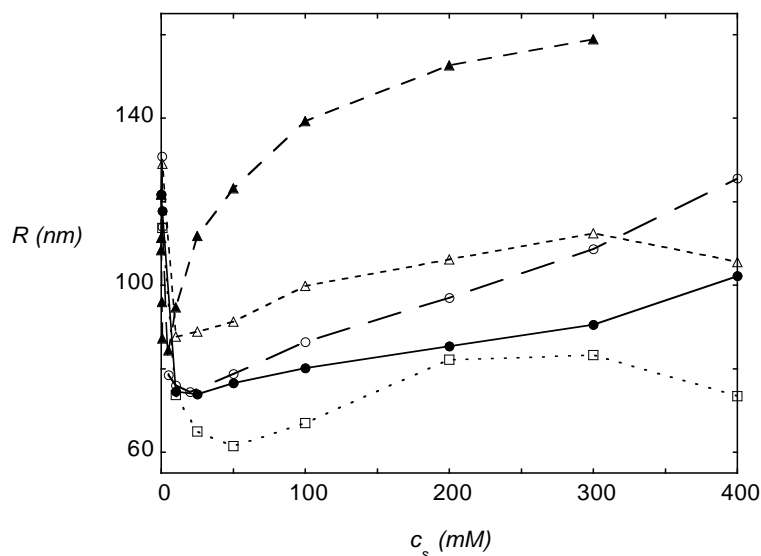


Figure 4.2: Effect of the alkali metal concentration on the equilibrium radius of DOPG vesicles. The graph shows the radius of DOPG vesicles after 15 freeze-thaw cycles in (●) LiCl, (○) NaCl, (▲) KCl, (△) RbCl, and (□) CsCl.

(Cevc, 1990), the electrophoretic mobility  $\mu$  of extruded vesicles with a radius of approximately 60 nm in 100 mM of an alkali chloride solution was measured. Figure 4.1 shows that the electrophoretic mobility of the DOPG vesicles is almost linearly related to the binding constants of the alkali cations. The stronger the cations bind to the phospholipid headgroup, the lower the surface charge, and therefore the electrophoretic mobility. The charge density on the DOPG vesicles therefore decreases in the presence of alkali cations in the order  $\text{Cs}^+ > \text{Rb}^+ > \text{K}^+ > \text{Na}^+ > \text{Li}^+$ .

The binding of the ions is expected to influence the equilibrium radius of DOPG vesicles. According to literature predictions the lowering of the surface charge will lead to a decrease in  $k_c^{el}$  (equation 4.3), (Winterhalter and Helfrich, 1988), Lekkerkerker 1989, (Kumaran, 2001). To observe this effect, solutions of 2 mg/ml DOPG in a series of alkali chloride concentrations were subjected to freeze-thaw cycles to obtain thermodynamically stabilized vesicles. The hydrodynamic radius of the resulting vesicles is a non-trivial function of the ionic strength for all mono-valent salts used as can be seen in figure 4.2. The overall behavior of  $R$  as a function of ionic strength appears to be the same for all salts tested. At low ionic strength, up to approximately 10-50 mM, the vesicle radius decreases, while at higher salt concentrations  $R$  increases with ionic strength. When the vesicle radii in 200mM salt are compared, those produced in CsCl are the smallest. The size of the vesicles increases when they are made in LiCl, NaCl, RbCl, and KCl, respectively. Figure 4.3 shows that, when the vesicle radius is plotted as a function of the binding constants of the alkali cations to the phosphatidylglycerol headgroup (Cevc, 1990), this gives

### 4.3 Results

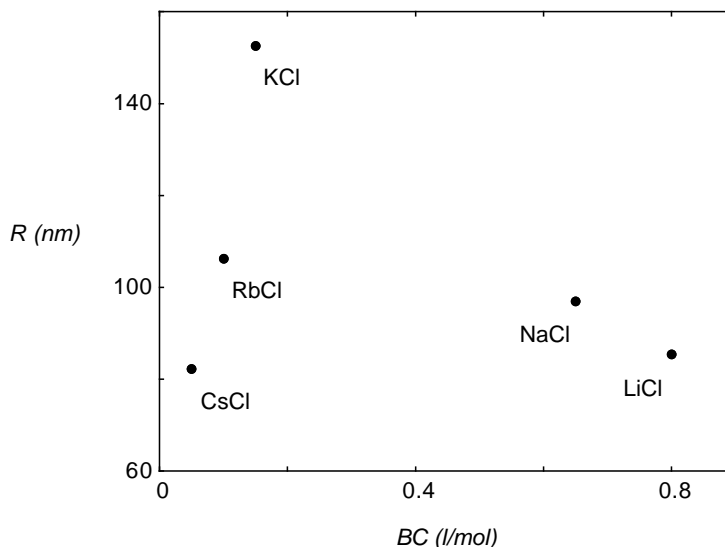


Figure 4.3: The radius of DOPG vesicles in 200mM alkali chloride solution as a function of the binding constant (BC) of the cation to the phospholipid headgroup. Binding constants were obtained from the literature (Cevc, 1990) (Appendix).

rise to a maximum in  $R$  for  $K^+$ .

Compared to mono-valent cations, divalent cations have higher hydration enthalpies and bind even stronger to DOPG (Appendix). To observe the effects of strong hydration and binding on the equilibrium radius, DOPG vesicles in  $MgCl_2$  and  $CaCl_2$  were subjected to freeze-thaw cycles. The effect of the divalent cations  $Mg^{2+}$  and  $Ca^{2+}$  on the equilibrium radius of DOPG vesicles is shown in figure 4.4. There are some striking differences between vesicles prepared in mono- and di-valent salts. The ionic strength regime in which vesicle radii could be determined was approximately ten times smaller in the presence of divalent salt. At concentrations above 2.5 mM  $CaCl_2$  and 5 mM  $MgCl_2$  vesicles started to aggregate. The size of the individual vesicles at high salt concentrations could therefore not be determined with dynamic light scattering. Another difference with the monovalent salts is that vesicles are much larger in the presence of divalent cations. The overall behavior of the vesicle radius in mono- and di-valent salt as a function of the salt concentration is comparable. However, the initial decrease in size at low ionic strength happens over a much smaller salt concentration range in  $MgCl_2$  and  $CaCl_2$  and the increase with salt concentration at higher ionic strength is much faster in the presence of divalent cations.

#### 4.3.2 Calculations

The working hypothesis is that the radius of the entropically stabilized vesicles is controlled by  $k_c$ . To determine what the effects of cation hydration and

## Effect of cations on vesicle stability

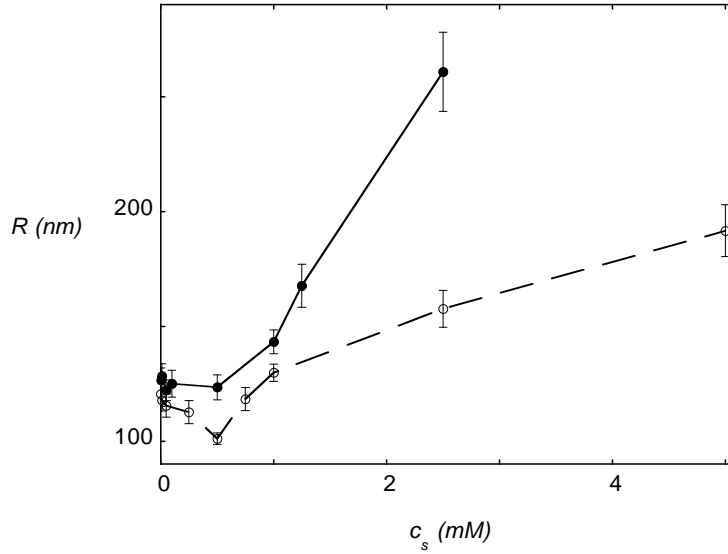


Figure 4.4: The effect of the  $MgCl_2$  (○) and  $CaCl_2$  (●) concentration on the equilibrium radius of DOPG vesicles, as obtained after 15 freeze-thaw cycles in salt solution.

binding on  $k_c$  are,  $k_c$  was determined from SCF calculations for cylindrically shaped vesicles ( $K = 0$ ). The general behavior of  $k_c$  as a function of ionic strength was approximately the same for all parameter sets tested. At low ionic strength  $k_c$  was observed to decrease whereas at high ionic strength  $k_c$  increased with the volume fraction of salt in the system. The effects of cation hydration and binding on  $k_c$  were first studied separately to obtain a better understanding.

Cation hydration was varied by changing  $\chi_{\text{cation-W}}$  while keeping  $\chi_{\text{anion-W}}$  constant at  $-2$ . In these calculations the cations were assumed not to bind specifically to the anionic headgroup;  $\chi_{\text{cation-X}} = 0$ . The results are comparable to those found earlier for changing anion hydration (Chapter 2). At all ionic strengths tested the more negative values for  $\chi_{\text{cation-W}}$  gave rise to the highest values for  $k_c$  (Fig. 4.5).

The influence of the binding of cations to the lipid headgroup on  $k_c$  is more complex. Cation binding was mimicked by choosing a negative  $\chi$ -parameter for the interaction between the cations and the segments X in the model lipid.

Due to the low density of X segments in the bilayer surface the values that have to be chosen for  $\chi_{\text{cation-X}}$  are rather high, before some effect is observed. This is a natural artefact of the (Bragg-Williams) mean-field approximation; in figure 4.6 we show the typical result. At low and intermediate salt concentrations, strong binding leads to decreased values of  $k_c$ . At high ionic strength the  $k_c$  curves belonging to different values of  $\chi_{\text{cation-X}}$  can cross and the behavior of  $k_c$  with  $\chi_{\text{cation-X}}$  becomes more complicated.

The results of varying  $\chi_{\text{cation-W}}$  and  $\chi_{\text{cation-X}}$  simultaneously can be seen in

### 4.3 Results

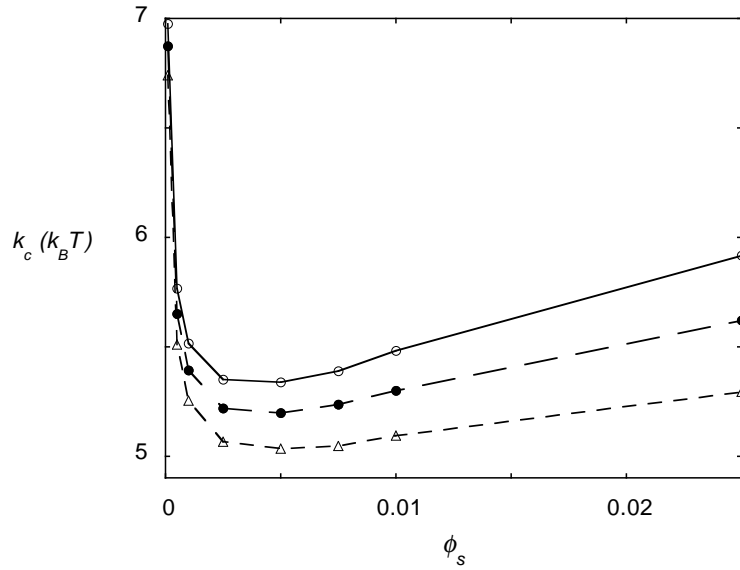


Figure 4.5: The mean bending modulus as a function of the ionic strength. Cation hydration has a profound influence on the mean bending modulus  $k_c$  predicted by SCF theory. Data are shown for  $\chi_{\text{cation-W}} = -3$  ( $\circ$ ),  $\chi_{\text{cation-W}} = -2$  ( $\bullet$ ),  $\chi_{\text{cation-W}} = -1$  ( $\Delta$ ),  $\chi_{\text{anion-W}}$  was kept constant at  $-2$ .

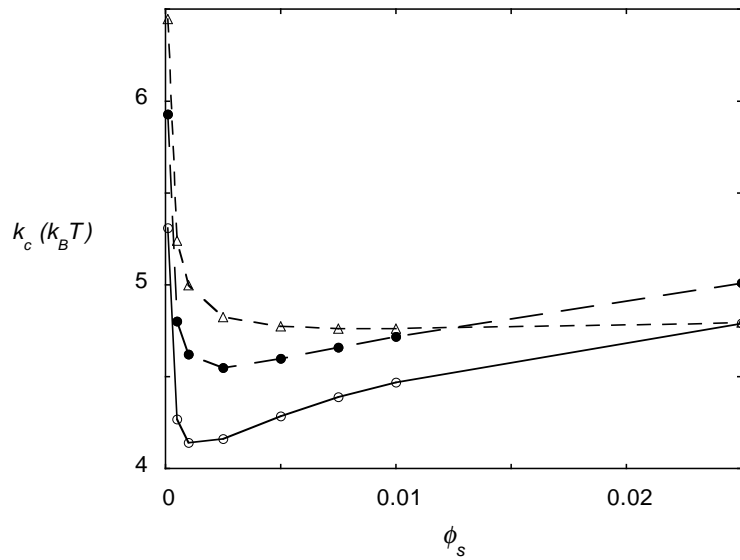


Figure 4.6: SCF predictions for the effect of the binding of cations to the segments  $X$  in the lipid headgroup on the mean bending modulus  $k_c$  of a charged lipid bilayer. Data is shown for  $\chi_{\text{cation-X}} = -5$  ( $\circ$ ),  $\chi_{\text{cation-X}} = -15$  ( $\bullet$ ),  $\chi_{\text{cation-X}} = -25$  ( $\Delta$ ).

## Effect of cations on vesicle stability

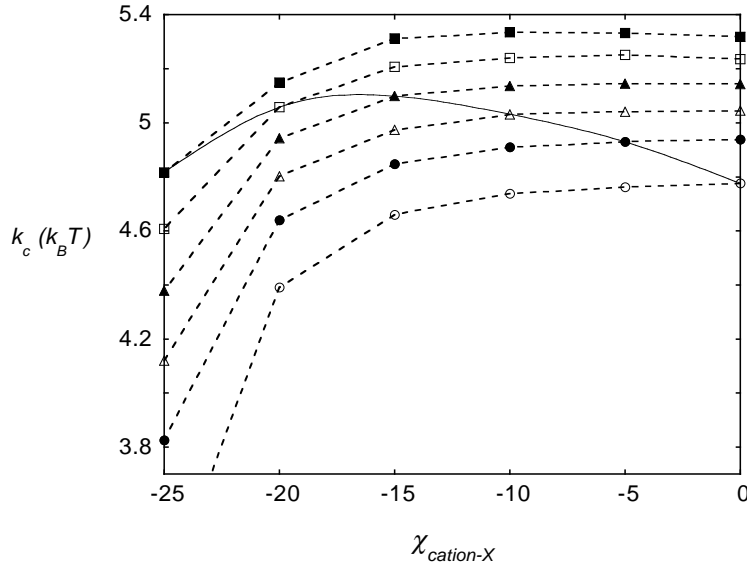


Figure 4.7: SCF predictions for the mean bending modulus  $k_c$  as a function  $\chi_{\text{cation-X}}$ . Data are shown for  $\chi_{\text{cation-W}} = 0$  ( $\circ$ ),  $\chi_{\text{cation-W}} = -0.5$  ( $\bullet$ ),  $\chi_{\text{cation-W}} = -1$  ( $\triangle$ ),  $\chi_{\text{cation-W}} = -1.5$  ( $\blacktriangle$ ),  $\chi_{\text{cation-W}} = -2$  ( $\square$ ),  $\chi_{\text{cation-W}} = -2.5$  ( $\blacksquare$ ). The solid line exemplifies the expected behavior of realistic cations.

figure 4.7. In this figure we present predictions for the overall mean bending modulus  $k_c$  for several values of degrees of cation hydration ( $\chi_{\text{cation-W}}$ ) as a function of the specific binding of the cation on the lipid headgroup ( $\chi_{\text{cation-X}}$ ). Stronger binding of ions to the lipid headgroup, and thus more negative values of  $\chi_{\text{cation-X}}$ , leads to a decrease in  $k_c$  for all  $\chi_{\text{cation-W}}$  values tested. Secondly, the more negative values of  $\chi_{\text{cation-W}}$  give rise to higher values of  $k_c$ .

Table 1 (Appendix) shows that, in reality, the most strongly hydrated ions, also have the largest binding constants and vice versa. As a result cation hydration and cation binding have antagonistic effects on  $k_c$  of the lipid membrane. The solid line in figure 4.7 exemplifies the expected behavior of real cations; it combines high  $\chi_{\text{cation-W}}$  and  $\chi_{\text{cation-X}}$  values with intermediate  $\chi_{\text{cation-W}}$  and  $\chi_{\text{cation-X}}$  and  $\chi_{\text{cation-W}}$  and  $\chi_{\text{cation-X}}$  values. When the hydration and binding properties of real ions are considered, the combination of high  $\chi_{\text{cation-X}}$  and low  $\chi_{\text{cation-W}}$  with low  $\chi_{\text{cation-X}}$  gives rise to a maximum in  $k_c$  as a function of  $\chi_{\text{cation-X}}$  (Fig. 4.7). The exact position of the maximum is difficult to predict, as it is difficult to determine the values of the  $\chi$ -parameters for realistic cations.

## 4.4 Discussion

The correlation between the measured radius  $R$  and predicted  $k_c$  as a function of the ionic strength has been discussed before (Chapter 2). For all salts tested

## 4.4 Discussion

here, the behavior of  $R$  with salt concentration can also be divided in a low and a high ionic strength regime. At low ionic strength the vesicle size decreases, whereas at high ionic strength a slight increase in  $R$  is observed with increasing salt concentration. Similar behavior is seen in all parameter settings for  $k_c$  as a function of the ionic strength.

The initial decrease in  $k_c$  and therefore in  $R$  at low salt concentration is mainly due to a decrease of the electric double layer thickness. As mentioned above, charged bilayers in salt solutions are surrounded by an electric double layer. This double layer has to bend with the lipid bilayer and it therefore increases  $k_c$ . Upon addition of more salt the thickness of the electric double layer decreases and therefore  $k_c$  decreases. This decrease is partly counteracted by a closer lipid packing when the headgroup charges get screened by counter ions. Closer packing of the lipids leads to thicker and stiffer membranes which results in an increased  $k_c$ . The observed changes in  $k_c$  with ionic strength are therefore not comparable to theoretical predictions on the relation between  $k_c^{el}$  and salt concentration (Winterhalter and Helfrich, 1988), (Lekkerkerker, 1989). In addition to the concentration, the valency of the counter ion has a large influence on  $\kappa^{-1}$ . Divalent counterions will cause the  $\kappa^{-1}$  to drop faster compared to monovalent ones. This is in agreement with the observation that the equilibrium vesicle radius, which is related to  $k_c$ , drops over a much smaller concentration range in the presence of  $\text{MgCl}_2$  or  $\text{CaCl}_2$  than with the alkali chlorides.

At a certain ionic strength, the effect of a decrease in electric double layer thickness becomes negligible compared to the increase in lipid bilayer thickness. This increase in the thickness of the lipid bilayer is not only caused by the effects of charge screening; difference in hydration between the cations also appear to play a role. Strong hydration and therefore more negative values of  $\chi_{\text{cation-W}}$  gives rise to higher values of  $k_c$  and, thus, larger vesicles. This observation is supported by a study on the effects of a series of anions on  $k_c$  and  $R$  of DOPG vesicles. In the presence of the more strongly hydrated  $\text{Cl}^-$  ions the freeze-thaw method gave bigger vesicles compared to the radii found in the presence of  $\text{Br}^-$  and  $\text{I}^-$  (Chapter 2). Calculations showed that when hydration is taken into account the bilayers become thicker with increasing anion hydration. It is however not yet clear whether the ions directly dehydrate the membrane, or if the effect is due to differences in solubility of the hydrated ions in the apolar part of the bilayer. The increase in the gel to liquid-crystalline phase transition temperature observed for the zwitterionic phospholipid dipalmitoylphosphatidylcholine in the presence of alkali chlorides (Koynova and Caffrey, 1998) supports the idea that the ions dehydrate the bilayer membrane and cause the lipids to pack into thicker membranes.

At very high ionic strength the vesicle radius passes through a maximum (Fig. 4.2). This maximum is probably related to a maximum in the bilayer thickness, and comparable to the maximum in the equilibrium thickness found for free nonionic film as a function of the salt concentration (Boomgaard van den and Lyklema, 1989). Although we do not understand this behavior it is



## Effect of cations on vesicle stability

probably related to the structure of the salt solution at high ionic strength.

The data on alkali chlorides presented here cannot be explained by ion hydration. In contrast to the data on equilibrium vesicles in the presence of different anions, the radii of DOPG vesicles in the presence of the alkali cations, do not increase with their hydration enthalpies ( $\text{Li}^+ > \text{Na}^+ > \text{K}^+ > \text{Rb}^+ > \text{Cs}^+$ ). Specific binding of the cations to the anionic DOPG headgroup is probably responsible for this anomaly. Unlike cations, anions are not expected to bind to similarly charged membranes. This makes their behavior apparently easier to interpret.

By adsorbing onto the negatively charged membrane, cations change the surface charge. The surface charge of phosphatidylglycerol vesicles is therefore expected to decrease in the order,  $\text{Cs}^+ > \text{Rb}^+ > \text{K}^+ > \text{Na}^+ > \text{Li}^+$ . Measurements on the electrophoretic mobility of extruded vesicles in 100 mM salt support this assumption (Fig. 4.1).  $k_c^{el}$  is predicted to scale with the surface charge density as  $k_c^{el} \propto \sigma^2$  (Winterhalter and Helfrich, 1988), (Lekkerkerker, 1989), (Kumaran, 2001); cation binding is therefore expected to decrease  $k_c$ . These analytical, theoretical predictions do however not account for changes in lipid packing which also change  $k_c$ . When the binding of ions to the lipid headgroup is included in the SCF calculations, which do allow for changes in lipid packing,  $k_c$  is still observed to decrease with increasing  $\chi_{\text{cation-X}}$  (Fig. 4.6). The decrease in  $k_c$  at low ionic strength is the largest for the cation that binds most strongly to the lipid headgroups, i.e. with the most negative  $\chi_{\text{cation-X}}$ . This means that cations do not only lower  $k_c$  by decreasing the double layer thickness, but also by lowering  $\sigma$  directly.

So far, the effects of cation hydration and binding were considered separately. Strong hydration tends to increase  $k_c$ , whereas strong binding leads to a decrease in  $k_c$ . However, the most strongly hydrated alkali cation  $\text{Li}^+$  also has the highest affinity for the DOPG headgroup. Weakly hydrated ions like  $\text{Cs}^+$ , on the other hand, bind only weakly to the PG headgroup. The opposing effects of ion hydration and cation binding are probably responsible for the observed dependence of  $R$  on the presence of the alkali cations. Indeed calculations in which  $\chi_{\text{anion-W}}$  and  $\chi_{\text{anion-X}}$  data are combined show that when combinations of low  $\chi_{\text{anion-W}}$  and  $\chi_{\text{anion-X}}$ , intermediate  $\chi_{\text{anion-W}}$  and  $\chi_{\text{anion-X}}$ , and high  $\chi_{\text{anion-W}}$  and  $\chi_{\text{anion-X}}$  values are compared, negatively charged bilayers have the highest  $k_c$  in the presence of a cation with intermediate binding and hydration properties (Fig. 4.7). This is in agreement with the finding that equilibrium DOPG vesicles are the largest in the presence of KCl.

Although the calculations on  $k_c$  are in good qualitative agreement with the experimental data on the effects of monovalent cations on the radii of entropically stabilized DOPG vesicles, they cannot fully account for the observed effects of the divalent cations,  $\text{Mg}^{2+}$  and  $\text{Ca}^{2+}$ . The decrease in double layer thickness is faster in the presence of divalent salts (equation 4.2) as can be observed from a comparison of figures 4.2 and 4.4. However, DOPG vesicles do not reach smaller radii in the presence of the strongly binding and strongly hydrated divalent cations compared to the monovalent ones (table 1), as would

## 4.5 Conclusions

be expected from the calculations presented in figure 4.7. A possible reason for this disagreement might be the aggregation of DOPG vesicles. Although all samples were inspected for visible aggregation, the formation of smaller aggregates that could not be distinguished by eye cannot be excluded. The concentration range, over which stable vesicles close to their equilibrium radius can be produced, might therefore be smaller than presented in figure 4.4.

## 4.5 Conclusions

When a DOPG suspension is subjected to freeze-thaw cycles in the presence of alkali chlorides, the equilibrium radii of the resulting vesicles increases in the order  $\text{CsCl} < \text{LiCl} < \text{NaCl} < \text{RbCl} < \text{KCl}$  over a large concentration range. This size increase is due to the combined effects of (cat)ion hydration and specific binding to the DOPG headgroup. SCF calculations showed that  $k_c$  increases with cation hydration. The alkali cations are therefore predicted to increase  $k_c$  and therefore  $R$  in the order  $\text{Li}^+$ ,  $\text{Na}^+$ ,  $\text{K}^+$ ,  $\text{Rb}^+$ ,  $\text{Cs}^+$ . However cations do also bind to the negatively charged phospholipid headgroup. According to our calculations this decreases  $k_c$  over a large concentration range. The most strongly binding cation should give rise to the smallest vesicles and  $R$  should decrease in the order  $\text{Li}^+$ ,  $\text{Na}^+$ ,  $\text{K}^+$ ,  $\text{Rb}^+$ ,  $\text{Cs}^+$ . A combination of these contrasting effects gives a maximum in  $k_c$  in the SCF calculations on charged lipid bilayers. This maximum is also found for DOPG vesicles in alkali chlorides. The maximum in  $R$  is found for  $\text{K}^+$  which has an intermediate hydration and PG-binding constant when compared with the other alkali cations.

## 4.6 Appendix

	$R$ (nm)	$\mu$ ( $10^{-6}\text{m}^2/\text{Vs}$ )	BC (l/mol)	$\Delta H_{hydr}$ ( $10^5\text{J/mol}$ )
$\text{Li}^+$	$61.74 \pm 1.76$	$-5.016 \pm 0.06$	0.8	-5.00
$\text{Na}^+$	$60.80 \pm 1.80$	$-5.353 \pm 0.08$	0.65	-3.90
$\text{K}^+$	$61.58 \pm 1.77$	$-6.020 \pm 0.04$	0.15	-3.10
$\text{Rb}^+$	$62.21 \pm 1.82$	$-6.137 \pm 0.06$	0.1	-2.80
$\text{Cs}^+$	$64.01 \pm 1.72$	$-6.273 \pm 0.04$	0.05	-2.50
$\text{Mg}^{2+}$			12	-18.9
$\text{Ca}^{2+}$			17	-15.6

Table 4.1: The measured radius  $R$  and the electrophoretic mobility  $\mu$  of extruded vesicles in 100 mM alkali chloride solution. Binding constants (BC) of the metal cations to the  $\text{PG}^-$  headgroup are obtained from Cevc (1990), the hydration enthalpies  $\Delta H_{hydr}$  are tabulated in (Verkerk et al., 1986).

## 4.6 Appendix

## Chapter 5

# Thermodynamic stability of dioleoylphosphatidylcholine and dioleoylphosphatidylglycerol vesicles: lipid- and surfactant-lipid mixtures

### Abstract

Vesicles made of more than one amphiphile can in principle be stabilized by a spontaneous curvature that selects a particular radius. This spontaneous curvature is due to non ideal lateral interactions that can cause the inner and outer monolayers of the bilayer to have considerably different compositions. But in mixtures of two bilayer-forming phospholipids, with comparable tail length, this is not expected. If stable vesicles are formed from these mixtures, they are most likely stabilized by entropy. It can be argued that the size of entropically stabilized vesicles is related to the (bare) mean bending modulus,  $k_c$ , of the bilayer. The  $k_c$  of bilayers consisting of more than one amphiphile decreases towards the equimolar composition. Vesicles of mixtures of the bilayer forming phospholipids dioleoylphosphatidylglycerol (DOPG) and dioleoylphosphatidylcholine (DOPC), and vesicles of the cationic surfactant cetyltrimethylammoniumbromide (CTAB) and the anionic phospholipid DOPG, indeed have a smaller equilibrium radius compared to the pure component vesicles. Self-consistent-field calculations show that this size decrease can be attributed to changes in  $k_c$  that correlate with changes in surface charge density. These calculations also show that bilayers with a spontaneous curvature can only be obtained when the constituent amphiphiles show an inclination for lateral phase separation.

## 5.1 Introduction

### 5.1 Introduction

For a long period of time vesicles were not believed to represent an equilibrium structure of surfactants in solution, but in the past decade several groups have reported on the spontaneous formation of vesicles. These spontaneous vesicles are often believed to be in thermodynamic equilibrium. It has been reported that mixtures of anionic and cationic surfactants, in particular, seem to be good candidates for spontaneously formed equilibrium vesicles (Jung et al., 2001). It is however not always clear how these vesicles are stabilized against the formation of multilamellar sheets.

There are in principle two ways for vesicles to be in thermodynamic equilibrium; they can either be stabilized by entropy or they can have a non zero spontaneous curvature. Both ways of stabilization give rise to vesicles of a particular size. Bilayers composed of one type of surfactant species are generally not believed to have a spontaneous curvature, as the two monolayers are similarly curved. Vesicles composed of one surfactant species can therefore only be stabilized by entropy. But in (cationic-anionic) surfactant mixtures complexation and non ideal behavior may allow for the formation of bilayers of which the two monolayers have a large difference in surfactant composition. This composition difference can in principle result in monolayers with opposite spontaneous curvature (Safran et al., 1990), (Safran et al., 1991). Others argue, however, that asymmetry between the inner and outer layers never plays a role in vesicles that are large compared to the bilayer thickness (Bergström et al., 1999) and that spontaneous vesicles are therefore usually entropically stabilized.

In the case of phospholipid bilayers entropic stabilization of vesicles is believed not to be possible due to the high value of the bilayers' mean bending modulus  $k_c$  (Lasic, 1990), (Lasic et al., 2001). In the literature, phospholipid bilayers are reported to have a  $k_c$  that is in the order of 10-40  $k_B T$  (Seifert and Lipowsky, 1995), (Meleard et al., 1998), (Rawicz et al., 2000). It is however not only  $k_c$  that determines how much energy is needed to curve a bilayer into a closed vesicle. The curvature energy,  $E_{ves}$ , of a spherical vesicle without a spontaneous curvature is equal to

$$E_{ves} = 4\pi(2k_c + \bar{k}) \quad (5.1)$$

In this equation  $\bar{k}$  is the Gaussian bending modulus. Although the value of  $k_c$  is positive and probably rather high for phospholipid vesicles, the sign of  $\bar{k}$  can be either positive or negative, but is usually assumed to be negative for bilayer membranes. This means that, in spite of the high values measured for  $k_c$ , entropic stabilization of phospholipid vesicles is still possible when  $k_c$  and  $-\bar{k}$  are in the same order of magnitude.

For charged phospholipid bilayers in salt solution,  $k_c$  and  $-\bar{k}$  are expected to be of the same order of magnitude. Both DOPG and DOPC form entropically stabilized vesicles over a large range of phospholipid and salt concentrations (Chapter 2). The curvature energy of the bilayer is apparently low enough in

## Lipid- and surfactant-lipid mixtures

these systems to make entropic stabilization of vesicles possible. The average radius of these vesicles scales as  $R \propto (c_{lipid})^{0.15 \pm 0.1}$  which points at stabilization by translational entropy and undulations (Simons and Cates, 1992), (Herve et al., 1993). When vesicles are stabilized by entropy their radius is determined by the persistence length of the bilayer, and therefore by  $k_c$ . The entropy of mixing will favor a population of small vesicles, but the minimum size of the vesicles is set by the persistence length of the bilayer.

Compared to bilayers of a single phospholipid species, bilayers of mixed composition are expected to have a decreased  $k_c$ . Arguments based on mixing entropy give rise to the assumption that  $k_c$  will decrease towards the equimolar composition. Entropically stabilized vesicles of phospholipid mixtures are therefore, in the absence of a spontaneous curvature, expected to be smaller.

Upon mixing of two differently charged surfactants, the surface charge density changes, and this also has profound effects on  $k_c$ . For low charge densities,  $k_c$  is predicted to scale with the surface charge density  $\sigma$  (Winterhalter and Helfrich, 1988), (Lekkerkerker, 1989), as  $k_c \propto \sigma^2$ . The combined effects of lipid mixing and changes in charge density are expected to be responsible for the changes in vesicle radius.

Here, the radius of mixed vesicles, composed of the anionic phospholipid DOPG and either the zwitterionic phospholipid DOPC or the cationic surfactant CTAB, obtained with the freeze-thaw method will be presented. The results will be discussed using SCF calculations on the thermodynamic and mechanical properties of mixed bilayers. The absence of a spontaneous curvature and similarities in behavior of the measured  $R$ , and the calculated  $k_c$  as a function of composition, indicate that the mixed vesicles are stabilized by entropy. Bilayers with a spontaneous curvature are only found when lateral phase separation is induced by strong repulsion between the headgroups or the tails of its constituent amphiphiles

## 5.2 Materials and Methods

### 5.2.1 Experiments

The anionic phospholipid dioleoylphosphatidylglycerol (DOPG) was purchased as a sodium salt, the zwitterionic phospholipid dioleoylphosphatidylcholine (DOPC) as a chloroform solution, from Avanti Polar lipids. The cationic surfactant cetyltrimethylammoniumbromide (CTAB) was obtained from BDH chemicals Ltd. Both phospholipids and the surfactant were used without any further purification. Analytical grade sodium bromide (NaBr) was bought from J.T. Baker Chemicals.

Vesicles were produced by the freeze-thaw method from mixtures of DOPG and DOPC, and from mixtures of DOPG and CTAB. Mixtures of DOPG and DOPC were obtained dissolving the phospholipids together in chloroform. The chloroform was removed by evaporation under a stream of nitrogen; the last

## 5.2 Materials and Methods

traces of solvent were removed from the lipid film under vacuum. Subsequently the dry lipid film was rehydrated with a NaBr solution of the desired ionic strength to a concentration of 2 mg lipid/ml. DOPG-CTAB mixtures were prepared by mixing stock solutions of the same ionic strength in the desired ratio. A 2 mg/ml DOPG solution was mixed with a equimolar CTAB solution. A problem in dealing with phospholipids is the fast oxidation and hydrolysis, all samples containing either DOPG or DOPC were therefore studied within four days after vesicle production.

Multilayered phospholipid vesicles are known to fragment into small vesicles when the solution is subjected to successive cycles of freezing and thawing (MacDonald et al., 1994). The method of freezing and thawing probably leads to fast equilibration, in spite of the low solubility of phospholipids (Chapter 2). Therefore, all mixtures were given a freeze-thaw treatment. 1 ml of a 2 mg/ml surfactant solution was immersed in liquid nitrogen until it was completely frozen. The samples were thawed in a water bath at approximately 313 K. During thawing the solutions were regularly vortexed. All samples were by eye checked for the occurrence of phase separation. The size of the vesicles or micelles in the solution was determined using dynamic light scattering.

The samples were analyzed using an ALV light-scattering apparatus with an argon ion laser as light source. The data was collected at a scattering angle of 90 degrees at a wavelength of 514 nm. During the measurements the temperature was kept at 293 K for the DOPG-DOPC mixtures. The size of the DOPG-CTAB vesicles was determined at 303 K, which is above the Krafft temperature of CTAB for all NaBr concentrations used. The hydrodynamic vesicle radius was obtained from a cumulant analysis of the intensity autocorrelation function.

### 5.2.2 Self-consistent-field calculations

Surfactants can self assemble in association colloids, such as micelles, vesicles, and bilayers. The self-consistent-field (SCF) theory can be used to evaluate the distribution of surfactant molecules in these association colloids. From the distribution functions it is possible to obtain the partition function and subsequently the thermodynamical and mechanical parameters of a lipid bilayer. Recently, Oversteegen showed how the bending moduli,  $k_c$  and  $\bar{k}$ , of a bilayer membrane can be determined unambiguously from SCF calculations (Oversteegen and Leermakers, 2000). Both  $k_c$  and  $\bar{k}$  from the Helfrich equation can be obtained by evaluating the curvature dependence of the interfacial tension,  $\gamma$ .

$$\gamma = \gamma_0 + \frac{1}{2}k_c(J - J_0)^2 + \bar{k}K \quad (5.2)$$

in which  $J$  is the mean curvature ( $J = \frac{1}{R_1} + \frac{1}{R_2}$ ) and  $K$  is the Gaussian curvature ( $K = \frac{1}{R_1R_2}$ ).  $R_1$  and  $R_2$  are the two radii of curvature that locally characterize the bilayer membrane. The curvature of the bilayer can be varied by changing the amount of surfactant molecules in the system. For a given amount of surfactant the constrained equilibrium density profiles and hence



## Lipid- and surfactant-lipid mixtures

the interfacial tension can be calculated. The Helfrich constants follow from the interfacial tension of both a spherical and a cylindrical vesicle as a function of the vesicle radius. For a cylindrical interface  $K = 0$ ,  $J = \frac{1}{R}$  and  $A = 2\pi R h$ , (where  $h$  is the length of the cylinder), and equation 5.2 can be written as

$$\gamma A = -2\pi k_c J_0 + \pi k_c J \quad (5.3)$$

For a spherical interface  $J^2 = 4K = \frac{4}{R^2}$ , and  $A = 4\pi R^2$ , equation 5.2 reduces to

$$\gamma A = -8\pi k_c J_0 R + 4\pi (2k_c + \bar{k}) \quad (5.4)$$

By varying the total curvature  $J$ ,  $k_c$  can be obtained from calculations in the cylindrical geometry. This  $k_c$  can subsequently be used to obtain  $\bar{k}$  from the data on the spherical geometry. The existence of a spontaneous curvature  $J_0$ , can be checked by extrapolating the intercept of the  $\gamma A(J)$  data to  $\gamma A = 0$ . A non-zero abscission points to the existence of such a non-zero spontaneous curvature. Information on the stability of the bilayer can be obtained from the bending moduli. Stable bilayers are only found if the curvature energy of a spherical vesicle  $E_{ves}$  is positive, this means that  $2k_c + \bar{k} > 0$  (when  $J_0 = 0$ ).

In the SCF calculations DOPG like molecules were modeled as linear chains with segment sequence  $C_{18} X_2 C_2 X_2 C_{18}$ . The two  $C_{18}$  -groups are the hydrophobic tails, while the hydrophilic headgroup is represented by the segment sequence  $X_2 C_2 X_2$ , in which each X carries a charge of  $-\frac{1}{4}$  e. Water was modeled by a simple solvent monomer W. The ionic strength of the solution was determined by cat- and anions with the size of water molecules, and with valency +1 e and -1 e, respectively. Ion hydration was taken into account by the choice of the Flory-Huggins interaction parameters,  $\chi_{\text{cation-W}} = -2$  and  $\chi_{\text{anion-W}} = -1$ . The more negative value for the cation reflects its stronger hydrogen-bonding properties in comparison with the anion, that typically tends to destroy water structure. The surfactant headgroup was made water soluble by choosing  $\chi_{X-W} = -2$ . In all calculations the following dielectric constants were used  $\epsilon_C = 2$ ,  $\epsilon_X = \epsilon_{\text{cation}} = \epsilon_{\text{anion}} = 5$ ,  $\epsilon_W = 80$ .

Experiments were done on mixtures of the anionic phospholipid DOPG and the zwitterionic phospholipid DOPC. Although DOPC is zwitterionic, data on the electrophoretic mobility of DOPC vesicles show that it carries a net negative charge in NaBr solution (Tatulian, 1983), (Tatulian, 1987). The phase diagram of DOPC in NaBr suggests the same; in a range of intermediate ionic strength an electric double layer develops at the periphery of the bilayer (Chapter 3). In the calculations DOPC was simulated by placing a small charge on the headgroup. The total charge on the surfactant representing DOPC was  $-\frac{2}{5}$  e instead of -1 e; this corresponds to a charge of  $-\frac{1}{10}$  e per segment X. Because the DOPG and DOPC like lipids only differ in headgroup charge, the critical micelle concentrations are similar. Therefore the mixing ratio of the phospholipid like molecules is comparable to the lipid ratio in the bilayer.

More information on the mixing of an anionic phospholipid with a cationic surfactant was obtained by doing calculations on mixtures of the DOPG like

## 5.3 Results

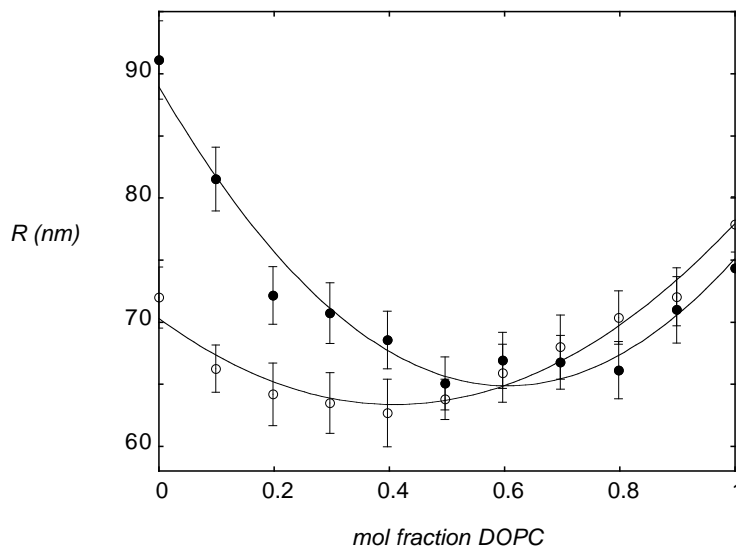


Figure 5.1: The radius of mixed DOPG-DOPC vesicles in 300 (●) and 50 (○) mM NaBr after 15 freeze-thaw cycles. The total lipid concentration during the freeze-thaw procedure was 2.5 mM.

molecule  $C_{18} X_2 C_2 X_2 C_{18}$  and a CTAB like molecule  $C_{15} Y_2 C_2 Y_2 C_2$ . The segment Y only differs from the segment X in its charge of +1 e instead of -1 e. For mixtures of a phospholipid and a surfactant the mixing ratios do not necessarily correspond to the ratio in the bilayer membrane. Therefore the exact amounts of lipid and surfactant in the membrane were always checked in the SCF calculations.

## 5.3 Results

### 5.3.1 Experiments

Thermodynamically stable vesicles can be produced by the freeze-thaw method from both DOPC and DOPG phospholipids (Chapter 2). When freeze-thawing is applied to mixtures of DOPG and DOPC a rather homodisperse population of stable vesicles is produced. The hydrodynamic radius of these mixed phospholipid vesicles is significantly lowered compared to the radii of vesicles made of a single phospholipid species. In 300 mM NaBr the absolute decrease in vesicle radius is as much as 25 nm compared to DOPG and 10 nm compared to DOPC vesicles (Fig. 5.1). This corresponds to a relative size decrease of 10-30%. The minimum in the radius does not occur at exactly equimolar composition. At high ionic strength pure DOPG vesicles are larger than DOPC vesicles and the minimum is shifted towards the side rich in DOPC. Whereas at low ionic strength DOPC vesicles are larger than DOPG and the minimum in  $R$  is on the DOPG rich side.

## Lipid- and surfactant-lipid mixtures

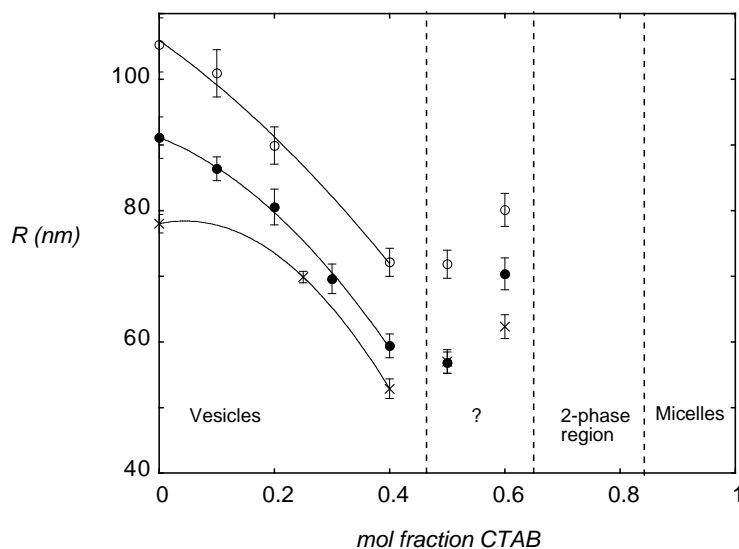


Figure 5.2: Radii of mixed DOPG-CTAB vesicles in 400 (○), 300 (●), and 200 (×) mM NaBr. The vesicles were prepared by the freeze-thaw method.

Applying the freeze-thaw method to mixtures of the anionic phospholipid DOPG and the cationic surfactant CTAB also results in vesicles that are, over the whole ionic strength range investigated, smaller than vesicles made of pure DOPG (Fig. 5.2). Higher salt concentrations resulted in larger vesicles over the composition range. In 300 mM NaBr the observed decrease in vesicle radius was as much as 30 nm or 30%. However, vesicles are only formed at the DOPG rich side of the composition axis. At high mole fractions of CTAB rod like micelles appear. The wormlike CTAB micelles increase in length with the percentage of DOPG in the aggregate and with increasing ionic strength. In the transition region between the micellar and vesicle phases the system phase separates into two phases. The exact nature of the aggregates in this region could not be determined with DLS. It is also not clear from DLS measurements whether the structures that appear at 50 and 60 mol% CTAB are vesicles.

### 5.3.2 Calculations

The SCF calculations show that mixing of the DOPG and DOPC like lipids never results in a non-zero spontaneous curvature. In all cases the surface tension  $\gamma(J, K)$  followed equation 5.3, or 5.4 with  $J_0 = 0$ . Figure 5.3 gives a typical example of a segment density profile through a cross section of a mixed vesicle bilayer. It shows that the profiles of the curved lipid bilayer are slightly asymmetric. The total headgroup concentration, for instance, is higher at the inner surface than at the outer surface of the bilayer, while the maximum in tail density is closer to the outside. The DOPG and DOPC like lipids are also asymmetrically distributed over the bilayer. The DOPC like lipid is more concentrated on the inside monolayer, and the highly charged

### 5.3 Results

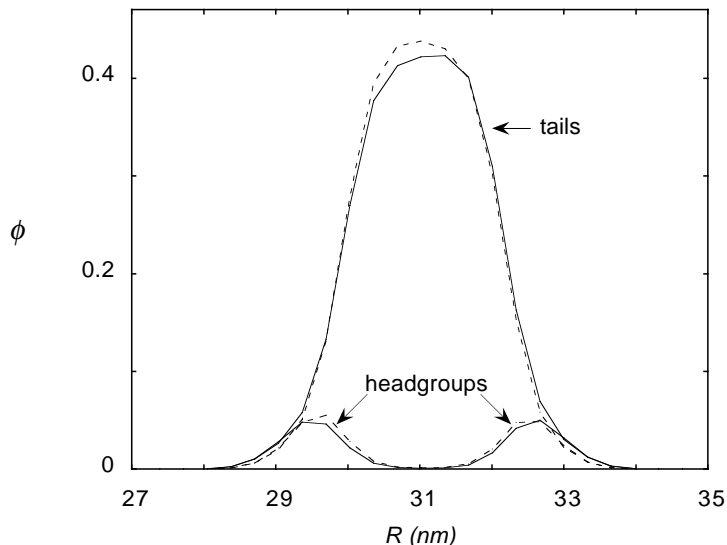


Figure 5.3: Volume fraction profile of a lipid bilayer consisting for 50% of a lipid with charge  $-1 e$  (solid line) and 50% of a lipid with charge  $-\frac{2}{5} e$  (dashed line). The calculations were performed at volume fractions of salt,  $\phi_s = 0.01$ .

DOPG like lipid has higher density on the outside monolayer of the vesicle. But this asymmetry never leads to a spontaneous curvature,  $J_0 \neq 0$ . Mixing mainly results in bilayers with a decreased  $k_c$  (Fig. 5.4). The position of minimum in  $k_c$  depended on the ionic strength and did not always occur at equimolar composition. At low salt concentrations the minimum in  $k_c$  was shifted towards the highly charged DOPG like lipid and with increasing ionic strength the minimum shifted towards lipid carrying less charge. The observed changes in  $k_c$  with composition are expected to be the result of lipid mixing in the bilayer, and changes in surface charge density.

To obtain more information on the effect of charge density on  $k_c$ , the charge on the headgroup was decreased from  $-1 e$  to  $-\frac{2}{5} e$  in steps of  $-\frac{1}{10} e$ . The results of these calculations are presented in figure 5.5. Instead of the expected decrease of  $k_c(\phi_s)$  (Winterhalter and Helfrich, 1988), (Lekkerkerker, 1989), a maximum in  $k_c$  versus headgroup charge was observed. At low ionic strength the maximum occurred at high surface charge, but with increasing ionic strength the maximum could be found at lower surface charges. The numerical data contain a little numerical noise, due to the fact that the so-called lattice artefacts are very hard to eliminate completely. This has some influence on the fitting of  $k_c$  from the numerical data.

The difference between the two calculated  $k_c$  curves (Fig. 5.4 and Fig. 5.5.) is expected to be related to mixing of lipids within the bilayer. Subtraction of the values for  $k_c$  at equal average surfactant charge, results in a curve with a minimum at equimolar composition (Fig. 5.6). The depth of this minimum decreases with increasing ionic strength. When the charges are completely

## Lipid- and surfactant-lipid mixtures

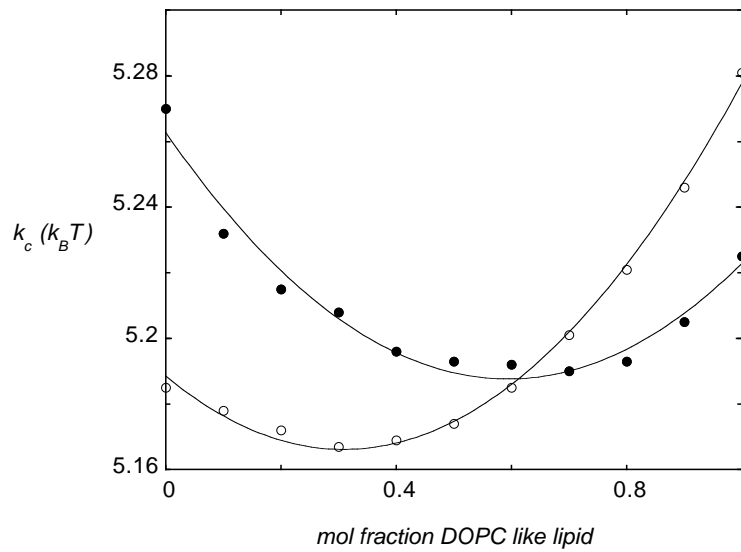


Figure 5.4: The mean bending moduli  $k_c$  of mixed lipid bilayers as a function of composition. SCF calculations were performed at volume fractions of salt,  $\phi_s = 0.005$  ( $\circ$ ), and  $\phi_s = 0.01$  ( $\bullet$ ). The charge on the DOPG like lipid was  $-1$  e, the DOPC like lipid carries a charge of  $-\frac{2}{5}$  e.

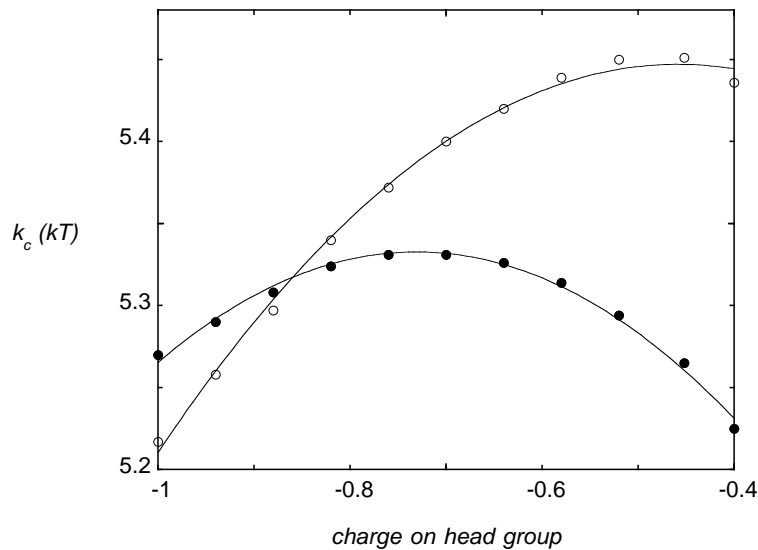


Figure 5.5:  $k_c$  of charged  $C_{18} X_2 C_2 X_2 C_{18}$  bilayers at volume fractions of salt,  $\phi_s = 0.0025$  ( $\circ$ ) and  $\phi_s = 0.01$  ( $\bullet$ ). The charge on the headgroup was varied between  $-1$  e and  $-\frac{2}{5}$  e.

### 5.3 Results

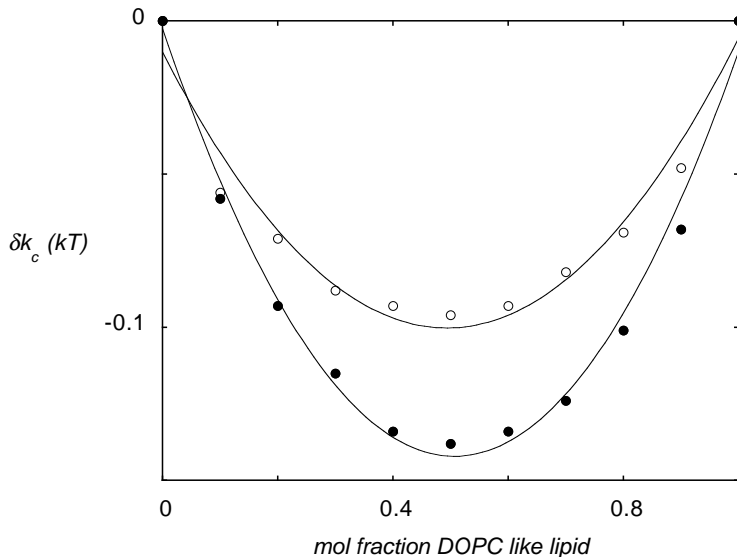


Figure 5.6: The effect of lipid mixing on  $k_c$  at volume fractions of salt,  $\phi_s = 0.01$  (●) and  $\phi_s = 0.025$  (○). The curves were obtained by subtraction of the  $k_c$  data on  $C_{18} X_2 C_2 X_2 C_{18}$  as a function of headgroup charge from the  $k_c$  data on mixing of two differently charged lipids.

screened, the molecules are in effect the same, and therefore mixing of the two differently charged lipids equals mixing of lipids of the same species.

To test whether mixtures of an anionic phospholipid and a cationic surfactant with comparable tail length resulted in vesicles with a spontaneous curvature, SCF calculations were performed on a mixture of a negatively charged  $C_{18} X_2 C_2 X_2 C_{18}$  lipid and a positively charged surfactant,  $C_{15} Y_2 C_2 Y_2 C_2$  in a salt solution. For the surfactant, the hydrophobic tail was chosen to consist of fifteen segments because this resulted in the preferential formation of micelles. At longer tail lengths bilayers were often the aggregates with the lowest free energy. Vesicles made of the lipid-surfactant mixture were not found to have a spontaneous curvature, at any composition or ionic strength.

The curvature energy,  $E_{ves}$ , decreased with increasing surfactant content (Fig. 5.7). At mole fractions of surfactant higher than 0.5,  $E_{ves}$  became negative and micellar aggregates were preferred over bilayers. The volume fraction of surfactant at which the transition from bilayer to micelle occurred depended slightly on the ionic strength. The position of the transition could be altered by changing the length of the hydrophobic tail of the surfactant. Shorter tail lengths resulted in a shift of the transition to lower volume fractions of surfactant.

In the regime where bilayers were the preferred aggregate structure ( $E_{ves} > 0$ ), the mean bending modulus  $k_c$  decreased with increasing fractions of surfactant in the membrane (Fig. 5.8). Exactly how  $k_c$  varies with surfactant concentration, depends on the ionic strength. For a given bilayer composition,

## Lipid- and surfactant-lipid mixtures

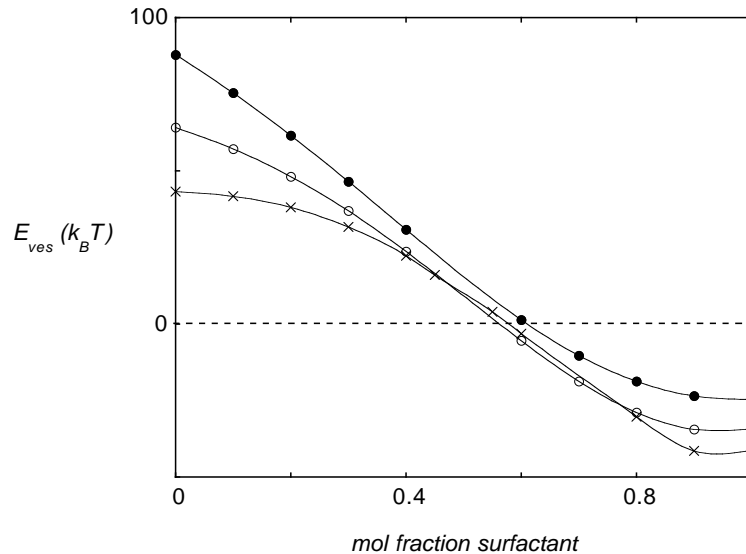


Figure 5.7: The curvature energy  $E_{ves} = 4\pi(2k_c + \bar{k})$  of a mixed bilayer of an anionic lipid and a cationic surfactant. When  $4\pi(2k_c + \bar{k}) < 0$  bilayers are no longer preferred, and micelles will form. Calculations were performed at volume fractions of salt,  $\phi_s = 0.05$  ( $\bullet$ ),  $\phi_s = 0.025$  ( $\circ$ ) and  $\phi_s = 0.01$  ( $\times$ ).

the higher ionic strengths always gave the higher values of  $k_c$ . Shorter surfactant tails gave similar results for both  $E_{ves}$  and  $k_c$ , but the shorter the tail the smaller the composition range in which bilayers were stable and the stronger the decrease in  $k_c$  with composition.

No evidence was found for the existence of a spontaneous curvature in our experiments on mixed bilayers. SCF calculations on a mixture of two oppositely charged surfactants never gave indications for a spontaneous curvature,  $J_0 \neq 0$ . All surfactant were always virtually equally distributed over the monolayers. A spontaneous curvature was only found for bilayers of which the two monolayers showed an inclination for demixing.

To obtain demixing of the apolar tails, a new lipid  $D_{18} X_2 D_2 X_2 D_{18}$  was introduced. This molecule was exactly the same as the  $C_{18} X_2 C_2 X_2 C_{18}$  lipid, but to get a bilayer in which the monolayers differed in composition,  $\chi_{D-C}$  was chosen to be 0.4 (Fig. 5.9). The choice of the  $\chi$ -parameter was rather critical. When  $\chi_{D-C} = 1$  complete demixing was observed, and the lipids preferred to form vesicles consisting only of either  $D_{18} X_2 D_2 X_2 D_{18}$  or  $C_{18} X_2 C_2 X_2 C_{18}$ . A much lower value for the  $\chi$ -parameter, e.g.  $\chi_{D-C} = 0.25$ , gave vesicles of which the monolayers contained both lipids, and no demixing was observed. Summarizing, the SCF calculations showed that vesicles only have a non-zero spontaneous curvature, if the amphiphiles demix. The resulting bilayer then consists of two monolayer sheaths that differ completely in composition. As the lipids have exactly the same headgroup size and tail length, the composition ratio between the amphiphiles determines the spontaneous curvature and

### 5.3 Results

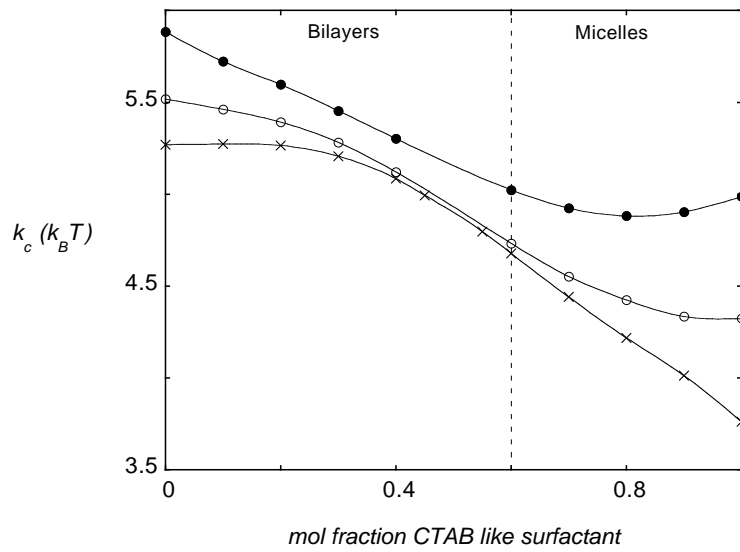


Figure 5.8: The mean bending modulus of a mixed bilayer of an anionic lipid and a cationic surfactant. Calculations were performed at volume fractions of salt,  $\phi_s = 0.05$  ( $\bullet$ ),  $\phi_s = 0.025$  ( $\circ$ ) and  $\phi_s = 0.01$  ( $\times$ ).

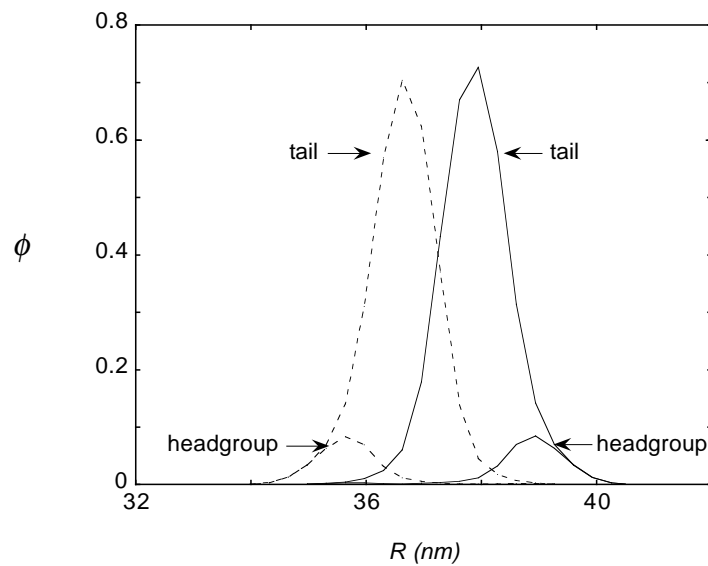


Figure 5.9: Volume fraction profile of a lipid bilayer consisting for 55% of the lipid  $C_{18} X_2 C_2 X_2 C_{18}$  (solid line) and 45% of  $D_{18} X_2 D_2 X_2 D_{18}$  (dashed line) at  $\phi_s = 0.01$  and  $\gamma A = 0$ . The monolayers are completely demixed at  $\chi_{D-C} = -0.4$ .



## Lipid- and surfactant-lipid mixtures

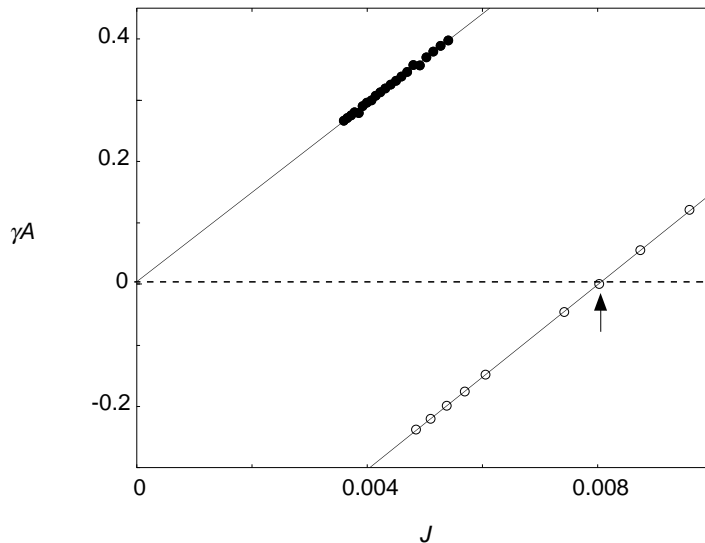


Figure 5.10: The dependence of  $\gamma A$  of the curvature  $J$  for bilayers containing  $C_{18} X_2 C_2 X_2 C_{18}$  and 50% ( $\bullet$ ) or 47.5% ( $\circ$ )  $D_{18} X_2 D_2 X_2 D_{18}$ . To obtain complete demixing of the lipid tails  $\chi_{D-C}$  was chosen to be 0.4,  $\phi_s = 0.01$ . The arrow indicates  $J_0$  for the 47.5%  $D_{18} X_2 D_2 X_2 D_{18}$  mixture.

therefore the vesicle size. From equation 5.3 it can be seen that, an equimolar mixture of  $D_{18} X_2 D_2 X_2 D_{18}$  and  $C_{18} X_2 C_2 X_2 C_{18}$  with  $\chi_{D-C} = 0.4$  has for reasons of symmetry a  $J_0 = 0$ . Away from equimolar composition vesicles have a  $J_0 \neq 0$ . For the example given in figure 5.10, a deviation from the equimolar ratio of 2.5% results in  $J_0 = 0.008$  or equivalently, a radius  $R_0 = 250$  lattice layers ( $\sim 75nm$ ). Because  $R_0$  is solely determined by the ratio in which the lipids are mixed, vesicles tend to become smaller with increasing amounts of either component. This size decrease is rather fast, and not far from equimolar composition the system again prefers to form vesicles consisting of either  $D_{18} X_2 D_2 X_2 D_{18}$  or  $C_{18} X_2 C_2 X_2 C_{18}$ . The composition range in which vesicles with a non-zero spontaneous curvature are found is very narrow.

## 5.4 Discussion

Previously we showed that there is a range of NaBr and phospholipid concentrations in which both DOPG and DOPC vesicles are thermodynamically stable (Chapter 2). Mixtures of DOPC and DOPG also form stable vesicles at intermediate salt and phospholipid concentrations. The radius of these mixed vesicles is slightly decreased compared to vesicles consisting of one phospholipid species only. SCF calculations on mixtures of phospholipid like surfactants show that the  $k_c$  of the mixed bilayer is also lowered. The similarity between the calculated  $k_c$  and measured  $R$  versus composition curves and the absence of a spontaneous curvature in the calculations, strongly suggests that these

## 5.4 Discussion

vesicles are stabilized by entropy. The translational entropy will prefer many small objects, but the minimum size of these objects will be set by the persistence length of the bilayer  $\xi_p$ . Therefore the vesicle radius  $R$  is expected to scale as  $R \propto \xi_p \propto e^{\frac{k_c}{k_B T}}$ . It is difficult to connect the measured values of  $R$  directly to the calculated values of  $k_c$ . The molecules in the calculations only mimic real phospholipid molecules, and various factors that influence the  $k_c$  are neglected. The present SCF calculations do neither correctly take into account the stiffness of the phospholipid tails, nor the collective modes of fluctuations in the bilayers. It is therefore expected that trends are more reliable than exact values.

Nevertheless, both the calculations and the experiments show that the minimum in the  $k_c$  and  $R$  versus composition curves occur off equimolar composition. Mixing several types of lipids in the bilayer leads to less dense bilayer packing and therefore to a decreased mean bending rigidity. This effect is expected to be the largest at equimolar composition. The observed changes in bending rigidity are apparently not only determined by effects of lipid mixing. Upon mixing of two phospholipids with a difference in headgroup charge, the total surface charge density also changes. This effect can be studied separately in the calculations by putting different charges on the headgroup. Charge density changes result in a maximum in  $k_c$  as a function of composition. In the literature  $k_c$  is predicted to scale with the surface charge density,  $\sigma$ , as  $k_c \propto \sigma^2$  (Winterhalter and Helfrich, 1988), (Lekkerkerker, 1989). This is not in agreement with the SCF calculations. The reason for this discrepancy can be found in the fact that changes in headgroup area with surface charge are implicitly excluded in the literature predictions. Uncharged surfactants pack into thicker membranes than charged ones, and this results in much stiffer membranes. As discussed before,  $k_c$  is determined by both changes in bilayer thickness and changes in the thickness of the diffuse double layer (Chapter 2). The maximum in the plots of  $k_c$  versus headgroup charge is caused by the opposite effects of electrostatics and membrane thickness. On the one hand  $k_c$  increases with increasing surface charge. On the other hand, the membrane becomes thinner with increasing headgroup repulsion and therefore  $k_c$  decreases with increasing surface charge.

If one evaluates the difference between figure 5.4 and figure 5.5, at equal surface charge and ionic strength, a curve is obtained with a minimum at the equimolar composition (Fig. 5.6). This curve represents the effect of surfactant mixing on  $k_c$ . The fact that the minimum is found at equimolar compositions for all ionic strengths supports the view that the sum effects of lipid mixing and changes in surface charge density completely determine the behavior of  $k_c$  and  $R$  with composition. Although it is often stated that  $k_c$  of surfactant films is dominated by the tails rather than by the heads of the constituent amphiphiles (Szleifer et al., 1988), (Lekkerkerker, 1989), both the SCF calculations and the experiments show that changes in the surface charge and headgroup area can result in measurable and significant changes in the radius of entropically

## Lipid- and surfactant-lipid mixtures

stabilized vesicles. Although the contribution of the surfactant headgroup to the mean bending modulus  $k_c$  is probably small compared to the contribution of the tails, it is certainly not negligible.

Two bilayer-forming phospholipids are not expected to give rise to vesicles that are stabilized by a spontaneous curvature term. This might be different for an oppositely charged micelle forming surfactant and a bilayer forming phospholipid. A mixture of the single tailed surfactant sodium dodecyl sulfate (SDS) and the double tailed surfactant didodecyldimethylammonium bromide (DDAB) was reported to form spontaneous thermodynamically stable catanionic vesicles (Marques, 2000). The stability of catanionic vesicles is usually explained by the theory developed by Safran (Safran et al., 1990), (Safran et al., 1991), which supposes the surfactants to divide asymmetrically over the two monolayers. The difference in monolayer composition may result in monolayers of opposite curvature, and hence a bilayer membrane with a spontaneous curvature. In our experiments mixtures of DOPG and CTAB give stable vesicles over a certain composition range. The similarity between the computed  $k_c$  and measured  $R$  as a function of ionic strength suggests, however, that these catanionic vesicles, like the mixed phospholipid vesicles, are stabilized by entropy. The absence of a spontaneous curvature in the SCF calculations on a mixture of a cationic surfactant and an anionic lipid suggests the same.

The phase behavior of the CTAB-DOPG mixture is not yet fully understood. Vesicles seem to be the predominating aggregate up to mol fractions of 0.4 CTAB. The fact that the calculated  $k_c$  shows similar dependence as the measured  $R$  both on composition and on ionic strength up to 0.4 mol fraction CTAB supports this idea. At higher fractions of CTAB the measured  $R$  and the calculated  $k_c$  are no longer comparable. Similarities in the phase behavior between our system and egg lecithin and CTAB/CTAC mixtures in 0.1 M NaCl (Gustafsson et al., 1997), (Almgren, 2000), suggest that in the region between 0.45 and 0.65 mol fraction CTAB the mixed vesicles probably coexist with a micellar phase. This possibly gives rise to open or perforated vesicles and wormlike micelles growing from the bilayer fragments. Morphological data (e.g. cryo-TEM) would be needed to shed more light on this issue. At even higher fractions of CTAB the system phase separates into a concentrated and a dilute micellar phase, from which bilayers gradually disappear.

No evidence was found for the existence of a spontaneous curvature in our experiments on mixed bilayers. SCF calculations on a mixture of two oppositely charged surfactants never gave indications for a spontaneous curvature,  $J_0 \neq 0$ . All surfactants were always virtually equally distributed over the monolayers. A spontaneous curvature was only found for bilayers of which the two monolayers showed an inclination for demixing. The idea that demixing is necessary for a spontaneous curvature is supported by the fact that mixtures of CTAB and sodium perfluorooctanoate do form vesicles that are stabilized by a spontaneous curvature whereas a mixture of CTAB and sodium octylsulfonate (SOS) forms vesicles that are stabilized by entropy (Jung et al., 2001). A mixture of hydrocarbon and fluorocarbon tails will have a strong tendency to demix

## 5.5 Summary

and therefore the monolayers will differ significantly in composition. CTAB and SOS both have hydrocarbon tails and mixing of these two surfactants will therefore lead to a bilayer of (almost) homogeneous composition. The SCF calculations also showed that the window of  $\chi_{C-D}$ -parameters in which monolayer demixing takes place is rather narrow. Lower values of  $\chi_{C-D}$  lead to bilayers in which the surfactants are completely mixed, while higher values of  $\chi_{C-D}$  lead to vesicles consisting of only one of the phospholipid like surfactants. This possibly explains why vesicles of a mixture of CTAB and perfluorohexanoate are not stabilized by a spontaneous curvature, but by entropy (Jung et al., 2001). The shorter length of the fluorated tail might not be enough to obtain monolayers that differ significantly in surfactant composition.

An other parameter that may play an important role in the development of a spontaneous curvature in a bilayer vesicle, is the gel to liquid-crystalline phase transition. Phase separation of the gel and liquid-crystalline phases may lead to patch formation, but it is not inconceivable that it can also result in a significant difference in composition of the two monolayers that make up the bilayer membrane. The composition difference that develops in this way may result in a vesicle with a spontaneous curvature.

The SCF calculations show that the range of parameters at which simple vesicles consisting of lipids and/or surfactants actually have a spontaneous curvature, is narrow. The discussion on the existence of vesicles that are stabilized by a  $J_0 \neq 0$  is therefore rather academic, and as shown in this article equilibrium vesicles are generally stabilized by entropy.

## 5.5 Summary

To produce mixed dioleoylphosphatidylglycerol (DOPG) dioleoylphosphatidylcholine (DOPC) vesicles that are expected to be close to their thermodynamic equilibrium, the freeze thaw method was used. The effect of phospholipid mixing on the vesicle radius,  $R$  was studied. The radius of the mixed phospholipid vesicles is decreased compared to pure DOPG or DOPC vesicles. The minimum in  $R$  does not occur at equimolar composition, suggesting that changes in charge density should be taken into account.

Self-consistent-field calculations on the mechanical properties of the bilayer showed that the membranes' mean bending modulus  $k_c$  has a minimum with composition if two differently charged lipid-like amphiphiles are mixed. The position of the minimum in  $k_c$  depends on the ionic strength, and does not occur exactly at equimolar composition. When  $k_c$  is calculated for phospholipid like molecules with different headgroup charges, a maximum in  $k_c$  is observed. The difference between the before mentioned  $k_c$  data has a minimum at equimolar composition for all ionic strengths, and thus represents the effect of lipid mixing only. The fact that a spontaneous curvature was never found in the calculations on mixtures of two phospholipid like surfactants and the similarity between the observed behavior of the measured  $R$  and the calculated  $k_c$  with composition

## Lipid- and surfactant-lipid mixtures

suggest that the mixed DOPG-DOPC vesicles are indeed stabilized by entropy.

Mixtures of the anionic phospholipid DOPG and the cationic surfactant cetyltrimethylammoniumbromide (CTAB) showed a rather complex phase behavior. At high DOPG concentrations bilayers were preferred, while at high CTAB concentrations (wormlike) micelles were formed. In the regime between the bilayer and micellar phase, complex intermediate structures and phase separation was found. When bilayers were stable, the freeze thaw method resulted in stable vesicles whose size decreased with increasing amounts of CTAB.

SCF calculations were presented on mixtures of a negatively charged phospholipid like molecule and positively charged surfactant. The calculations show that bilayers are not always stable. When high amounts of the surfactant were present in the membrane,  $E_{ves}$  became negative. In the regime where stable bilayers were found,  $k_c$  decreased with increasing amount of surfactant. Again, the mixed bilayers never showed any sign of a spontaneous curvature. Even for much shorter surfactant tail lengths the lipid and the surfactant were, to first order, homogeneously distributed over the monolayers. This means that the vesicles must be stabilized by entropy. The close similarity between the measured  $R$  and calculated  $k_c$  as a function of composition and ionic strength again suggests the same.

Bilayers with a spontaneous curvature could only be obtained for surfactant or lipid mixtures when the constituent amphiphiles showed an inclination for lateral phase separation.

## 5.5 Summary

## Chapter 6

# Self-consistent field predictions for the Gaussian bending modulus $\bar{k}$ , and possible implications for membrane fusion

### Abstract

Vesicles are often used as model systems to study membrane fusion. Recently it was argued that phospholipid vesicles can be thermodynamically stable, which has potential impact on their fusion capacity. Being off equilibrium must a stimulus for vesicles to fuse. It is generally believed that the bilayers' Gaussian bending modulus  $\bar{k}$  may play an important role in vesicle fusion, apart from the off equilibrium size of the vesicles. The tendency of a membrane to form the saddle surfaces required for fusion depends on the value of  $\bar{k}$ . For stable bilayer vesicles  $\bar{k}$  is negative. When  $\bar{k}$  becomes positive, the membrane can lower its free energy by the formation of saddle surfaces and by lowering the number of vesicles in solution. Here we report self-consistent field predictions on the effect of various kinds of additives on the value of  $\bar{k}$ . Additives such as alkanes, which bring  $\bar{k}$  close to zero and increase the equilibrium vesicle radius, tend to promote fusion. Fusion inhibitors, such as micelle forming surfactants, on the other hand, lower the equilibrium vesicle radius and render  $\bar{k}$  more negative.

## 6.1 Introduction

### 6.1 Introduction

Membrane fusion is of fundamental importance in the life of a cell. It is essential in various intra- and intercellular processes, such as exo- and endocytosis, membrane genesis, viral infection, and fertilization. The fusion event requires major rearrangements of lipids in the contact region between the membranes. Although in biological systems fusion is probably mediated by proteins, the physical properties of the bilayer are thought to be of major importance (Chernomordik et al., 1995)(Lee and Lentz, 1998). This is, e.g., reflected by the fact that the fusogenicity of vesicles is highly dependent on their size and on the membrane composition (Haque et al., 2001).

Vesicle fusion is thought to proceed via the formation of stalk intermediates (Kozlov and Markin, 1983), (Siegel, 1993), (Siegel, 1997)(Siegel, 1999). The energy cost for the formation of a stalk is highly dependent on the bilayer composition. Lipids have a certain molecular shape, which determines the preferred aggregate structure (Israelachvili et al., 1976), (Israelachvili et al., 1977). The surfactant parameter  $P = \frac{v}{al}$ , in which  $l$  is the total length of the lipid,  $v$  the volume, and  $a$  the effective headgroup area of the lipid, is a convenient concept to quantify the preference of a surfactant for a certain interfacial geometry (Mitchell and Ninham, 1981). Cone-shaped lipids, which have a  $P > 1$ , prefer to form inverted hexagonal  $H_{II}$ , or inverted cubic  $C_{II}$  phases. These lipids are predicted to destabilize the bilayer structure and promote fusion by lowering the energy of stalk formation. Recently, it was shown that a stalk is indeed an intermediate in the transition from a lamellar to an  $H_{II}$  phase (Yang and Huang, 2002).

To calculate the energy needed for stalk formation the Helfrich equation (Helfrich, 1973) is frequently used. In this equation the effects of the Gaussian curvature elasticity are neglected as  $\bar{k}$  does not vary with topology (Siegel, 1999), (Kozlovsky and Kozlov, 2002), (Markin and Albanesi, 2002). A problem with this description of the energy needed for stalk formation is that it uses the mean bending modulus  $k_c$  as measured for large non-interacting unilamellar vesicles, but for highly curved surfaces in close contact  $k_c$  is not expected to be independent of the curvature (Chapter 3) nor of the inter bilayer distance. Hence large errors may be made in the estimation of energy needed for the formation of fusion intermediates. A second problem arises from the introduction of a spontaneous monolayer curvature, based on the surfactant parameters of its individual constituents. In the calculations of bilayer properties this approach can certainly be questioned. The spontaneous curvature of a bilayer is the curvature that minimizes the free energy and is not directly related to the surfactant parameter of the individual molecules. An alternative approach to describe fusion and the influence of fusion inhibitors and promoters is therefore useful as will be discussed here.

The Helfrich equation (Helfrich, 1973) describes the surface tension of a bilayer as a second order expansion in the mean curvature  $J$  ( $J = \frac{1}{R_1} + \frac{1}{R_2}$ ) and the Gaussian curvature  $K$  ( $K = \frac{1}{R_1 R_2}$ );  $R_1$  and  $R_2$  are the two radii of



curvature. When we assume that the equilibrium membrane is tensionless, the equation originally posed by Helfrich becomes

$$\gamma = -k_c J_0 J + \frac{1}{2} k_c J^2 + \bar{k} K \quad (6.1)$$

This equation defines the important physical membrane properties  $k_c$ ,  $\bar{k}$ , and  $J_0$ . The rigidity of the bilayer is determined by the mean bending modulus,  $k_c$ . The spontaneous curvature  $J_0$  is thought to be the curvature that minimizes the curvature energy of a cylindrically curved interface. The Gaussian bending modulus  $\bar{k}$  is particularly interesting to us, as it determines the membrane topology rather than its rigidity. The value of  $\bar{k}$  is a measure for the tendency of the bilayer to form saddle surfaces. Such surfaces are important in fusion intermediates. For negative values of  $\bar{k}$  the bilayer will prefer to form vesicles or bilayer sheets, but for positive values of  $\bar{k}$  the bilayer can lower its free energy by the formation of (many) saddle surfaces for which  $\frac{1}{R_1 R_2} < 0$  (cubic phases). For negative values of  $\bar{k}$  the system will gain  $4\pi\bar{k}$  energy for each vesicle, this makes it favorable to form many small objects. But when  $\bar{k}$  becomes positive the system provides  $4\pi\bar{k}$  for each vesicle, it will therefore tend to reduce the number of vesicles. From this reasoning it follows that a prerequisite for bilayers to fuse might be  $\bar{k} \gtrsim 0$ .

Although this criterion seems reasonable, it is obviously not sufficient to explain why the very small vesicles obtained after sonication show a greater inclination for fusion than larger vesicles with the same composition (Nir et al., 1982). As shown recently, charged phospholipid vesicles can be thermodynamically stable (Chapter 2). They are protected against the formation of multilamellar sheets by their surface charge, undulations, and translational entropy. The equilibrium size of these vesicles is determined by the persistence length of the bilayer  $\xi_p$ , which is directly related to  $k_c$ . The extent to which the actual vesicle radius deviates from the equilibrium radius might also be of great importance in vesicle fusion.

It is conceivable that for full fusion to occur, both of the before-mentioned criteria have to be fulfilled. There are however some problems in testing this hypothesis. Up till now, to the best of our knowledge, no experimental data on  $\bar{k}$  of lipid bilayers is available. As it is very difficult to determine  $\bar{k}$  experimentally, there is little hope that such information will be obtained soon. The only means to get some insight into the effects of fusion promoters and inhibitors on  $\bar{k}$  are molecularly realistic model calculations.

The aim of this report is to generate more information on the roles of  $\bar{k}$  and  $k_c$  in vesicle fusion. For this purpose we will use self-consistent-field calculations that have shown to be useful in the prediction of bilayer properties before (Chapter 2). The effects of additives with different surfactant parameters on  $\bar{k}$  and  $k_c$  of a stable bilayer membrane will be presented. The results will be discussed in relation to literature experiments on vesicle fusion.

## 6.2 Materials and Methods

## 6.2 Materials and Methods

The Self Consistent Field (SCF) theory can be used to evaluate the distribution of surfactant molecules in association colloids. These self assembled objects can be either micelles, vesicles, or bilayers. Recently, Oversteegen showed how the structural, thermodynamic and mechanical parameters of a lipid bilayer can be determined unambiguously from SCF calculations (Oversteegen and Leermakers, 2000),

In the calculations the curvature of the bilayer can be varied by changing the number of lipid molecules in the system. For each given number of lipid molecules the topology constrained equilibrium density profiles can be calculated. The parameters in the Helfrich equation can subsequently be determined from the resulting interfacial tensions. Calculations on a cylindrical interface give access to  $k_c$ . Because in this geometry  $K = 0$ ,  $J = \frac{1}{R}$  and the area  $A = 2\pi Rh$  (where  $h$  is the length of the cylinder), equation 6.1 can be rewritten as

$$\gamma A = -2\pi k_c J_0 + \pi k_c J \quad (6.2)$$

By varying  $R$  and therefore the number of lipid molecules in the system,  $k_c$  can be obtained from the slope of the  $\gamma A$  versus  $J$  plots. For all the systems presented here, extrapolation of the  $\gamma A$  versus  $J$  always gave an abscissa of zero; they do not have a spontaneous curvature, i.e. they have  $J_0 = 0$ . The  $k_c$  obtained in this way can be used to extract  $\bar{k}$  from similar calculations on a spherical interface. For a sphere,  $J^2 = 4K = \frac{4}{R^2}$  and  $A = 4\pi R^2$ , so that equation 6.1 becomes

$$\gamma A = -8\pi k_c J_0 R + 4\pi(2k_c + \bar{k}) \quad (6.3)$$

As  $J_0 = 0$ ,  $\bar{k}$  follows directly from  $\gamma A$ , using  $k_c$  from the cylindrical system.

Bilayer stability depends on the value of both  $k_c$  and  $\bar{k}$ . Stable bilayers can only exist if the total free energy of bending is positive. In a spherical geometry this means that  $-2k_c < \bar{k} \leq 0$ . Micellar aggregates will prevail when  $-2k_c > \bar{k}$ . For  $\bar{k} > 0$  the bilayers will no longer be stable against the formation of connecting handles for which  $\frac{1}{R_1 R_2} < 0$ , and as a result the system will form C<sub>II</sub> or H<sub>II</sub> phases.

### 6.2.1 Parameters

The implementation of the SCF model used in this study cannot deal with branched molecules, Therefore, the phospholipids and additives were all modeled as linear chains. The effects of more complicated molecules, such as, e.g., cholesterol, on the mechanical properties of the bilayer could not be tested.

The standard charged phospholipid-like molecule, used in most calculations, was a linear chain with segment sequence C<sub>18</sub>X<sub>2</sub>C<sub>2</sub>X<sub>2</sub>C<sub>18</sub>, in which the X segments each carry a charge of  $-\frac{1}{4}$  e. The two C<sub>18</sub>-groups represent the hydrophobic tails, the X<sub>2</sub>C<sub>2</sub>X<sub>2</sub> group stands for the hydrophilic headgroup. To

test the effect of the size of the headgroup on  $k_c$  and  $\bar{k}$ , the C segments were removed from the headgroup, and the amount of segments X in the molecule was changed, while keeping the total headgroup charge constant at  $-1$  e.

Phospholipids were mixed with different kinds of additives. As the additives do not all have the same solubility, the amount of molecules that ended up in the bilayer was calculated, and given in the figures. The effect of mixing phospholipids which differ in effective headgroup charge was obtained by adding a molecule  $C_{18}Y_2C_2Y_2C_{18}$  to the  $C_{18}X_2C_2X_2C_{18}$  bilayer. The segments Y in this molecules all carry a charge of  $-\frac{1}{10}$  e. Micelle forming surfactants with  $P < \frac{1}{3}$ , were represented by a molecule with segment sequence  $C_{18}X_2C_2X_2$ . This molecule is very similar to the phospholipid like molecule; it only misses one of the hydrophobic tails. Surfactants with  $P > 1$  tend to form inverted phases. In the calculations such molecules were represented as  $C_{18}Z$ , in which the segment Z carries no charge. As the chains in our model behave like Gaussian chains, putting a charge on the headgroup resulted in surfactants for which  $P < 1$ . Additives that accumulate in the hydrophobic part of the bilayer membrane, such as alkanes, are modeled as  $C_{18}$  molecules.

In all the calculations water was modeled by a simple solvent monomer W. The ionic strength of the solution was determined by two monomer types, cation and anion, with valency  $+1$  and  $-1$ , respectively. The hydration of ions was taken into account by the choice of the Flory-Huggins interaction parameters,  $\chi_{W-cation} = -2$  and  $\chi_{W-anion} = -1$ . The more negative value for  $\chi_{anion-X}$  reflects the stronger hydrogen bonding property of the cation. The surfactant headgroup was made soluble in water by choosing  $\chi_{X-W} = \chi_{Y-W} = \chi_{Z-W} = -2$ . In the calculations on the effect of the headgroup size on  $k_c$  and  $\bar{k}$ , the total of the interaction parameters of the headgroup with water was kept constant by changing  $\chi_{X-W}$ . In all calculations the following segment type dielectric constants were used  $\epsilon_C = 2$ ,  $\epsilon_X = \epsilon_{cation}, \epsilon_{anion} = 5$ ,  $\epsilon_W = 80$ . The local dielectric constants were subsequently computed from a volume fraction weighted average.

## 6.3 Results

Most phospholipids prefer to form bilayers and are therefore assumed to have a  $P$  between  $\frac{1}{2}$  and  $1$  (Mitchell and Ninham, 1981). Mixing of two phospholipid like molecules that meet this criterion and that differ only in headgroup charge results in a bilayer of which the  $k_c$  is decreased compared to the single component bilayer (Fig. 6.1). The lipid composition at which the minimum in  $k_c$  occurs depends on the ionic strength of the solution. As discussed before, the observed changes in  $k_c$  are the result of surfactant mixing in the bilayer and changes in surface charge density (Chapter 4).

The changes in  $\bar{k}$  that occur upon mixing two different phospholipid species, are shown in figure 6.2.

Bilayers composed of highly charged lipids always have a more negative  $\bar{k}$

### 6.3 Results

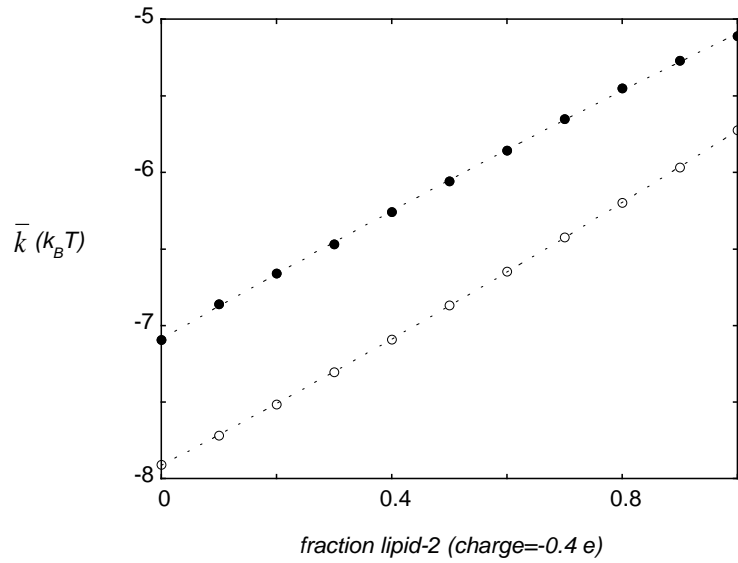


Figure 6.1: The mean bending modulus  $k_c$  of a binary lipid bilayer as a function of composition. The bilayer consisted of  $C_{18}X_2C_2X_2C_{18}$  with charge  $-1 e$  and  $C_{18}Y_2C_2Y_2C_{18}$  with charge  $-\frac{2}{5} e$ . Results are shown for two levels of ionic strength,  $\phi_s = 0.005$  ( $\circ$ ) and  $\phi_s = 0.01$  ( $\bullet$ ).

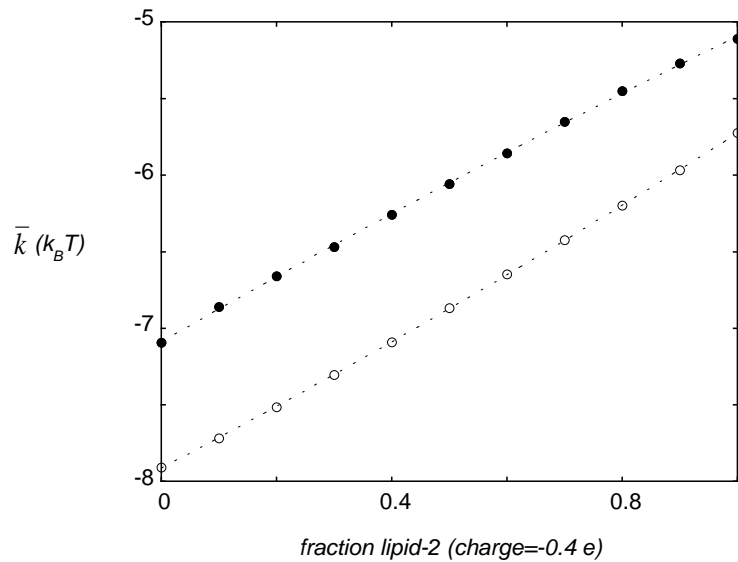


Figure 6.2: The Gaussian bending modulus  $\bar{k}$  of a mixed lipid bilayer as a function of composition. The bilayer consisted of  $C_{18}X_2C_2X_2C_{18}$  with charge  $-1 e$  and  $C_{18}Y_2C_2Y_2C_{18}$  with charge  $-\frac{2}{5} e$ . Results are shown for  $\phi_s = 0.005$  ( $\circ$ ) and  $\phi_s = 0.01$  ( $\bullet$ ).

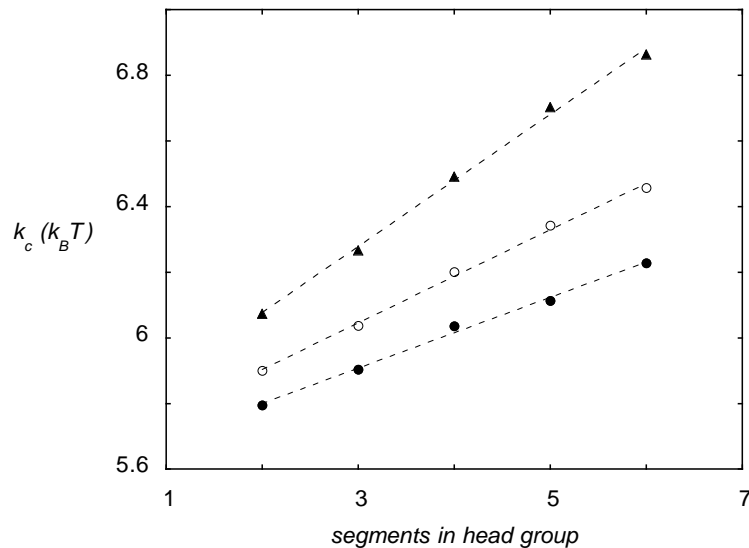


Figure 6.3:  $k_c$  as a function of headgroup size at the ionic strengths,  $\phi_s = 0.005$  ( $\bullet$ ),  $\phi_s = 0.01$  ( $\circ$ ), and  $\phi_s = 0.02$  ( $\blacktriangle$ ). The size of the lipid headgroup was varied by changing the amount of X segments while keeping the total headgroup charge and hydrophilicity constant

than those composed of lipids that carry less charge (Chapter 2). Therefore  $\bar{k}$  becomes less negative with increasing amounts of the less charged  $C_{18}Y_2C_2Y_2C_{18}$  in the bilayer. While  $k_c$  has a minimum as a function of the composition, the increase in  $\bar{k}$  is almost linear with the composition. Increasing the ionic strength results in less negative values of  $\bar{k}$ . When the ionic strength is changed from  $\phi_s = 0.005$  to  $\phi_s = 0.01$ , the  $\bar{k}$  curve is shifted upwards (Fig. 6.2).

Phosphatidylethanolamine is a phospholipid for which  $P > 1$ ; it may form  $H_{II}$  phases in excess water. It has been suggested these lipids destabilize the bilayer state and promote membrane fusion (Haque et al., 2001). To test whether the changes in surfactant parameter result in the expected changes in  $k_c$  and  $\bar{k}$ , the size of the headgroup was varied at constant lipid tail length. In the calculations, the size of the hydrophilic headgroup of a phospholipid like molecule was varied at a constant headgroup charge of  $-1 e$ , and the total affinity of the headgroup for water was also kept constant. As can be seen in figure 6.3 and 6.4, the headgroup size of the lipid molecule affects both  $k_c$  and  $\bar{k}$ . At all ionic strengths,  $k_c$  increases, while  $\bar{k}$  becomes more negative with increasing headgroup size. Lipids with  $P > 1$ , are cone shaped; they have a small headgroup compared to their tail length. In the SCF-calculations, a small headgroup results in lower values of  $k_c$  and less negative values of  $\bar{k}$ , compared to lipids with a larger headgroup.

Surfactants with  $P < \frac{1}{3}$  form spherical micelles in excess water. In naturally occurring membranes, lysolipids are probably the most well known micelle forming surfactants. The incorporation of lysolipids into phospholipid bilayers is known to inhibit fusion of apposing membranes. To test how  $k_c$  and  $\bar{k}$  of a

### 6.3 Results

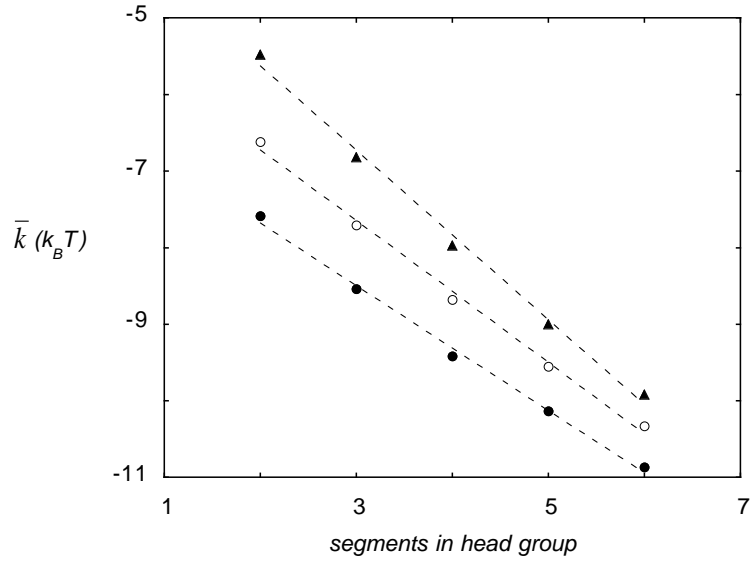


Figure 6.4:  $\bar{k}$  as a function of headgroup size at the ionic strengths,  $\phi_s = 0.005$  (●),  $\phi_s = 0.01$  (○), and  $\phi_s = 0.02$  (▲). The size of the lipid headgroup was varied by changing the amount of X segments while keeping the total headgroup charge constant at  $-1$  e.

lipid bilayer react on a surfactant with  $P < \frac{1}{3}$ ,  $C_{18}X_2C_2X_2$  was incorporated into the  $C_{18}X_2C_2X_2C_{18}$  membrane.

Figure 6.5 and 6.6 shows  $k_c$  and  $\bar{k}$  as a function of the bilayer composition in the region where  $4\pi(2k_c + \bar{k}) > 0$ . Mixed  $C_{18}X_2C_2X_2C_{18}$ - $C_{18}X_2C_2X_2$  bilayers do not remain stable over the whole composition range. The value of  $4\pi(2k_c + \bar{k})$  becomes negative at high fractions of  $C_{18}X_2C_2X_2$ , and the surfactant mixture will prefer to form micellar phases. The bilayer (vesicle) to micelle transition is a function of the ionic strength. With increasing salt concentration the transition shifts to higher fractions of surfactant in the bilayer. For the ionic strengths shown, the behavior of both  $k_c$  and  $\bar{k}$  with composition is comparable. With increasing amounts of the micelle forming surfactant in the bilayer  $k_c$  decreases; the membrane becomes more flexible. The more of the  $C_{18}X_2C_2X_2$  is taken up by the membrane, the more negative  $\bar{k}$  becomes. This means that, upon incorporation of  $C_{18}X_2C_2X_2$  in the membrane, the system will have a tendency to increase the number of vesicles and that it will cost more energy to form the saddle surfaces that are needed in vesicle fusion.

Surfactants with a  $P > 1$  tend to form inverted phases like the  $H_{II}$  and  $C_{II}$  phases. In contrast to the surfactants mentioned before, molecules that tend to form inverted phases promote fusion. When the bilayer forming phospholipid like molecule  $C_{18}X_2C_2X_2C_{18}$  is mixed with a molecule,  $C_{18}Z$ , that has a  $P > 1$ ,  $k_c$  decreases (Fig. 6.7). Bilayers apparently become less rigid upon addition of  $C_{18}Z$ . The effect of the amount of inverse phase former on  $\bar{k}$  is the opposite of that of a micelle forming surfactant; for all ionic strengths  $\bar{k}$  becomes less

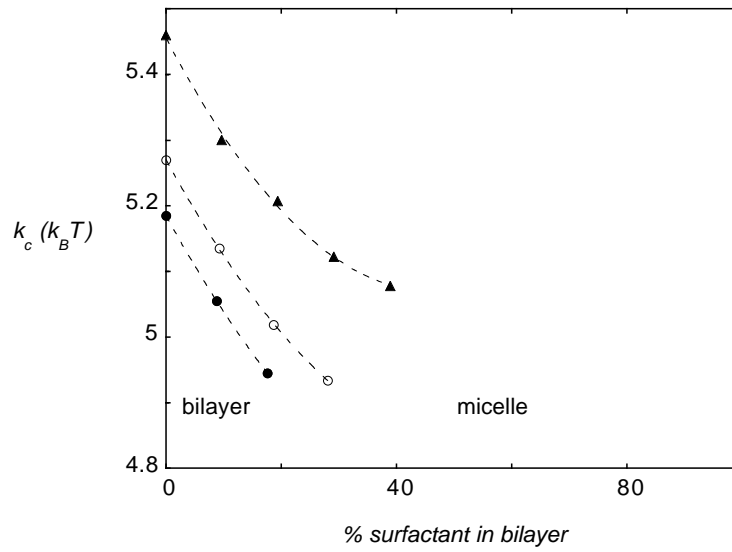


Figure 6.5:  $k_c$  as a function of the amount of micelle forming surfactant in the charged lipid bilayer at  $\phi_s = 0.005$  ( $\bullet$ ),  $\phi_s = 0.01$  ( $\circ$ ), and  $\phi_s = 0.02$  ( $\blacktriangle$ ).

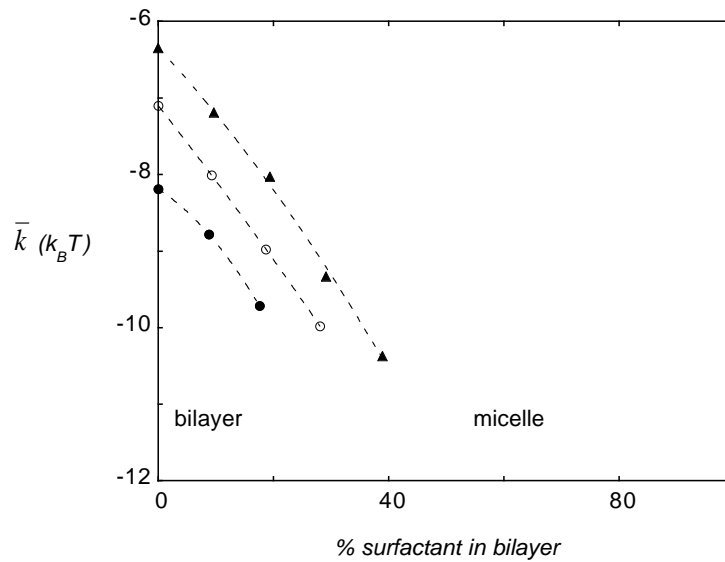


Figure 6.6:  $\bar{k}$  as a function of the amount of micelle forming surfactant in the charged lipid bilayer at  $\phi_s = 0.005$  ( $\bullet$ ),  $\phi_s = 0.01$  ( $\circ$ ), and  $\phi_s = 0.02$  ( $\blacktriangle$ ).

## 6.4 Discussion

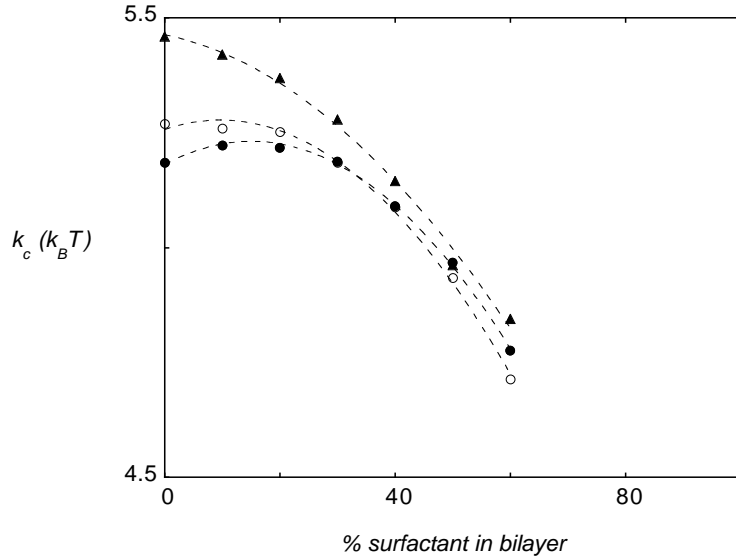


Figure 6.7:  $k_c$  as a function of the amount of inverted phase forming surfactant in the charged lipid bilayer at  $\phi_s = 0.005$  ( $\bullet$ ),  $\phi_s = 0.01$  ( $\circ$ ), and  $\phi_s = 0.02$  ( $\blacktriangle$ ).

negative with increasing amounts of  $C_{18}Z$  in the bilayer (Fig. 6.8). Hence, the formation of saddle surfaces will cost less energy when an inverted phase forming surfactant is added to the phospholipid bilayer. High amounts of  $C_{18}Z$  in the bilayer eventually gave a  $\bar{k} \approx 0$ . Adding more of the inverted phase forming surfactant to the bilayer resulted in the transition from a lamellar to an inverted phase. The lamellar to inverted phase transition is a function of the ionic strength with increasing salt concentration it shifts to lower amounts of  $C_{18}Z$  in the membrane.

Besides surfactants, other molecules can also significantly change membrane properties. Alkanes, and other hydrocarbon compounds that tend to make the membrane thicker are known to promote vesicle fusion (Basanez et al., 1998), (Malinin et al., 2002). To study the effect of mixing such molecules with phospholipids on  $k_c$  and  $\bar{k}$ ,  $C_{18}X_2C_2X_2C_{18}$  lipids were mixed with  $C_{18}$  alkanes. As a result of the alkanes in the bilayer both  $\bar{k}$  and  $k_c$  increased (Fig. 6.9 and Fig. 6.10). When a certain amount of alkane is taken up by the membrane,  $\bar{k}$  even becomes zero. The percentage  $C_{18}$  at which  $\bar{k} = 0$  depends on the ionic strength. The higher the ionic strength, the lower the amount of alkane needed to obtain  $\bar{k} = 0$ . As  $\bar{k} > 0$ , bilayers were no longer stable against the formation of inter bilayer connections, and no SCF solution could be generated.

## 6.4 Discussion

Upon fusion two vesicles become one and the system gains or loses  $4\pi\bar{k}$  energy, depending on the sign of  $\bar{k}$ . It is however unclear in which step of the



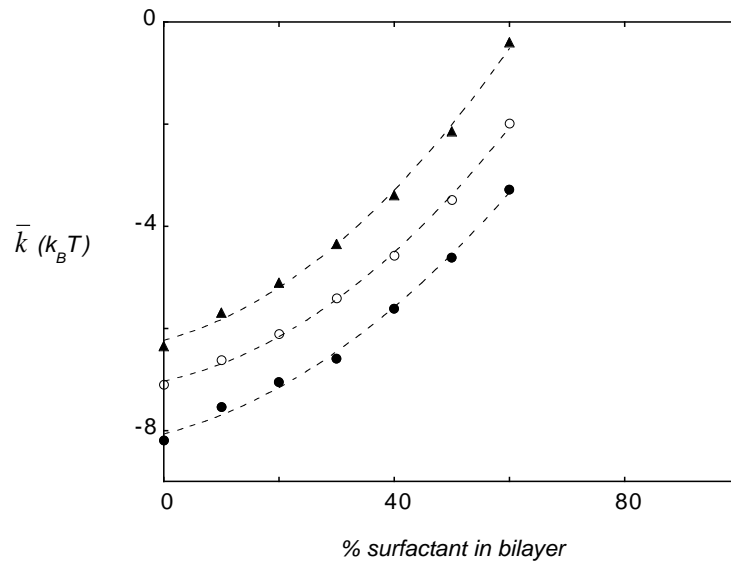


Figure 6.8:  $\bar{k}$  as a function of the amount of inverted phase forming surfactant in the charged lipid bilayer at  $\phi_s = 0.005$  ( $\bullet$ ),  $\phi_s = 0.01$  ( $\circ$ ), and  $\phi_s = 0.02$  ( $\blacktriangle$ ).

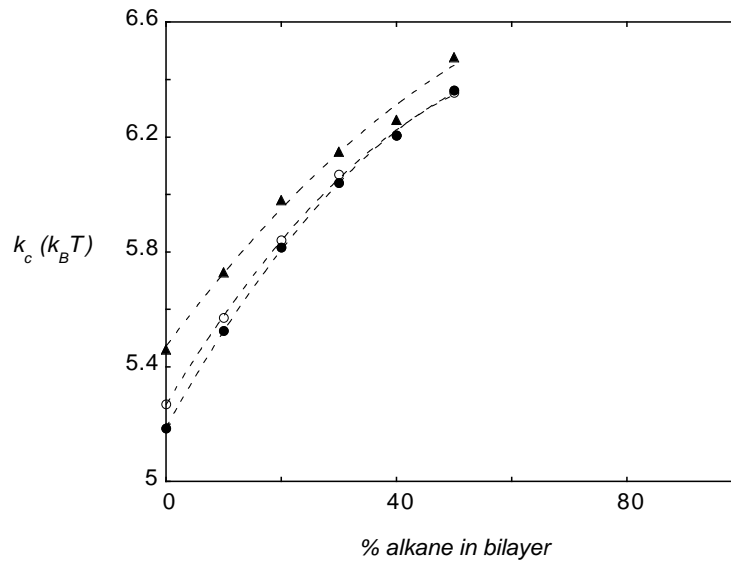


Figure 6.9:  $k_c$  as a function of the percentage of  $C_{18}$  alkane in charged  $C_{18}X_2C_2X_2C_{18}$  bilayer at  $\phi_s = 0.005$  ( $\bullet$ ),  $\phi_s = 0.01$  ( $\circ$ ), and  $\phi_s = 0.02$  ( $\blacktriangle$ ).

## 6.4 Discussion

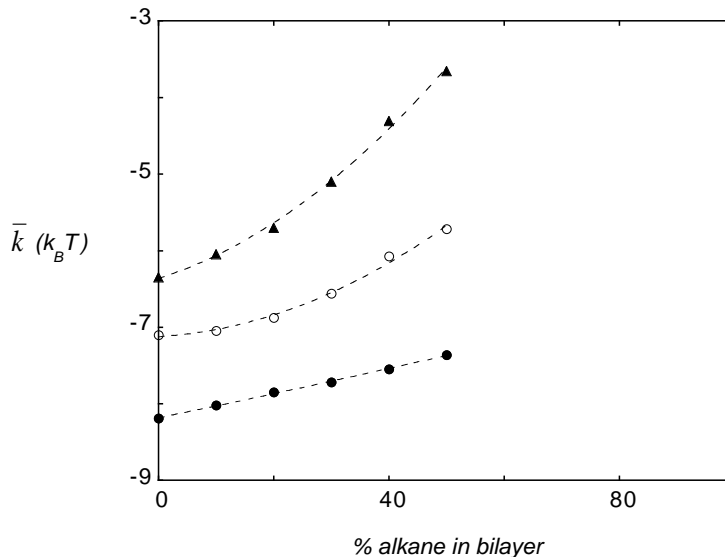


Figure 6.10:  $\bar{k}$  as a function of the percentage of  $C_{18}$  alkane in a charged  $C_{18}X_2C_2X_2C_{18}$  bilayer at  $\phi_s = 0.005$  (●),  $\phi_s = 0.01$  (○), and  $\phi_s = 0.02$  (▲).

fusion this happens, and theoretical predictions on the energy needed for stalk formation therefore usually neglect  $\bar{k}$  (Siegel, 1999), (Kozlovsky and Kozlov, 2002), (Markin and Albanesi, 2002). The energy needed to form a stalk is then calculated from  $k_c$  that is known from experiments for some systems. These experimentally obtained values of  $k_c$  refer to large, non interacting vesicles. However, both  $k_c$  and  $\bar{k}$  are very likely a function of the curvature (Chapter 3) in the limit of high curvature typically present in stalks. The inter bilayer distance is also expected to have an influence on the bending moduli, especially when the membranes are charged. This makes the prediction on the energy of stalk formation very uncertain. An evaluation of the energetic and entropic changes upon vesicles fusion might give an alternative way to predict whether additives inhibit or promote fusion.

When the surface of a phospholipid bilayer is effectively charged, its vesicles can be thermodynamically stable. The charge protects the vesicles against the formation of multilamellar phases. In the absence of a spontaneous curvature, the energy needed to curve the flat bilayer into a closed vesicle will have to be compensated by entropy. The formation of closed spherical vesicles from a charged bilayer will lead to an elimination of unfavorable edges, and the system gains mixing entropy.

Previously it was shown that both the entropy of mixing and undulations play a role in the entropic stabilization of charged phospholipid vesicles (Chapter 3). The mixing entropy favors many small vesicles, but the lower limit to the vesicle radius is set by the persistence length  $\xi_p$  of the bilayer. The membrane persistence length is related to the mean bending modulus  $k_c$  by

$\xi_p \propto e^{\frac{4\pi k_c}{k_B T}}$ . The vesicle radius,  $R$  is therefore expected to scale as

$$R \propto \xi_p \propto e^{\frac{4\pi k_c}{k_B T}} \quad (6.4)$$

where  $k_B$  is the Boltzmann constant, and  $T$  is the temperature. This scaling relation couples the equilibrium vesicle radius directly to  $k_c$ . Increases in  $k_c$  should therefore result in larger equilibrium vesicles.

In spite of the low solubility of phospholipids in water, vesicles will try to reach their equilibrium radius and gain entropy. Whether the system gains entropy by fusion depends on the value of  $k_c$ . If vesicles are much smaller than the equilibrium radius, fusion is expected to proceed. Additives that increase  $k_c$  and thus the equilibrium vesicle radius are for this reason expected to enhance fusion by supplying a driving force.

But this fusion criterion is probably not sufficient; it also should be not too costly for the bilayers to form fusion pores. The formation of fusion pores is related to the Gaussian bending modulus  $\bar{k}$ , which determines the tendency of a bilayer to form saddle surfaces, when  $\bar{k}$  becomes positive the membrane can only lower its free energy by the formation of a saddle surface for which  $\frac{1}{R_1 R_2} < 1$ . Once  $\bar{k} \approx 0$  it will cost (almost) no energy to form fusion pores and the system will not lose energy when the number of objects are reduced.

Mixtures of DOPC and DOPG were studied previously (Chapter 4). The radius of the mixed phospholipid vesicles showed a minimum as a function of the composition. This minimum shifted toward higher DOPC content with increasing ionic strength. A similar behavior of  $k_c$  as a function of both the composition and the ionic strength can be seen in figure 6.1. For a detailed discussion of this behavior we refer to (Chapter 4), but the good agreement between the measured  $R$  and the calculated  $k_c$  indicates that our calculations on both  $k_c$  and  $\bar{k}$  of bilayers of mixtures of phospholipid like molecules must be qualitatively correct.

For phospholipids, both  $\bar{k}$  and  $k_c$  depend on the size of the hydrophilic headgroup (Fig. 6.3). The larger the headgroup, the larger  $k_c$  and the more negative  $\bar{k}$ . Although vesicles would favor a larger radius with increasing headgroup size, it becomes more difficult to form fusion pores, and the reduction in number of vesicles upon fusion will cost the system  $4\pi\bar{k}$  per vesicle. This idea is supported by the fact that the threshold concentration of  $\text{Ca}^{2+}$  needed to fuse unilamellar vesicles composed of different charged phospholipids increases with increasing headgroup size, phosphatidic acid < phosphatidylserine < phosphatidylglycerol. Large unilamellar vesicles of phosphatidylinositol, which has a very large headgroup, are even entirely resistant to  $\text{Ca}^{2+}$  induced fusion (Arnold, 1995).

Surfactants that have  $P < \frac{1}{3}$  are predicted to inhibit fusion. The inhibition of fusion by several micelle-forming surfactants is a well known fact in the literature. Lysolipids prevent syncytia formation in baculovirus-infected cells (Vogel et al., 1993), exocytotic fusion of sea urchin egg of cortical granules (Vogel et al., 1993), and the fusion of DOPE vesicles (Yeagle et al., 1994). Besides lysolipids, other micelle forming substances like palmitoylcarnitine and

## 6.4 Discussion

gangliosides are also reported to inhibit phospholipase-C-promoted vesicle fusion (Basanez et al., 1998), (Goni et al., 1994).

The inhibition of fusion by lysolipids and other micelle-forming surfactants has been attributed to the fact that they increase the energy needed for stalk formation by generating a positive spontaneous curvature. It is however more likely that a more negative  $\bar{k}$  is responsible for this phenomenon; the system has to pay  $4\pi\bar{k}$  per vesicle for each fusion event. With increasing amounts of lysolipid in the bilayer  $k_c$  is predicted to decrease. This means that, if  $k_c$  remains independent of the curvature (as is assumed in the literature), it will cost less energy to bend the bilayer into the highly curved stalks. This is however not the only consequence of a decrease in  $k_c$ ; the repulsive undulation pressure between phospholipid bilayers was experimentally found to increase with the incorporation of lysolipids (McIntosh et al., 1995). Lower values of  $k_c$  lead to an increase in the repulsive undulation pressure. The prediction that  $k_c$  decreases when a micelle forming surfactant is taken up in the membrane is also supported by measurements on the equilibrium radius of vesicles composed of mixtures of dioleoylphosphatidylglycerol (DOPG) and cetyltrimethylammonium bromide (CTAB). The radii of these vesicles decrease with an increasing amount of CTAB in the bilayer (Chapter 4).

The increase in undulation repulsion and the smaller equilibrium radius that results from the decrease in  $k_c$  will probably both help to prevent vesicle fusion. But the decrease in  $\bar{k}$  with increasing amount of micelle-forming surfactant in the bilayer will make vesicle fusion energetically very unfavorable.

When  $P > 1$ , surfactants are capable of forming inverted phases. Added to a phospholipid bilayer, these surfactants are predicted to promote stalk formation by inducing a negative monolayer curvature. Experiments show that these surfactants do indeed promote fusion in various systems. Unsaturated fatty acids, such as arachidonic acid, prefer inverted phases, and promote both lipid and vesicle content mixing in phospholipid-C promoted vesicle fusion (Basanez et al., 1998). These molecules also induce fusion of aggregated chromaffin granules (Creutz, 1981), and promote  $\text{Ca}^{2+}$ -induced fusion of phospholipid vesicles (Glaser and Gross, 1994).

The SCF calculations performed here predict that  $\bar{k}$  becomes less negative with increasing amounts of a surfactant with  $\frac{v}{a} > 1$ . It therefore becomes less unfavorable to form one vesicle out of two, and the formation of a fusion pore will also cost less energy as  $\bar{k}$  approaches zero. For positive values of  $\bar{k}$  the system will even gain energy from vesicle fusion.

The mean bending modulus  $k_c$  is predicted to become smaller upon the addition of amphiphiles with  $P > 1$ . The equilibrium radius of vesicles will therefore decrease with increasing amounts of the inverted-phase-forming surfactant. The decrease in  $k_c$  is expected to inhibit the growth of vesicles that are large compared to their equilibrium radius, but vesicles that are small with respect to  $\xi_p$  are still expected to grow in size. This probably explains why unsaturated fatty acids promote fusion of sonicated (Glaser and Gross, 1994), and cholesterol-containing extruded (Basanez et al., 1998) vesicles. The antag-

onistic effects of  $k_c$  and  $\bar{k}$  on fusion when surfactants with  $P > 1$  are added to the bilayer will in some cases result in a competition between energy gain and entropy loss. It is therefore to some extent uncertain whether or not the addition of inverted phase formers to a phospholipid bilayer will promote vesicle fusion.

Hydrocarbon solvents, such as hexadecane, are known to promote vesicles fusion (Walter et al., 1994) (Basanez et al., 1998), (Malinin et al., 2002). This phenomenon has been suggested to be caused by the partitioning of the alkanes between the phospholipid tails thereby increasing the monolayer curvature and decreasing the energy needed for stalk formation (Chen and Rand, 1998). Our calculations show that upon the addition of alkanes both  $k_c$  and  $\bar{k}$  increase. The increase in  $\bar{k}$  is due to the increased effective area of the hydrophobic tails while the size of the headgroup remains almost constant. This effectively leads to  $P > 1$  and with increasing amounts of alkane the system tends to form inverted phases for which  $\bar{k} > 0$ . The increase in  $k_c$  can be understood in terms of the bilayer thickness. As alkanes partition into the center of the bilayer, the membrane becomes thicker, and therefore the bilayers' persistence length  $\xi_p$  increases. Summarizing, both the formation of fusion intermediates and the subsequent growth into larger vesicles are promoted by the addition of alkanes.

The calculated trends in both  $k_c$  and  $\bar{k}$  as a function of composition appear helpful in understanding the effects of additives on vesicle fusion. The amount of additive needed to meet  $\bar{k} \approx 0$  is however rather high in the calculations compared to the experiments. This may be due to the rather localized action of the inhibitors or promoters in the experiments, while in the calculations the molecules are homogeneously distributed (laterally along the bilayer) and fluctuations in composition are ignored. The fact that all (complex) molecules in the SCF calculations behave as flexible chains has probably also contributed to this discrepancy. Although trends in  $k_c$  and  $\bar{k}$  are reliable, the amount of additive needed to promote fusion is probably overestimated.

The calculations presented here do not contain any information on the energy and structure of the fusion intermediate; they can only be used to evaluate the energy and entropy of the system before and after fusion. Since we expect the bending moduli to change when bilayers are brought into close contact, calculations on  $k_c$  and  $\bar{k}$  as a function of inter bilayer distance would be useful, especially with respect to the energy of the highly bent fusion intermediates such as the stalk.

## 6.5 Conclusions

Membrane fusion can be rationalized in terms of the bending constants,  $k_c$  and  $\bar{k}$ . Vesicles gain both energy and entropy when they fuse, provided  $k_c$  and thus  $\xi_p$  is large with respect to the vesicle size, and  $\bar{k} \geq 0$ . Vesicles tend to grow to their equilibrium radius which is determined by  $k_c$ . When the radius is smaller

## 6.5 Conclusions

than the equilibrium radius vesicles gain entropy upon fusion. Upon fusion two objects become one; if  $\bar{k} < 0$  the system will lose  $4\pi\bar{k}$  with each fusion event, whereas this amount of energy will be gained when  $\bar{k} > 0$ . This brings us to the conclusion that additives that increase both  $k_c$  and  $\bar{k}$  promote vesicle fusion, whereas additives that decrease both bending moduli behave as fusion inhibitors. Surfactants that decrease  $k_c$  and increase  $\bar{k}$  are expected to promote fusion only when the vesicles are rather small with respect to their equilibrium radius. Numerous experimental observations reported in the literature are in line with the fusion criteria that we defined on the basis of the results of our SCF calculations.

# Chapter 7

## Osmotic shrinkage and reswelling of giant vesicles composed of dioleoylphosphatidylglycerol and cholesterol

### Abstract

The osmotic shrinkage of giant unilamellar DOPG (dioleoylphosphatidylglycerol) vesicles in a hypertonic osmotic solution leads to vesiculation of the phospholipid bilayer (raspberry mode of shrinkage). The size of the daughter vesicles that appear inside the giant is an increasing function of the cholesterol content. The radius of the daughter vesicles increases from  $0.2 \mu\text{m}$  to  $3.0 \mu\text{m}$  when the cholesterol content is changed from 0 to 40 %. It is argued that the size selection of the daughters is regulated by the membrane persistence length, which is an exponential function of the mean bending modulus. From the kinetics of shrinkage as well as the lysis upon osmotic inflation it is estimated that after an osmotic gradient of 200 mM approximately 11 % of the daughter vesicles remain attached to the mother giant.

## 7.1 Introduction

### 7.1 Introduction

Living cells that are subject to osmotic stress, by either drying, freezing, or exposure to a medium of higher osmolarity, tend to dehydrate. This dehydration directly reduces the volume, which gives rise to an excess of membrane area. In some systems, the area to volume ratio is reestablished by vesiculation of the plasma membrane, for example, during plasmolysis in onion epidermal cells (Oparka et al., 1990) and in the Gram-negative bacterium *Escherichia coli* (Schwarz and Koch, 1995). In guard-cell protoplasts shrinkage causes vesicular retrieval of the plasma membrane into the cytoplasm (Kubitscheck et al., 2000). In the dry axis of desiccation-tolerant soybean seeds (Chabot and Leopold, 1982) and the dry radicle of cowpea seeds (Bliss et al., 1984) a clustering of vesicles is seen along the margins of the plasma membrane, which is not observed in the hydrated state. The vesiculation upon dehydration may however result in serious damage to the plasma membrane upon subsequent rehydration when area expansion is necessary. This is illustrated by the reaction of protoplasts from cold acclimated and non acclimated rye leaves. In the acclimated protoplast, vesicles remain continuous with the plasma membrane upon freezing-induced contraction (Gordon-Kamm and Steponkus, 1984b), whereas the non acclimated protoplasts vesiculate without remaining attached to the plasma membrane (Gordon-Kamm and Steponkus, 1984a). This loss of contact of the vesicles with the plasma membrane leads to a reduction in surface area. When vesicles do not remain attached to the plasma membrane, lysis of the protoplast during thawing may occur. Apparently, lipid material is needed for area expansion, but insufficient amounts of this membrane material are readily accessible. The same conclusions were drawn from a study on the stress-strain relation of these protoplasts. When the protoplast is volumetrically contracted in a medium of elevated osmolarity and its membrane loses material, a re-expansion to the original size may lyse the plasma membrane if the membrane cannot incorporate sufficient new material fast enough (Wolfe and Steponkus, 1981), (Wolfe and Steponkus, 1983). Inability to reincorporate vesicles into the plasma membrane of the expanding protoplast has also been suggested as the cause of imbibitional damage in desiccation-tolerant organisms (Chabot and Leopold, 1982).

Membrane vesiculation upon osmotic contraction seems not to be reserved for biological membranes, or their lipid extracts (Steponkus and Lynch, 1989). Giant egg-PC vesicles were observed to retain their spherical shape during osmotic shrinkage (Boroske et al., 1981). Recently, it was reported that the volume reduction of a giant vesicle, in a hypertonic osmotic solution, is accompanied by the formation of daughter vesicles inside the shrinking giant (Bernard et al., 2002). This 'raspberry mode' of shrinkage was observed for vesicles of varying composition, but not for pure DPPC vesicles. It was therefore suggested that the vesiculation is driven by a non-homogeneous distribution of the lipids in the bilayer, which gives rise to a non vanishing spontaneous curvature (Bernard et al., 2002). We believe that the spontaneous curvature as follows



## Osmotic shrinkage of giant vesicles

from the Helfrich equation (Helfrich, 1973) is very specific and not needed to explain the reported observations. Instead, we propose that the membrane persistence length controls the physical behavior of the phospholipid bilayer during osmotic shrinkage.

In this report we present a study on the behavior of unilamellar giant DOPG vesicles containing different amounts of cholesterol under hypertonic osmotic stress. The formation of daughter vesicles inside the shrunken giants is followed as function of both composition and osmotic gradient. We show that the radius of the daughter vesicles can be estimated from the initial size and the osmotic gradient. Furthermore, we introduce a model to estimate both the membrane permeability for water and the fraction of vesicles that stay attached to the giant vesicle during osmotic shrinkage. To check the values found with this model for the fraction of daughter vesicles that stay attached, the reversibility of the shrinkage process is analyzed.

## 7.2 Materials and Methods

Dioleoylphosphatidylglycerol (DOPG) was obtained from Avanti Polar Lipids, cholesterol was from Sigma. To obtain giant (unilamellar) vesicles the lipids were dissolved in chloroform that was subsequently evaporated under a stream of nitrogen, leaving a thin lipid film on the wall of a glass tube. The last traces of solvent were removed from the lipid film by drying under vacuum for at least 4 hours. The glass tube was subsequently filled with a 50 mM sucrose solution and allowed to equilibrate for 48-72 hours. This procedure resulted in a heterogeneous population of spherical vesicles, some of which were unilamellar and large enough for analysis with an optical microscope.

The reaction of the giant vesicles on osmotic gradients of 50, 125, and 200 mM were followed with an optical microscope by direct observation of the vesicle radius as a function of time. All observations were made at room temperature which is above the gel to liquid crystalline phase transition temperature of the lipid(mixtures) used.

To be able to change the osmotic pressure of the vesicle-containing medium, a counting chamber was covered with a normal cover glass and the sucrose solution containing the giant vesicles was injected into one of the grooves. Due to capillary forces the area under the cover glass also filled with a thin layer of vesicle-containing solution. An osmotic gradient was established by filling the other groove with a glucose solution of different ionic strength. As the convection resulting from the concentration gradient is relatively slow in the thin layer, vesicles could be followed during osmotic contraction. This setup made it also possible to remove the solution from the grooves, leaving the thin layer of solution between the cover slide and the counting chamber intact. In this way the solution could easily be replaced and the reversibility of the osmotic contraction of the vesicles could be studied.

### 7.3 Results and Analysis

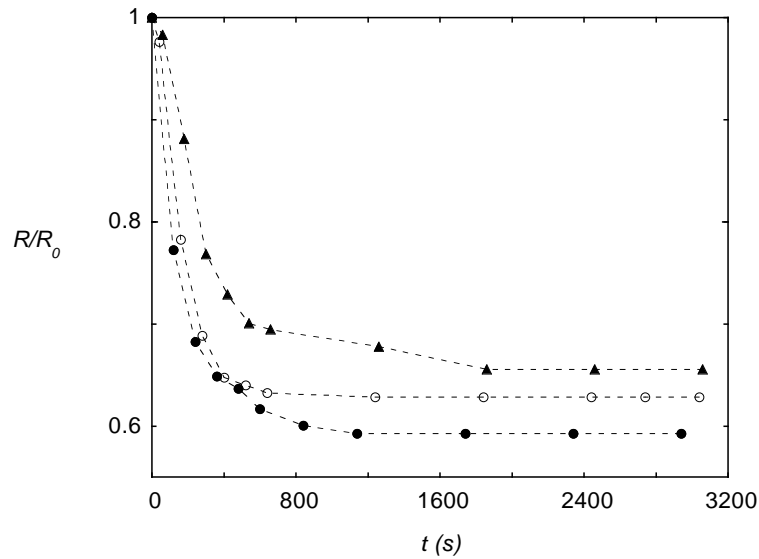


Figure 7.1: Relative shrinkage of vesicles with a radius of approximately  $20 \mu\text{m}$  subjected to an osmotic gradient of  $200 \text{ mM}$  glucose. The vesicles were composed of DOPG(●), DOPG-20 % cholesterol(○), or DOPG-40 % cholesterol (▲).

### 7.3 Results and Analysis

The gentle rehydration of the lipid film gave a suspension that contained a mixture of giant vesicles that was heterogeneous in both size and lamellarity. From this population of vesicles, unilamellar specimens were selected by looking for minimal contour contrast and absence of internal structure. These vesicles were subsequently followed in time during osmotic shrinkage and rehydration.

During osmotic shrinkage all vesicles tested remained approximately spherical, and no large shape fluctuations or shape instabilities were observed. Figure 7.1 shows the relative size decrease of giant vesicles of different composition with a radius of  $\sim 20 \mu\text{m}$  during exposure to an osmotic gradient of  $200 \text{ mM}$  glucose. More of these experiments were done with differently sized vesicles ( $20 \mu\text{m} < R < 40 \mu\text{m}$ ) and osmotic gradients of  $50 \text{ mM}$  and  $100 \text{ mM}$ . For these conditions similar behavior of  $R$  as a function of time was observed

Initially, the vesicle radius  $R$  decreased with time. The rate of size decrease was reproducible for vesicles composed of the same lipid species, but varied among vesicles of different composition. The more cholesterol the vesicle membrane contained the slower the rate of size decrease. After approximately 40 minutes the decrease in size had stopped for vesicles of all composition. Apparently osmotic equilibrium had been reached and therefore the vesicle radius remained constant in time (Fig. 7.1). The final  $R/R_0$  was a function of the composition (Fig. 7.1). DOPG vesicles that contained higher amounts of cholesterol always shrunk less when they were osmotically dehydrated.

## Osmotic shrinkage of giant vesicles

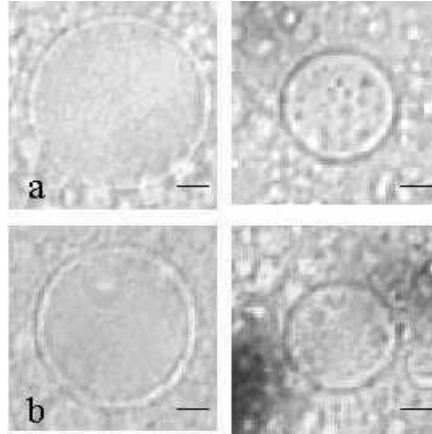


Figure 7.2: DOPG vesicles containing 20 % (a) and 40 % (b) cholesterol before ( $t=0$  s) (left) and after (right) osmotic contraction ( $t=3600$  s). The shrunken vesicles contains daughter vesicles that are approximately  $1.8 \mu\text{m}$  (a) and  $3.0 \mu\text{m}$  (b) in radius. The bar indicates  $10 \mu\text{m}$ .

The decrease in radius in a hypertonic solution was seen for all vesicles tested, but the giants did not always contain visible daughter vesicles. In vesicles composed of DOPG and 40 % cholesterol, daughter vesicles were clearly observed and approximately  $3.0 \mu\text{m}$  in radius (Fig. 7.2). The size of these daughter vesicles decreased with increasing amounts of cholesterol in the bilayer. In giants composed of pure DOPG daughter vesicles were never observed, probably because they were too small. During osmotic shrinkage the vesicles were always observed to appear inside the giant vesicle, outward extrusions were never seen.

As mentioned before, a possible explanation for the fact that daughter vesicles were never observed inside DOPG giants might be the limited resolution of the optical microscope. To test this hypothesis the size of the daughter vesicles was calculated from the osmotic gradient and the decrease in vesicle radius. The model used for these calculations assumes that the total membrane area is conserved during shrinkage, and that membrane is impermeable to both sucrose and glucose. If we assume that the total surface area is conserved by the formation of  $n$  daughter vesicles of radius  $r$ , the equilibrium area  $A(\infty)$  of the giant vesicle after shrinkage is given by:  $A(\infty) = 4\pi R(\infty)^2 = 4\pi R_0^2 - 4\pi n(\infty)r^2$ . This gives the following expression for the number of daughter vesicles  $n$ :

$$n(\infty) = \frac{R_0^2 - R(\infty)^2}{r^2} \quad (7.1)$$

Because the membrane is (almost) impermeable to sucrose and glucose the osmotic gradient will determine the end volume  $V_{end}$  of the shrunken giant. This  $V(\infty)$  is given by:  $V(\infty) = \frac{c_0}{\Delta c + c_0} (\frac{4}{3}\pi R_0^3)$ . At the same time  $V(\infty) = \frac{4}{3}\pi (R(\infty)^3 - n(\infty)r^3)$ . This gives the following expression for the radius of the

### 7.3 Results and Analysis

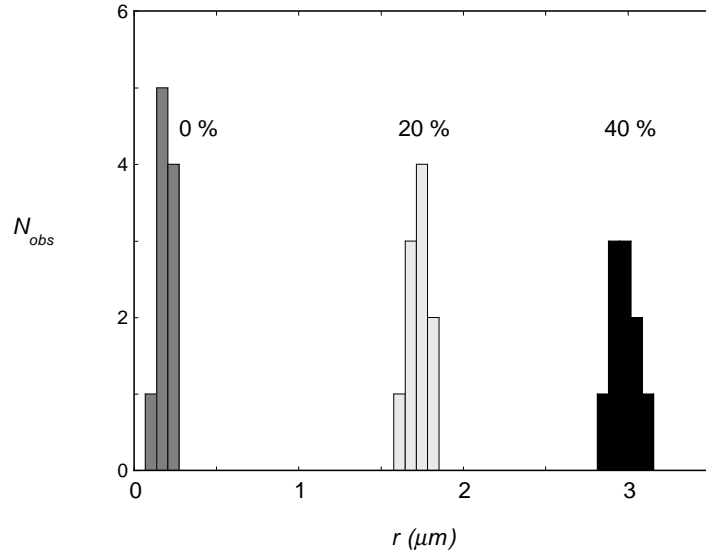


Figure 7.3: Histogram showing the radius of the daughter vesicles calculated from the concentration gradient and the vesicle radii before and after application of the osmotic gradient. The vesicles are composed of DOPG and cholesterol. The percentage cholesterol in the DOPG bilayer is indicated. For each composition 10 individual experiments were performed.

daughter vesicles inside the giant:

$$r = \frac{R(\infty)^3 - \frac{c_0}{c_0 + \Delta c} R_0^3}{R_0^2 - R(\infty)^2} \quad (7.2)$$

When equation 7.2 is used to obtain the radius of the DOPG daughter vesicles it gives  $r = 0.2 \pm 0.1 \mu\text{m}$ , which is indeed below the resolution of the optical microscope. For DOPG vesicles containing cholesterol much larger radii are found for the daughter vesicles (Fig. 7.3). The size of the daughter vesicles seems to depend strongly on composition;  $r$  increases from  $0.2 \mu\text{m}$  in pure DOPG vesicles to approximately  $3.0 \mu\text{m}$  in vesicles containing 40 % cholesterol. The values calculated for  $r$ , are very close to the radii of the daughter vesicles observed with optical microscopy (compare Fig. 7.2 and Fig. 7.3).

Now that the radii of the daughter vesicles are known, the water permeability of the bilayer can be obtained from the decrease of the vesicle radii in time (Fig. 7.1). Because the lipid bilayer is almost impermeable to glucose and sucrose, the hypertonic glucose solution outside withdraws water from the vesicle. The speed with which this loss of water through the membrane takes place is determined by the permeability for water of the bilayer,  $P$  ( $\mu\text{m}/\text{s}$ ). The water permeability of the bilayer  $P$  is given by the molar flow of water ( $v_w$  is molar volume of water) through the membrane  $J$ , and the concentration difference over the bilayer membrane  $\Delta c$

$$\frac{1}{A} \frac{dV}{dt} = P v_w \Delta c \quad (7.3)$$

## Osmotic shrinkage of giant vesicles

The loss of water from the vesicle takes place over a certain membrane area  $A$ . This area is not necessarily given by  $4\pi R^2$ , as some area might be hidden by vesicles that remain attached to their mother. Therefore the areal fraction from vesicles that remain attached to the bilayer  $\alpha$ , is introduced. The area that is accessible for water transport at any time is now given by:

$$A(t) = 4\pi [R(t)^2 + \alpha(R^2 - R(t)^2)] \quad (7.4)$$

During osmotic shrinkage  $\Delta c$  decreases. Because  $c(t) = c_0(V_0/V(t))$ ,  $\Delta c = c(t) - c_0$  can be calculated at any time, therefore equation 7.3 can be rewritten to

$$\frac{dR}{dt} = \frac{Pv_w}{(R(t)^2 + \frac{2}{3}rR(t))} \left( \frac{c_0R_0^3}{(R(t)^3 + rR(t)^2 - rR_0^2)} - c_b \right) ((1-\alpha)R(t)^2 + \alpha R_0^2) \quad (7.5)$$

in which  $c_b$  is the final concentration in- and outside the vesicle. As explained above,  $r$  is already known from the  $R/R_0$  ratio. From equation 7.5 it follows that besides the membrane permeability  $P$ , the amount of vesicles that remain attached to the bilayer  $\alpha$  can in principle be estimated from the change of the vesicle radius in time. The initial slope of the  $R$  versus time curves appears to be sensitive to  $P$ , whereas the value of  $\alpha$  can be found from the  $R(t)$  at higher values of  $t$ . We note that equation 7.5 can be solved analytically, but this results in a lengthy, complicated implicit relation between  $R$  and  $t$ . Therefore, equation 7.5 was fitted directly to the derivative of the observed size decrease in time (Fig. 7.4). Unfortunately, our experiment has too low a time resolution to obtain a reliable value for the permeability  $P$  of pure DOPG vesicles. The decrease of  $R$  in time is just too fast for these vesicles (Fig. 7.1), and therefore  $P$  is underestimated. For sufficiently high amounts of added cholesterol the process of shrinkage was slow enough to obtain more reliable data. For vesicles composed of DOPG with 20% cholesterol  $P=15.3\pm 3.4 \mu\text{m/s}$  whereas DOPG vesicles containing 40% cholesterol had a  $P$  of  $6.6 \pm 0.5 \mu\text{m/s}$ . The more cholesterol the DOPG bilayer contained the less permeable it became for water. The values found for  $\alpha$  did not differ much between vesicles of different composition. According to our model  $14 \pm 4 \%$  of the daughter vesicles remained attached to the mother giant.

Some of the vesicles that were followed in time had a water permeability that was much lower than the presented values. These lower values are probably associated with multilamellar vesicles (Boroske et al., 1981), and these cases were disregarded. Besides low optical contrast, the membrane permeability seems to be a good criterion for unilamellarity.

During shrinkage the daughter vesicles can either stay attached to their mother, or loose contact with the outer membrane. When the daughter vesicles remain in contact with their mother, they can easily be reincorporated into the membrane during osmotic inflation. When contact is lost the possibilities to increase the surface area upon osmotic inflation will be much more limited.

### 7.3 Results and Analysis

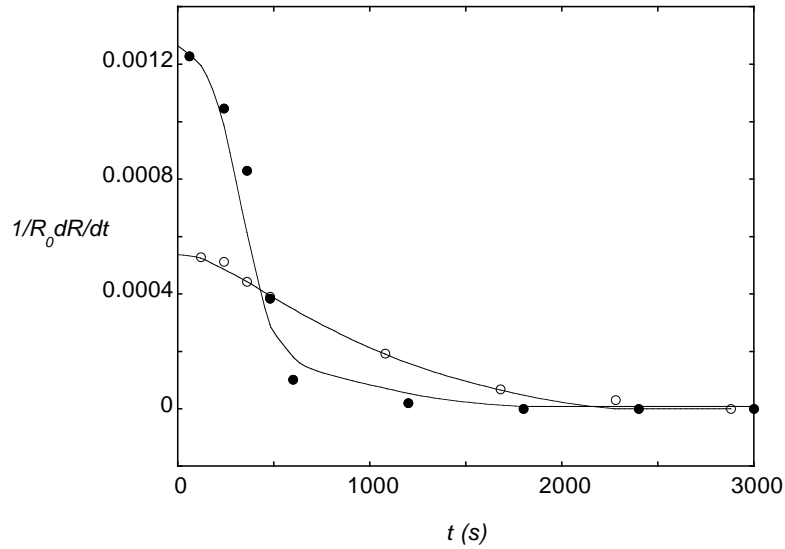


Figure 7.4: The measured  $\frac{1}{R_0} \frac{dR}{dt}$  as a function of time for giant vesicles composed of DOPG-20 % cholesterol (●) and DOPG-40 % cholesterol (○) in an initial osmotic gradient of 200 mM. The data was fitted with equation 7.5, which resulted in  $P=11.2$  and  $\alpha=0.15$  for DOPG vesicles containing 20 % cholesterol and in  $P=7.4$  and  $\alpha=0.17$  for those containing 40 % cholesterol.

To test whether some vesicles indeed remain continuous with the giant, as the values found for  $\alpha$  suggest, shrunken vesicles were subsequently subjected to a hypotonic glucose solution. To be able to determine whether the daughter vesicles remain attached to their mother, the reaction of unilamellar vesicles on osmotic inflation was tested first.

When fresh unstressed unilamellar (non-raspberry) vesicles were subjected to a hypotonic solution ( $\Delta c=50$  mM) they were able to increase their surface area by 4-9 %, depending on composition before they lysed. The more cholesterol the DOPG bilayer contained the smaller the area increase that had occurred before lysis. For bilayers composed of DOPG only an area increase of  $9.0 \pm 1.2$  % was measured, whereas DOPG bilayers containing 40 % cholesterol were able to increase their surface area by only  $4.1 \pm 1.3$  %.

To test whether the daughter vesicles remained attached to their mother, the reswelling experiment was repeated for the raspberry vesicles. The solution was replaced by a 50mM glucose solution, forcing the vesicles to grow in size. None of the vesicles was able to regain their original radius; the size increase was limited to approximately 22-28 % of the membrane surface area after shrinkage (Fig. 7.5). The maximum area increase depended slightly on composition. Vesicles composed of DOPG alone were able to increase their surface area by  $28 \pm 1.9$  %, whereas the vesicles composed of DOPG with 40 % cholesterol could increase their surface area by  $21 \pm 1.5$  % before they lysed.

During osmotic inflation the giant vesicles could in principle also increase their surface area by fusion with other stressed vesicles. Indeed, fusion of a

## Osmotic shrinkage of giant vesicles

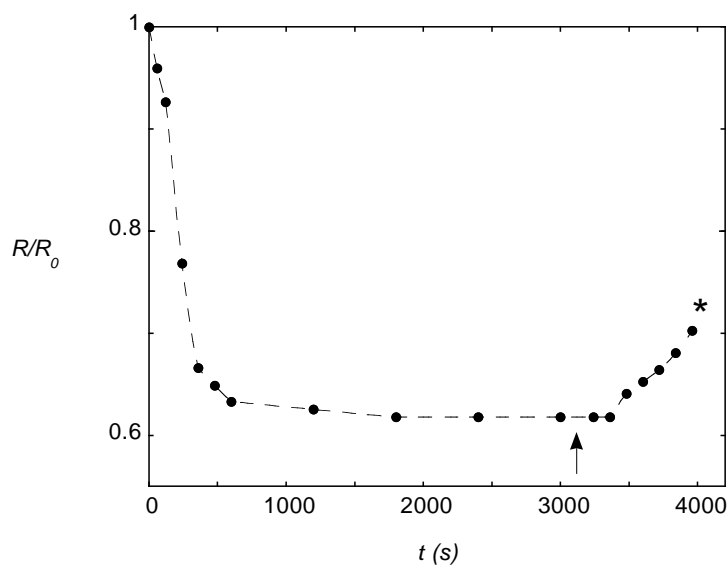


Figure 7.5: The relative change in radius of a vesicle composed of DOPG-20 % cholesterol upon de- and subsequent re-hydration. Rehydration was established by replacing the 250 mM sugar solution by a 50 mM glucose solution. After  $t=3000$  s the gradient was reversed (arrow), the vesicle lysed after  $t=4100$  s (\*).

shrunken giants with other giants was observed twice. This kind of fusion events also resulted in a faster relative size increase than the one presented in figure 7.5. In figure 7.6 the very rare fusion of two shrunken DOPG vesicles that have been osmotically dehydrated can be seen. The fusion of the vesicles was rather fast, full fusion had taken place within 4 minutes.

## 7.4 Discussion

Recently, giant unilamellar vesicles were reported to form inverted daughter vesicles when their internal volume is reduced by an osmotic gradient (Bernard



Figure 7.6: Fusing DOPG giants upon osmotic inflation after dehydration in a hypertonic glucose solution ( $\Delta c = 200$  mM). The photographs were taken two minutes apart.

## 7.4 Discussion

et al., 2002). The authors suggest that the observed wrinkling is associated with micro-segregation of the components of the vesicle membrane and that it is therefore only observed in multicomponent membranes. Vesicles composed of pure DPPC were reported not to exhibit this raspberry mode of shrinkage. In our experiments we showed that the radius of vesicles composed of DOPG decreases during osmotic deflation (Fig. 7.1). During this shrinkage the visible contours of the DOPG vesicles remains spherical. Indeed, we never observed any daughter vesicles inside the shrunken giants. Further analysis of the data (equation 7.2) suggests, however, that the one-component DOPG vesicles do also show the raspberry mode of shrinkage. The size of the inverted daughter vesicles is however calculated to be just  $0.2 \mu\text{m}$  and therefore too small to be observed by optical microscopy (Fig. 7.3). The observation that one-component vesicles are able to vesiculate makes the argument that the observed shrinkage is due to micro-segregation of the components in the vesicle membrane (Bernard et al., 2002) very unlikely .

An alternative explanation is suggested by the experiments in which cholesterol is added to the DOPG bilayer. Substances such as cholesterol are expected to increase the mean bending modulus  $k_c$  of the DOPG bilayer. The changes in  $k_c$  upon the incorporation of varying percentages of cholesterol in a DMPC bilayer have been measured and are indeed large (Duwe et al., 1990). With the incorporation of cholesterol into the DOPG bilayer, daughter vesicles became visible inside the mother giant after exposure to a hypertonic solution (Fig. 7.2). The size of the daughter vesicles was observed to increase with increasing cholesterol content (Fig. 7.3). Furthermore, the size of the daughter vesicles seems to be independent of the applied osmotic gradient. Hypertonic osmotic solution, which imposed a gradient of 50, 100, or 200 mM over the vesicle membrane all generated vesicles of the same size. The size of the daughter vesicles could only be influenced by changing the bilayer composition. This makes it very likely that the radius of the daughter vesicles is controlled by the persistence length  $\xi_p$ , and therefore the bare (intrinsic)  $k_c$  of the bilayer membrane. The bilayer has no resistance against shape fluctuations over length scales larger than  $\xi_p$ . This means that the effective mean bending modulus of the bilayer  $k_c^{eff}$  is not independent of the vesicle radius  $R$ . The renormalized mean bending modulus  $k_c^{eff}(R)$  is given by:

$$k_c^{eff}(R) = k_c - a \frac{k_B T}{4\pi} \ln \left[ \frac{R}{l} \right]$$

in which  $l$  is a length scale proportional to the size of the molecules, and  $a$  is a numerical constant of order unity. As  $\xi_p \propto l e^{\frac{4\pi k_c}{k_B T}}$ ,  $k_c^{eff}$  becomes zero when  $R \approx \xi_p$ . The same argument holds for the Gaussian bending modulus  $\bar{k}$ , and therefore the curvature energy given by  $E_{ves} = 4\pi(2k_c + \bar{k})$  will become zero at length scales much larger than  $\xi_p$ . This means that it will cost no curvature energy to form vesicles inside the giant provided that these vesicles are at least of the same order of magnitude as the persistence length. This relation also



## Osmotic shrinkage of giant vesicles

illustrates that substances that increase  $k_c$  such as cholesterol (Duwe et al., 1990) will increase the size of the daughter vesicles. Although the scaling relation will, in reality, be complicated by interactions between the (charged) vesicles (Simons and Cates, 1992), (Chapter 3), an increase in  $r$  with increasing cholesterol content is still observed.

In the dehydration experiments presented here, daughter vesicles always appeared on the inside of the mother giant; outward extrusions were never observed during osmotic shrinkage. The main reason for this might be the underpressure inside the vesicle. The faster decrease in vesicle volume with the same decrease in area when vesicles bud to the inside instead of to the outside might be a good explanation for this phenomenon. The development of outward extrusions during dehydration (by freezing) was however observed for giant vesicles composed of plasma membrane lipid extracts from cold acclimated rye leaves (Steponkus and Lynch, 1989). Giant vesicles made of the lipid extracts from non acclimated rye leaves showed the expected vesiculation to the inside upon freezing-induced dehydration. This difference in reaction on dehydration can only be explained by the difference in lipid composition between these two giant vesicles. Although it is unlikely that there are large differences in lipid composition between the two monolayers of the bilayer some degree of asymmetry in lipid composition is needed to explain the differences in behavior of the giant unilamellar vesicles of lipid extracts of acclimated and non acclimated rye leaves to dehydration. The asymmetry in monolayer composition must be a result of the special tendencies of some components or because of interactions between different lipids. This asymmetry in composition between the individual monolayers of the membrane is less likely in the simple two-component bilayers studied here.

The incorporation of cholesterol into the bilayer is expected to change not only  $k_c$  but also other physical properties of the lipid membrane. Cholesterol is known to fluidize gel phase membranes, and to increase the packing order in liquid crystalline bilayers. The increased packing order in the liquid crystalline phase is expected to decrease the water permeability of the bilayer. The incorporation of cholesterol in the DOPG bilayer does indeed influence the permeability of the lipid bilayer as can be seen from the slowing down of the kinetics of size decrease in figure 7.1. With increasing cholesterol content it becomes more difficult for water molecules to cross the membrane so that  $P$  decreases. Qualitatively, the decrease in membrane permeability with increasing cholesterol content has been observed before for DOPG bilayers (Yan and Eiseenthal, 2000). The permeability constants for cholesterol containing membranes obtained here are smaller than the literature values for pure phospholipid bilayers (Boroske et al., 1981), (Olbrich et al., 2000). The order of magnitude is however comparable, and therefore our data appears to be reliable.

From the literature data (Bernard et al., 2002) it is not perfectly clear whether the daughter vesicles remain attached to the mother giant during and after osmotic shrinkage. With the model used here to obtain  $P$  from the osmotic

## 7.4 Discussion

shrinkage experiments, it is possible to estimate the fraction of vesicles that remain attached to the mother giant. When an osmotic gradient of 200 mM was applied, approximately 15 % of the vesicles was found to remain attached to the mother membrane. The fraction of vesicles that remained attached turns out to be independent of the membrane composition.

When unstressed vesicles are subjected to a hypotonic osmoticum they are able to increase their surface area by 4-9 %. This is in agreement with the  $\delta A/A=3$  % reported for giant lechitin vesicles (Kwok and Evans, 1981) and the  $\delta A/A=4-6$  % (Rutkowski et al., 1991) or the  $\delta A/A=10$  % (Hallet et al., 1993) that were reported for small DOPG vesicles. The  $\delta A/A$  values measured decreased with increasing cholesterol content of the DOPG bilayer. This trend in maximal area increase before lysis of vesicles in a series of cholesterol contents agrees with the results obtained for cholesterol containing DMPC vesicles (Needham et al., 1988), and is usually ascribed to the increased bilayer cohesion by the addition of cholesterol. The fact that the vesicles always lysed at the same relative area increase suggests that critical fluctuations in lipid density within the bilayer may be the origin of the failure. This agrees with the idea of a critical rupture tension above which long term survival of the vesicle is very unlikely (Evans and Needham, 1986), (Evans and Needham, 1987).

When the same osmotic inflation experiments are done with vesicles that have first been dehydrated by a hypertonic osmoticum, an increase in area of 22-28 % is possible. This is significantly more than the 4-8 % area increase that is normally observed before lysis. The larger surface area increase that can be achieved after osmotic deflation suggests that some of the daughter vesicles remain attached to their mother and are readily available when an area increase is required. Fusion of other expanding vesicles in the medium with the expanding giant is rarely observed, and therefore a very unlikely mechanism of area increase. Besides, this fusion mechanism would just be as likely in normal (non-raspberry) expanding vesicles. Fusion of vesicles inside the giant with the outer membrane is expected to be a matter of chance and kinetically as slow as fusion from the outside; the good reproducibility of our data does not support fusion with daughter vesicles in the giant's interior. A study on model systems has shown that vesicle swelling actually inhibits fusion (Malinin et al., 2002), which also supports our assumption.

The differences in  $\delta A/A$  values between shrunken vesicles of different composition are comparable to those of  $\delta A/A$  values obtained for normal unilamellar vesicles. This suggests that these differences are caused by the differences in elasticity of the lipid bilayer. The amount of material incorporated during osmotic inflation is thus comparable for all lipid compositions. It amounts to approximately 11 % of all the vesicles that were formed during shrinkage. This percentage is in good agreement with the fraction of vesicles that remain attached during shrinkage obtained from fitting the decrease of  $R$  in time (14 %).

# Bibliography

- Almgren, M. Mixed micelles and other structures in the solubilization of bilayer lipid membranes by surfactants. *Biochim. Biophys. Acta*, 1508:146–163, 2000.
- Arnold, K. Cation-induced vesicle fusion modulated by polymers and proteins. In R. Lipowsky and E. Sackmann, editors, *Handbook of Biological Physics*, volume 1, chapter 19, pages 904–957. Elsevier Science B.V., 1995.
- Barchini, R., H.P. van Leeuwen, and J. Lyklema. Electrodynamics of liposome dispersions. *Langmuir*, 16:8238–8247, 2000.
- Basanez, G., F.M. Goni, and A. Alonso. Effect of single chain lipids on phospholipase C-promoted vesicle fusion. A test for the stalk hypothesis of membrane fusion. *Biochemistry*, 37:3901–3908, 1998.
- Bergström, M., J.S. Pedersen, P. Schurtenbergen, and S.U. Egelhaaf. Small-angle neutron scattering (SANS) study of vesicles and lamellar sheets formed from mixtures of an anionic and a cationic surfactant. *J. Phys. Chem. B.*, 103:9888–9897, 1999.
- Bernard, A.L., M.A. Guedeau-Boudeville, L. Jullien, and J.M. di Meglio. Raspberry vesicles. *Biochim. Biophys. Acta*, 1567:1–5, 2002.
- Bliss, R.D., K.A. Platt-Aloia, and W.W. Thomson. Changes in plasmalemma organization in cowpea radicle during imbibition in water and NaCl solutions. *Plant Cell Environ.*, 7:601–606, 1984.
- Boomgaard van den, T. and J. Lyklema. Salt effects in free nonionic films. *Langmuir*, 245:245–249, 1989.
- Boroske, E., M. Elwenspoek, and W. Helfrich. Osmotic shrinkage of giant egg-lecithin vesicles. *Biophys. J.*, 34:95–109, 1981.
- Cevc, G. Membrane electrostatics. *Biochim. Biophys. Acta*, 1031:311–382, 1990.
- Chabot, J.F. and A.C. Leopold. Ultrastructural changes of membranes with hydration in soybean seeds. *Amer. J. Bot.*, 69:623–633, 1982.

## BIBLIOGRAPHY

- Chen, Z. and R.P. Rand. Comparative study of the effects of several n-alkanes on phospholipid hexagonal phases. *Biophys. J.*, 74:994–952, 1998.
- Chernomordik, L., M.M. Kozlov, and J. Zimmerberg. Lipids in biological membrane fusion. *J. Membrane Biol.*, 146:1–14, 1995.
- Creutz, C.E. cis-Unsaturated fatty acids induce the fusion of chromaffin granules aggregated by synexin. *J. Cell Biol.*, 91:247–256, 1981.
- Daicic, J.A., A. Fogden, Carlson I., H. Wennerström, and B. Jonsson. Bending of ionic surfactant monolayers. *Phys. Rev. E*, 54:3985–3998, 1996.
- Duwe, H.P., J. Kaes, and E. Sackmann. Bending elastic moduli of lipid bilayers: modulation by solutes. *J. Phys. France*, 51:945–962, 1990.
- Eisenberg, M., T. Gresalfi, T. Riccio, and S. McLaughlin. Adsorption of monovalent cations to bilayer membranes containing negative phospholipids. *Biochemistry*, 23:5213–5223, 1979.
- Emons, A.M.C., W.J. Vos, and H. Kieft. A freeze fracture analysis of the surface of embryogenic and non-embryogenic suspension cells of *Daucus carota*. *Plant Science*, 87:85–97, 1992.
- Evans, E. and D. Needham. Giant vesicle bilayers composed of mixtures of lipids, cholesterol and polypeptides. *Faraday Discuss. Chem. Soc.*, 81:267–280, 1986.
- Evans, E. and D. Needham. Physical properties of surfactant bilayer membranes: thermal transitions, elasticity, rigidity, cohesion, and colloidal interactions. *J. Phys. Chem.*, 91:4219–4228, 1987.
- Fogden, A., J. Daicic, and A. Kidane. Undulating charged fluid membranes and their bending constants. *Phys. II France*, 7:229–248, 1997.
- Glaser, P.E. and R.W. Gross. Plasmamylethanolamine facilitates rapid membrane fusion: a stopped-flow kinetic investigation correlating the propensity of a major plasma membrane constituent to adopt an HII phase with its ability to promote membrane fusion. *Biochemistry*, 33:5805–5812, 1994.
- Goni, F.M., J.N. Nieva, B. Basanez, G. Fidelio, and A. Alonso. Phospholipase-C-promoted liposome fusion. *Biochem. Soc. Trans.*, 22:839–844, 1994.
- Gordon-Kamm, W.J. and P.L. Steponkus. The behavior of the plasma membrane following osmotic contraction of isolated protoplasts: Implications in freezing injury. *Protoplasma*, 123:83–94, 1984a.
- Gordon-Kamm, W.J. and P.L. Steponkus. The influence of cold acclimation on the behavior of the plasma membrane following osmotic contraction of isolated protoplasts. *Protoplasma*, 123:161–173, 1984b.

## BIBLIOGRAPHY

- Gustafsson, J., G. Orådd, and M. Almgren. Disintegration of the lecithin lamellar phase by cationic surfactants. *Langmuir*, 13:6956–6963, 1997.
- Hallet, F.R., J. Marsh, B.G. Nickel, and J.M. Wood. Mechanical properties of vesicles II A model for osmotic swelling and lysis. *Biophys. J.*, 64:435–442, 1993.
- Hammoudah, M.M., S. Nir, J. Bentz, E. Mayhew, T.P. Stewart, S.W. Hui, and R.J. Kurland. Interactions of La<sup>3+</sup> with phosphatidylserine vesicles, binding, phase transition, leakage, 31P-NMR and fusion. *Biochim. Biophys. Acta*, 645:102–114, 1981.
- Haque, M.E., T.J. McIntosh, and B.R. Lentz. Influence of lipid composition on physical properties of PEG-mediated fusion of curved and uncurved model membrane vesicles: "nature's own" fusogenic lipid bilayer. *Biochemistry*, 40: 4340–4348, 2001.
- Helfrich, W. Elastic properties of lipid bilayers: theory and possible experiments. *Z. Naturforsch.*, 28c:693–703, 1973.
- Herve, P., D. Roux, A.M. Bellocq, F. Nallet, and T. Gulik-Krzywicki. Dilute and concentrated phases of vesicles at thermal equilibrium. *J. Phys. II France*, 3:1255–1270, 1993.
- Hobbs, P.R. and R.L. Obendorf. Interaction of initial seed moisture and imbibitional temperature on germination and productivity of soybean. *Crop Science*, 12:664–667, 1972.
- Hoekstra, F.A., J.H. Crowe, and L.M. Crowe. Germination and ion leakage are linked with phase transitions of membrane lipids during imbibition of *Typha latifolia* pollen. *Physiol. Plant.*, 84:29–34, 1992.
- Hoekstra, F.A., E.A. Golovina, A.C. Van Aelst, and M.A. Hemminga. Imbibitional leakage from anhydrobiotes revisited. *Plant Cell Environ.*, 22: 1121–1131, 1999.
- Hoekstra, F.A. and E.W. Van der Wal. Initial moisture content and temperature of imbibition determine extent of imbibitional injury in pollen. *J. Plant. Physiol.*, 133:257–262, 1988.
- Israelachvili, J.N., D.J. Mitchell, and B.W. Ninham. Theory of self-assembly of hydrocarbon amphiphiles into micelles and bilayers. *J. Chem. Soc. Faraday Trans. II*, 72:1525–1568, 1976.
- Israelachvili, J.N., D.J. Mitchell, and B.W. Ninham. Theory of self-assembly of lipid bilayers and vesicles. *Biochim. Biophys. Acta*, 470:185–201, 1977.

## BIBLIOGRAPHY

- Jung, H.T., B. Coldren, J.A. Zasadzinski, D.J. Iampietro, and E.W. Kaler. The origins of stability of spontaneous vesicles. *Proc. Natl. Acad. Sci. U.S.A.*, 98:1353–1357, 2001.
- Kaler, E.W., A.K. Murthy, B.E. Rodriguez, and J.A. Zasadzinski. Spontaneous vesicle formation in aqueous mixtures of single-tailed surfactants. *Science*, 245:1371–1374, 1989.
- Klößen, B. and W. Helfrich. Cryotransmission electron microscopy of a superstructure of fluid dioleoylphosphatidylcholine (dopc) membranes. *Biophys. J.*, 73:3016–3029, 1997.
- Koynova, R. and M. Caffrey. Phases and phase transitions of the phosphatidylcholines. *Biochim. Biophys. Acta*, 1376:91–145, 1998.
- Kozlov, M.M. and V.S. Markin. Possible mechanism of membrane fusion. *Biofizika*, 28:255–261, 1983.
- Kozlovsky, Y. and M.M. Kozlov. Stalk model of membrane fusion: solution of energy crisis. *Biophys. J.*, 82:882–895, 2002.
- Kraayenhof, R., G.J. Sterk, H.W. Wong Fong Sang, K. Krab, and R.M. Epanand. Monovalent cations differentially affect membrane surface properties and membrane curvature, as revealed by fluorescent probes and dynamic light scattering. *Biochim. Biophys. Acta*, 1282:293–302, 1996.
- Kubitschek, U., U. Homann, and G. Thiel. Osmotically evoked shrinking of guard-cell protoplasts causes vesicular retrieval of plasma membrane into the cytoplasm. *Planta*, 210:423–431, 2000.
- Kumaran, V. Effect of surface charges on the curvature moduli of a membrane. *Phys. Rev. E*, 64:1–9, 2001.
- Kwok, R. and E. Evans. Thermoelasticity of large lecithin bilayer vesicles. *Biophys. J.*, 35:637–652, 1981.
- Lasic, D.D. On the thermodynamic stability of liposomes. *J. Colloid Interface Sci.*, 140:302–304, 1990.
- Lasic, D.D., R. Joannic, B.C. Keller, P.M. Frederik, and L. Auvray. Spontaneous vesiculation. *Adv. Colloid Interface Sci.*, 89:337–349, 2001.
- Lee, J. and B.R. Lentz. Secretory and viral fusion may share mechanistic events with fusion between curved lipid bilayers. *Proc. Natl. Acad. Sci. USA*, 95: 9274–9279, 1998.
- Leermakers, F.A.M., A.L. Rabinovich, and N.K. Balabaev. Self-consistent-field modeling of hydrated unsaturated lipid bilayers in the liquid-crystal phase and comparison to molecular dynamic simulations. *Phys. Rev. E*, 67:011910 1–17, 2003.

## BIBLIOGRAPHY

- Lekkerkerker, H.N.W. Contribution of the electric double layer to the curvature elasticity of charged amphiphilic monolayers. *Physica A*, 159:319–328, 1989.
- MacDonald, R.C., F.C. Jones, and R. Qui. Fragmentation into small vesicles of dioleoylphosphatidylcholine bilayers during freezing and thawing. *Biochim. Biophys. Acta*, 1191:362–370, 1994.
- Madani, H. and E.W. Kaler. Aging and stability of vesicular dispersions. *Langmuir*, 6:125–132, 1990.
- Malinin, V.S., P. Frederik, and B.R. Lentz. Osmotic and curvature stress affect PEG-induced fusion of lipid vesicles but not mixing of their lipids. *Biophys. J.*, 82:2090–2100, 2002.
- Markin, V.S. and J.P. Albanesi. Membrane fusion: stalk model revisited. *Biophys. J.*, 82:693–712, 2002.
- Marques, E.F. Size and stability of catanionic vesicles: effects of formation path, sonication, and aging. *Langmuir*, 16:4798–4807, 2000.
- Marsh, D. General discussion. In D.A. Young, editor, *Lipid vesicles and membranes*, Faraday discussions of the chemical society, pages 63–64, London, 1986. Royal society of chemistry.
- Mayer, A. Membrane fusion in eukaryotic cells. *Annu. Rev. Cell Dev. Biol.*, 18:289–314, 2002.
- McIntosh, T.J., S. Advani, R.E. Burton, D.V. Zhelev, D. Needham, and S.A. Simon. Experimental tests for protrusion and undulation pressures in phospholipid bilayers. *Biochemistry*, 34:8520–8532, 1995.
- Meijer, L.A., F.A.M. Leermakers, and J. Lyklema. Modeling the interactions between phospholipid-bilayer membranes with and without additives. *J. Phys. Chem.*, 99:17282–17293, 1995.
- Meijer, L.A., F.A.M. Leermakers, and J. Lyklema. Self-consistent-field modeling of complex molecules with united atom detail in inhomogeneous systems. Cyclic and branched foreign molecules in dimristoylphosphatidylcholine membranes. *J. Chem. Phys.*, 110:6560–6579, 1999.
- Meleard, P., C. Gerbeaud, P. Bardusco, N. Jeandaine, M.D. Mitov, and L. Fernandez-Puente. Mechanical properties of model membranes studied from shape transformations of giant vesicles. *Biochimie*, 80:401–413, 1998.
- Mitchell, D.J. and B.W. Ninham. Micelles, vesicles and microemulsions. *J. Chem. Soc., Faraday Trans. 2*, 77:601–629, 1981.
- Morse, D.C. and S.T. Milner. Statistical mechanics of closed fluid membranes. *Phys. Rev. E*, 52:5918–5945, 1995.

## BIBLIOGRAPHY

- Needham, D., T.J. McIntosh, and E. Evans. Thermomechanical and transition properties of dimyristoylphosphatidylcholine/cholesterol bilayers. *Biochemistry*, 27:4668–4673, 1988.
- Nir, S., J. Wilschut, and J. Bentz. The rate of fusion of phospholipid vesicles and the role of bilayer curvature. *Biochim. Biophys. Acta*, 688:275–278, 1982.
- Olbrich, K., W. Rawicz, D. Needham, and E. Evans. Water permeability and mechanical strength of polyunsaturated lipid bilayers. *Biophys. J.*, 79:321–327, 2000.
- Olsson, U. and H. Wennerström. On the ripening of vesicle dispersions. *J. Phys. Chem. B*, 106:5135–5138, 2002.
- Oparka, K.J., D.A.M. Prior, and N. Harris. Osmotic induction of fluid-phase endocytosis in onion epidermal cells. *Planta*, 180:555–561, 1990.
- Oversteegen, S.M. and F.A.M. Leermakers. Thermodynamics and mechanics of bilayer membranes. *Phys. Rev. E*, 62:8453–8461, 2000.
- Platt, K.A., M.J. Oliver, and W.W. Thomson. Membranes and organelles of dehydrated Selaginella and Tortula retain their normal configuration and structural integrity. *Protoplasma*, 178:57–65, 1994.
- Rabinovich, A.L., P.O. Ripatti, N.K. Balabaev, and F.A.M. Leermakers. Molecular dynamics simulations of hydrated unsaturated lipid bilayers in the liquid-crystal phase and comparison to self consistent field modeling. *Phys. Rev. E*, 67:011909 1–14, 2003.
- Rawicz, W., K.C. Olbrich, T. McIntosh, D. Needham, and E. Evans. Effect of chain length and unsaturation on elasticity of lipid bilayers. *Biophys. J.*, 79:328–339, 2000.
- Ópik, H. The ultrastructure of coleoptile cells in dry rice (*Oryza sativa* L.) grains after anhydrous fixation with osmium tetroxide vapour. *New Phytol.*, 85:521–529, 1980.
- Ópik, H. The fine structure of some dry seed tissues observed after completely anhydrous chemical fixation. *Ann. Bot.*, 56:453–466, 1985.
- Rutkowski, C.A., L.M. Williams, T.H. Haines, and H.Z. Cummins. The elasticity of synthetic phospholipid vesicles obtained by photon correlation spectroscopy. *Biochemistry*, 30:5688–5696, 1991.
- Safran, S.A., P. Pincus, and D. Andelman. Theory of spontaneous vesicle formation in surfactant mixtures. *Science*, 248:354–356, 1990.
- Safran, S.A., P.A. Pincus, D. Andelman, and F.C. MacKintosh. Stability and phase behavior of mixed surfactant vesicles. *Phys. Rev. A*, 43:1071–1078, 1991.



## BIBLIOGRAPHY

- Schwarz, H. and A.L. Koch. Phase and electron microscopic observations of osmotically induced wrinkling and the role of endocytotic vesicles in the plasmolysis of the Gram-negative cell wall. *Microbiology*, 141:3161–3170, 1995.
- Seifert, U. and R. Lipowsky. Morphology of vesicles. In R. Lipowsky and E. Sackmann, editors, *Handbook of biological physics*, volume 1, pages 403–460. Elsevier, Amsterdam, 1995.
- Siegel, D.P. Energetics of intermediates in membrane fusion: comparison of stalk and inverted micellar intermediate mechanisms. *Biophys. J.*, 65:2124–2140, 1993.
- Siegel, D.P. The mechanism of lamellar-to-inverted hexagonal phase transitions in phosphatidylethanolamine: implications for membrane fusion mechanism. *Biophys. J.*, 73:3089–3111, 1997.
- Siegel, D.P. The modified stalk mechanism of lamellar/inverted phase transitions and its implications for membrane fusion. *Biophys. J.*, 76:291–313, 1999.
- Simons, B.D. and M.E. Cates. Vesicles and onion phases in dilute surfactant solutions. *J. Phys. II France*, 2:1439–1451, 1992.
- Singer, J.S. and G.L. Nicholson. The fluid mosaic model of the structure of cell membranes. *Science*, 175:720–731, 1972.
- Staelin, L.A. and R.L. Chapman. Secretion and membrane recycling in plant cells: novel intermediary structures visualized in ultrarapidly frozen sycamore and carrot suspension-culture cells. *Planta*, 171:43–57, 1987.
- Steponkus, P.L. and D.V. Lynch. The behavior of large unilamellar vesicles of rye plasma membrane lipids during freeze/thaw induced osmotic excursions. *Cryo-Letters*, 10:43–50, 1989.
- Szleifer, I., E. Kramer, and A. Ben-Shaul. Curvature elasticity of pure and mixed surfactant films. *Phys. Rev. Lett.*, 60:1966–1969, 1988.
- Tatulian, S.A. Effect of lipid phase transition on the binding of anions to dimyristoylphosphatidylcholine liposomes. *Biochim. Biophys. Acta*, 736:189–195, 1983.
- Tatulian, S.A. Binding of alkaline-earth metal cations and some anions to phosphatidylcholine liposomes. *Eur. J. Biochem.*, 170:413–420, 1987.
- Thomson, W.W. and K.A. Platt. Conservation of cell order in desiccated mesophyll of *Selaginella lepidophylla*. *Ann. Bot.*, 79:439–447, 1997.

## BIBLIOGRAPHY

- Verkerk, G., J.B. Broens, W. Kranendonk, R.J. Van der Puijl, J.L. Sikkema, and C.W. Stam. *Binas*. Wolters-Noordhof, Groningen, the Netherlands, 1986.
- Vogel, S.S., E.A. Leikina, and L.V. Chernomordik. Lysophosphatidylcholine reversibly arrests exocytosis and viral fusion at a stage between triggering and membrane merger. *J. Biol. Chem.*, 268:25764–25768, 1993.
- Walter, A., P.L. Yeagle, and D.P. Siegel. Diacylglycerol and hexadecane increase divalent cation-induced lipid mixing rates between phosphatidylserine large unilamellar vesicles. *Biophys. J.*, 66:366–376, 1994.
- Wilschut, J., N. Duzgunes, D. Hoekstra, and Papahadjopoulos D. Modulation of membrane fusion by membrane fluidity: temperature dependence of divalent cation induced fusion of phosphatidylserine vesicles. *Biochemistry*, 24: 8–14, 1985.
- Winterhalter, M. and W. Helfrich. Effect of surface charge on the curvature elasticity of membranes. *J. Phys. Chem.*, 92:6865–6867, 1988.
- Wolfe, J. and P.L. Steponkus. The stress-strain relation of the plasma membrane of isolated plant protoplasts. *Biochim. Biophys. Acta*, 643:663–668, 1981.
- Wolfe, J. and P.L. Steponkus. Mechanical properties of the plasma membrane of isolated plant protoplasts. *Plant Physiol.*, 71:276–285, 1983.
- Yan, E.C.Y. and B.E. Eisenhal. Effect of cholesterol on molecular transport of organic cations across liposome bilayers probed by second harmonic generation. *Biophys. J.*, 79:898–903, 2000.
- Yang, L. and H.W. Huang. Observation of a membrane fusion intermediate structure. *Science*, 297:1877–1879, 2002.
- Yeagle, P.L., F.T. Smith, J.E. Young, and T.D. Flanagan. Inhibition of membrane fusion by lysophosphatidylcholine. *Biochemistry*, 33:1820–1827, 1994.

# Summary

## Imbibitional damage

Most seeds, yeasts, and pollen have the amazing property that they can survive a state of very strong dehydration and subsequent rehydration; this is called desiccation tolerance. Desiccation tolerance is not reserved for these systems; it can even be found in some higher plants and animals. However, although the structural integrity of the cells is preserved in the dry state, problems sometimes arise during rehydration. When dry cells take up water too quickly, they may suffer imbibitional injury. This kind of damage is especially common in seeds of (sub)tropical crops, and it is particularly severe at very low water content, or temperature. The main target of injury appears to be the plasma membrane, that loses its ability to serve as a (semi-permeable) barrier between the intra- and extra-cellular space. Imbibitional damage is therefore usually characterized by an enormous loss of intra-cellular substances, and the subsequent death of the affected cells.

The nature of the damage is probably related to the dramatic increase in the membrane surface area to cell volume ratio upon dehydration. The cells cope with the excess surface area by vesiculation and folding of the plasma membrane. This can however give problems during rehydration of the cells when the kinetics of protoplast growth exceed those of membrane expansion. If the membrane is not able to unfold and to recruit membrane material from the vesicles fast enough the plasma membrane will rupture.

It is not entirely clear why in some cases the vesicles and folds cannot be incorporated into the plasma membrane fast enough. Although the reason for this might well be hidden in a complex biochemical machinery, it is very plausible the generic physical and chemical aspects play an important role as well. The work in this thesis is therefore focused on obtaining more knowledge on the thermodynamic and mechanical characteristics of (model)membranes.

## Vesicle stability

In this thesis it is established that the size of negatively charged phospholipid vesicles is probably a thermodynamically regulated quantity. Independent of the initial vesicle size distribution the freeze thaw method gives rise to vesicles

of a certain radius. If the solubility of the individual phospholipids is high enough (low ionic strength) vesicles having the same radius were obtained by ripening of the vesicle solution. Furthermore, the dependence of the vesicle radius on the lipid concentration corresponded to the scaling relation predicted in the literature for vesicles stabilized by undulations and translational entropy. Translational entropy will favor the formation of many small vesicles, but by bending the bilayer on a length scale much smaller than its persistence length  $\xi_p$ , the membrane will lose undulation entropy. The vesicle radius  $R$  of entropically stabilized vesicles will therefore be set, in first order, by the bending modulus of the bilayer  $k_c$  which is related to  $\xi_p$ .

To obtain insight into the behavior of  $k_c$  of a charged lipid bilayer as a function of ionic strength we performed self-consistent field calculations. Indeed, when the experimentally obtained vesicle radius was correlated with the theoretical predictions for  $k_c$  very similar ionic strength dependences were found. Unfortunately we were unable to directly compare data from experiments with calculations; the exact relation between  $k_c$  and the vesicles radius still needs to be investigated.

Although the size of the vesicles obtained by the freeze thaw method did not depend on the initial vesicle size distribution, the ionic strength had a large influence on the final vesicle radius. At low ionic strength the vesicle radius  $R$  decreased whereas at high ionic strength it increased with salt concentration. This can be attributed to the combined effects of the thickness of the bilayer and the electric double layer thickness on  $k_c$  and thus on  $R$ . At low ionic strength the decrease in double layer thickness dominates over the increase in bilayer thickness.

The increase in bilayer thickness is partly due to the closer packing of the phospholipids as their negative charge gets screened by the counter ions present in solution. Ions however also dehydrate the membrane and this adds to the increase in bilayer thickness with increasing ionic strength. The amount of dehydration of the membrane by ions depends on the ion hydration, as was observed in both the calculations on  $k_c$  and measurements of dioleoylphosphatidylglycerol (DOPG) vesicle radii. In the series  $\text{Cl}^-$ ,  $\text{Br}^-$ ,  $\text{I}^-$ , chloride is the most strongly hydrated ion; it therefore tends to dehydrate the membrane more than bromide and iodide. The increase in vesicle radius at high ionic strength is therefore faster in the presence of NaCl compared to NaBr and NaI.

The influence of cations on the equilibrium radius of charged lipid vesicles is more difficult to understand. The picture sketched above is complicated by specific binding of cations to the negatively charged phospholipid headgroup. The most strongly hydrated alkali cations also have the highest binding affinity. By binding, cations decrease the surface charge density on the bilayer. Theory predicts that  $k_c$  should scale with the square of the surface charge density. Cation hydration and binding have opposed effects on  $k_c$ ; this means that in a series of the alkali chlorides  $\text{Li}^+$ ,  $\text{Na}^+$ ,  $\text{K}^+$ ,  $\text{Rb}^+$ ,  $\text{Cs}^+$ , at a certain ionic strength, a maximum in equilibrium DOPG radius is found for the vesicles in

KCl.

Charge plays a very important role in stabilization of the vesicle phase. Vesicles composed of the zwitterionic lipid dioleoylphosphatidylcholine (DOPC) are not stable against the formation of lamellar sheet phases when their surface charge is approximately zero. Anions are known to bind specifically to the choline headgroup; they thereby increase the surface charge on the vesicles. At high enough surface charge the vesicle phase is preferred over the formation of lamellar sheets. The salt and lipid concentration range over which stable phosphatidylcholine vesicles are found depends on the binding constant of the anion. In the presence of anions with low binding affinity such as  $\text{Cl}^-$  the vesicular phase is small or non-existent, while in the presence of the more strongly binding  $\text{Br}^-$  and  $\text{I}^-$  the vesicular phase becomes larger.

From the above it is clear that one-component vesicles can be stabilized against the formation of multilamellar sheets by their surface charge, translational entropy, and undulations. There has however been an extensive discussion in the literature on the role of a spontaneous curvature in the stabilization of the vesicle phase. In bilayers composed of surfactant mixtures an asymmetric distribution of molecules over the monolayers could in principle give rise to a non zero spontaneous curvature. SCF calculations show however that to obtain vesicles with a spontaneous curvature, very specific circumstances are needed. There is a very narrow regime of interaction energies between the components where phase separation over the monolayers occurs, and where the formation of vesicles of different composition is not favored over the formation of a mixed vesicle. In these cases there are compositions where vesicles with a spontaneous curvature can be found. The composition range is however small as the curvature changes fast with changes in monolayer composition.

In most circumstances, equilibrium vesicles of mixed composition are most likely stabilized by entropy. This is demonstrated in a study of the radius of phospholipid-phospholipid and phospholipid-surfactant mixtures prepared by the freeze-thaw method. The radius of vesicles of these mixtures behaved comparable to  $k_c$  obtained in SCF calculations as a function of both salt concentration and composition. The vesicles of mixed composition have a smaller equilibrium radius compared to one-component vesicles. Due to changes in surface density the minimum in  $k_c$  and  $R$  does not occur at equimolar composition for a bilayer composed of a mixture of DOPC and DOPG.

## Vesicle fusion

Vesicles are often used as model systems to study membrane fusion. We argued that the vesicle radius is in principle a thermodynamically regulated quantity. This observation has potential impact on fusion studies, as being off equilibrium must be a stimulus for vesicles to fuse. Besides being off equilibrium the value of the bilayers Gaussian bending modulus  $\bar{k}$  may also play a role. For negative values of  $\bar{k}$  bilayers are stable. But when  $\bar{k}$  approaches zero or becomes positive

the membrane can lower its free energy by the formation of connectors and reducing the number of objects in solution.

From the literature it is known that alkanes promote fusion of vesicles, while micelle forming surfactants are fusion inhibitors. To observe the reaction of  $k_c$  and  $\bar{k}$  on additives, the bending moduli of phospholipid like membranes containing alkane and surfactant like molecules were determined from SCF calculations. These calculations showed that additives such as alkanes tend to increase  $k_c$  (and thus the equilibrium vesicle radius) and bring  $\bar{k}$  close to zero. Micelle forming surfactants on the other hand were predicted to lower  $k_c$  and give rise to more negative values of  $\bar{k}$ . From this, it follows that when the vesicle radius is smaller than the equilibrium radius and  $\bar{k} \geq 0$  fusion can occur. Unfortunately our analysis can only be used to evaluate the energy and entropy of a system before and after fusion. Whether fusion really takes place is expected to depend on the energy costs of the highly bent fusion intermediates.

## Osmotic shrinkage and reswelling

When giant vesicles are subjected to a hypertonic osmotic gradient they behave very similar to plasma membranes. To deal with the arising excess membrane area the giants split off small vesicles to their inside. As a result the giant vesicles remain spherical during the shrinkage process. The size of the daughter vesicles does not depend on the extent of water loss, but it is a function of the membrane composition. Experiments, in which the cholesterol content of a DOPG bilayer is varied, suggest that the size of the daughter vesicles is related to the mean bending modulus  $k_c$  of the bilayer. The incorporation of cholesterol gives rise to stiffer membranes (higher  $k_c$ ) and therefore to larger daughter vesicles. The fact that giant vesicles composed of only DOPG also vesiculate upon dehydration, indicates that it is very unlikely that a spontaneous curvature plays a role in the determination of the size of the daughter vesicles.

The vesiculation of the plasma membrane upon osmotic contraction might make it difficult for the membrane to expand to its original size during osmotic inflation. If the daughter vesicles stay attached to the mother bilayer they can be readily incorporated into the bilayer. When they lose contact the increase in surface area is limited by the finite extensibility of the bilayer. From the kinetics of shrinkage it is possible to estimate the number of daughter vesicles that remain attached to the bilayer. It was found that in an hypertonic osmotic gradient of 200 mM approximately 14 % of the vesicles remain attached to the giant. This number was found to be independent of the bilayer composition. Experiments in which the osmotic gradient was reversed confirm this result. In a hypotonic osmotic gradient only a limited increase in surface area is possible (22-28%), indicating that 11 % of the daughter vesicles could be incorporated into the giant's membrane.

## Outlook

As pointed out in the introductory chapter of this thesis, cells of desiccation tolerant organisms change their membrane surface area during de- and re-hydration by fission from and fusion of vesicles with the plasma membrane, respectively. This mechanism of dealing with changes in the membrane area to cell volume ratio is of course much more general. Because the relative elastic expansion of biological membranes is limited to about 5%, cells have to make use of a membrane reservoir of vesicles when larger changes in area are necessary. When cells do not have access to this membrane reservoir they rupture upon expansion.

Although in biological systems an intricate protein machinery and the cytoskeleton probably play a very important role in fission from and fusion with the plasma membrane it is remarkable that giant lipid vesicles, which lack the biological machinery, deal in a similar way with changes in the surface area to volume ratio (chapter 7). To us, this indicates that the physical and mechanical properties of the bilayer membrane are sufficient to orchestrate vesiculation and fusion. However, biological systems are usually off-equilibrium and therefore much more complex than the phospholipid vesicle. The increases the concentration of different salts and the partitioning of (amphiphilic) substances into the bilayer that occur during dehydration of desiccation tolerant organisms are expected to have impact on the physical and mechanical properties of the biomembrane. Although this thesis mainly considers equilibrium systems, the information on the equilibrium size and bending moduli of phospholipid vesicles in different salts, salt concentrations (chapters 2 -5) and in the presence of amphiphiles (chapter 6) will give some insight into the behavior of off-equilibrium biological systems.

The insights obtained on the size regulation and stability of lipid vesicles presented in this thesis might therefore help us to obtain a deeper understanding of imbibitional damage, but also of related biological systems, in which changes in surface area to cell volume ratio take place. Based on this, one can start to design strategies to overcome imbibitional damage.





# Samenvatting

Alle levende planten en dieren bestaan voor een groot deel uit water. Water is daarom essentieel voor al het leven op aarde. Toch kunnen sommige zaden, pollen, sporen en gist een toestand van bijna totale uitdroging overleven. Wanneer droge zaden water opnemen groeit er een plant uit, en wanneer je water toevoegt aan gedroogd gist kun je het gebruiken in de productie van bijvoorbeeld brood en bier. Behalve deze relatief simpele organen en organismen zijn er ook hele planten en dieren die uitdroogtolerant zijn. Ze gebruiken deze eigenschap om droge seizoenen door te komen. Zo overleeft de wederopstandingsplant *Craterostigma pumilum* die voorkomt op Mount Elgon in Kenia uitdroging (Fig. 7.7).

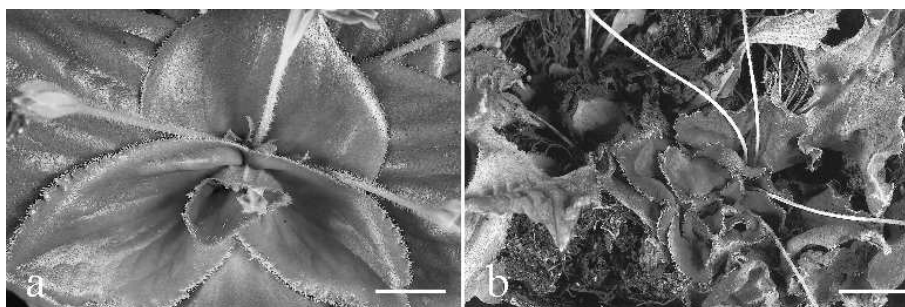


Figure 7.7: De wederopstandingsplant *Craterostigma pumilum* voor (a) en na (b) drogen. Het schaalstreepje op de foto is 1 cm lang.

De cellen waaruit uitdroogtolerante organismen zijn opgebouwd, kunnen drogen van 30 % tot 95 % droge stof zonder hun levensvatbaarheid te verliezen. Maar het verlies van zoveel water brengt enorme veranderingen met zich mee. Cellen worden omgeven door een celmembraan, en wanneer cellen drogen van 30 naar 95 % droge stof is nog maar de helft van het membraan oppervlak nodig om de cel te omspannen. De cellen kunnen dit teveel aan membraan oppervlak proberen kwijt te raken door vouwing en afsplitsing van een hoeveelheid vloeistof die omgeven die door membraanmateriaal (Fig. 7.8). Deze kleine blaasjes worden vesikels genoemd. Vlak onder de celmembraan van droge zaden wordt vaak een laag met vesikels gezien maar de celmembraan is ook sterk gevouwen (hoofdstuk 1 Fig. 1.2) Dit geeft aan dat cellen zowel vouwing als vesiculatie gebruiken om de veranderingen in oppervlakte/volume

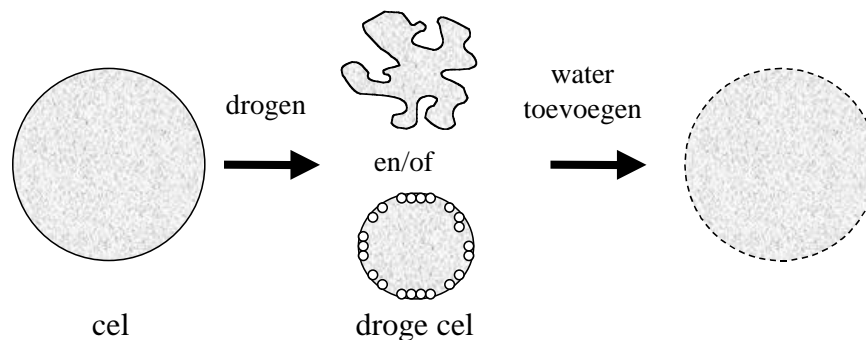


Figure 7.8: Een droge cel kan verandering in de membraan oppervlakte en cel volume verhouding opvangen door vormverandering en/of afsplitsing van kleine vesikels.

verhouding om te gaan.

Hoewel uitdroogtolerante organen en organismen uitdroging in principe kunnen overleven, gaat er wel eens wat fout tijdens het opnemen van water. Als koud in plaats van handwarm water wordt toegevoegd aan gist, zal het brood dat er mee gebakken wordt niet rijzen; de gist overleeft de opname van koud water niet. Ook sommige zaden zijn gevoelig voor opname van koud water, de zaailingen die er uit ontstaan zijn vaak abnormaal en vervormd. De permanente schade die droge uitdroogtolerante organismen oplopen tijdens wateropname wordt imbibitieschade genoemd.

Imbibitieschade is waarschijnlijk een gevolg van een gebrek aan membraanmateriaal. Als de cellen een deel van hun membraan materiaal kwijt raken door vesiculatie tijdens droging, moet dit materiaal weer opgenomen worden als de cel water opneemt (Fig. 7.8). Wanneer dit niet snel genoeg lukt is het membraan te klein om de cel te omspannen en zal het knappen (hoofdstuk 1 Fig. 1.3). Als dit gebeurt bij eencellige organismen zoals gisten, sterven ze. Bij meercellige organismen, zullen enkele cellen sterven en dat zal veelal leiden tot misvormingen.

Het is niet duidelijk waarom de kleine vesikels soms niet in de celmembraan kunnen worden opgenomen, of waarom de cel niet goed ontvouwd. De fysische en mechanische eigenschappen van celmembraan spelen waarschijnlijk een belangrijke rol bij vesiculatie, vouwing, fusie en ontvouwing. Maar omdat complexe biochemische reacties die in cellen plaatsvinden ook essentieel zijn wordt het probleem meestal uit deze hoek benaderd en worden de eigenschappen van het membraan onderbelicht. In dit proefschrift is daarom gekeken naar de stabiliteit en mechanische eigenschappen van membranen. Omdat membranen zoals die voorkomen in planten en dieren erg complex zijn is al het onderzoek gedaan aan een modelsysteem voor het biologische membraan. Celmem-

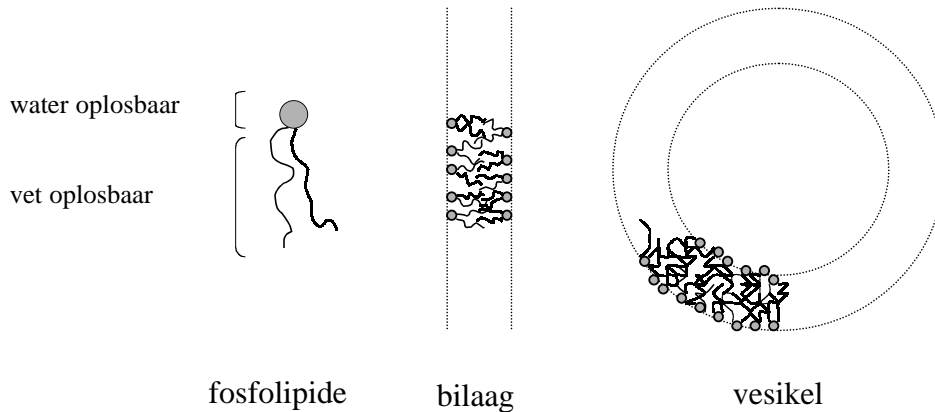


Figure 7.9: Fosfolipiden zijn moleculen met een wateroplosbare kop en twee vetoplosbare staarten. In water vormen deze moleculen bilagen die kunnen sluiten tot vesikels.

branen bestaan uit lipiden en eiwitten, het modelsysteem is eenvoudiger het bestaat alleen uit fosfolipiden. Deze fosfolipiden bestaan uit een (vaak negatief elektrisch geladen) kopgroep die makkelijk in water oplost en twee vetachtige staarten die contact met water willen vermijden (Fig. 7.9). Om aan de wensen van zowel de kopgroepen als de staarten te voldoen vormen fosfolipiden in water bilagen. In deze bilagen staan de kopgroepen in contact met water terwijl de vetoplosbare staarten elkaar opzoeken in de binnenkant van de bilaag (Fig. 7.9). Als de bilaag gesloten wordt tot een blaasje noemen we het een vesikel (Fig. 7.9). In dit proefschrift zijn vesikels gemaakt en gebruikt om meer te begrijpen van de stabiliteit en mechanische eigenschappen van celmembranen.

Vesikels kunnen op verschillende manieren gemaakt worden; zo kunnen hele kleine vesikels worden geproduceerd door een hoeveelheid lipiden in een waterige oplossing bloot te stellen aan ultrasoon geluid, en wat grotere door bilagen door een filter met een bepaalde poriegrootte te drukken, hele grote vesikels worden gevormd in een wisselend elektrisch veld. Een nadeel van al deze methodes is dat het moeilijk/niet mogelijk is om met een techniek altijd dezelfde vesikel grootte te produceren. In hoofdstuk 2 en hoofdstuk 3 van dit proefschrift wordt een methode om vesikels te maken beschreven die wel altijd dezelfde vesikel grootte (straal) geeft. Door de vesikeloplossing enkele keren te bevriezen in vloeibaar stikstof en te ontdooien wordt onafhankelijk van de begin grootte altijd dezelfde maat vesikels geproduceerd. Als de fosfolipiden waaruit de bilaag bestaat een elektrische lading dragen, kunnen vesikels zelfs vanzelf naar deze straal evolueren.

De straal van de vesikels die met de vries-dooi methode worden gevormd, wordt gereguleerd door entropie. Entropie is een maat voor het aantal realiseringmogelijkheden in een systeem; hoe meer realiseringmogelijkheden, hoe

hoger de entropie. Een systeem zal altijd streven naar een zo hoog mogelijke entropie, in ons geval zal het proberen zoveel mogelijk kleine vesikels te maken van de aanwezige fosfolipiden. Omdat de bilagen een zekere stijfheid hebben zit er echter een limiet aan de kleinste maat die de vesikels kunnen bereiken. De evenwichts grootte van de vesikels wordt daarom bepaald door de stijfheid van het membraan. Een maat voor die stijfheid is de buigingsmodulus van de bilaag  $k_c$ . De vesikel straal is dus gekoppeld aan een mechanische eigenschap van de bilaag.

Er zijn veel parameters die invloed hebben op  $k_c$ . Factoren die ervoor zorgen dat de fosfolipiden in de bilaag dichter pakken maken dat het membraan dikker en dus stijver wordt. Maar er zijn nog andere factoren die  $k_c$  beïnvloeden; omdat het membraan een negatieve elektrische lading draagt wordt  $k_c$  niet alleen bepaald door de dikte van de bilaag. De negatieve lading op de kopgroep van het fosfolipide trekt positieve ladingen uit de oplossing aan. Daardoor ontstaat er een laag waar zich veel positief geladen deeltjes bevinden rond het membraan; de elektrische dubbellaag. Deze elektrische dubbellaag moet meebuigen met de fosfolipide bilaag en heeft daarom ook invloed op  $k_c$ .

De belangrijkste positief geladen deeltjes die in een cel voorkomen zijn metaal ionen. De positief geladen metaaldeeltjes noemen we cationen. In hoofdstuk 4 wordt de invloed van verschillende cationen op de buigingsmodulus  $k_c$  en de evenwichtsstraal  $R$  van vesikels besproken. Door te binden aan de negatief geladen kopgroepen van de fosfolipiden verlagen de cationen de hoeveelheid lading op de vesikels, daardoor wordt de elektrische dubbellaag dunner. Maar omdat er minder lading op de fosfolipiden zit stoten ze elkaar minder af en kunnen ze dus dichter pakken in de bilaag, het membraan wordt hierdoor dikker. Het dikker worden van de bilaag en het dunner worden van de elektrische dubbellaag hebben een tegengesteld effect op  $k_c$ . Het gedrag van  $k_c$  onder invloed van verschillende cationen is daarom moeilijk te begrijpen.

De tot nu toe besproken modelsystemen waren gemaakt van slechts een soort fosfolipide terwijl biologische membranen uit veel verschillende soorten lipiden bestaan. Daarom is ook gekeken naar bilagen van mengsels van fosfolipiden en fosfolipiden en zeepachtige moleculen. In bilagen van mengsels van lipiden kunnen de monolagen waaruit het membraan is opgebouwd een verschillende samenstelling hebben. Omdat de bilaag in een vesikel gekromd is, is er wat meer ruimte voor de kopgroepen in de buitenste monolaag, en wat meer ruimte voor de staarten in de binnenste monolaag. Het is daarom denkbaar dat moleculen met een grote kopgroep zich voornamelijk ophopen in het buitenste monolaag van de bilaag in een vesikel. Dit verschil in monolaag samenstelling zou er voor kunnen zorgen dat een vesikel een spontane kromming aanneemt. De spontane kromming zal sterk afhangen van de samenstelling van het mengsel. Hoewel dit scenario heel plausibel lijkt laten we in hoofdstuk 5 zien dat een spontane kromming bijna nooit voorkomt. De straal van vesikels die bestaan uit mengsels van fosfolipiden of fosfolipiden en zepen, wordt bepaald door de buigingsmodulus  $k_c$ .

Uit het voorgaande komt naar voren dat  $k_c$  bepalend is voor de grootte van

## Samenvatting

vesikels die gestabiliseerd worden door entropie. De buigingsmodulus  $k_c$  van het membraan zal waarschijnlijk ook bepalen op welke lengte schaal het membraan kan vouwen en hoe groot de afgesplitste vesikels zullen worden als er water onttrokken wordt aan cellen. Er is echter nog een parameter die van groot belang kan zijn in fusie en vesiculatie; de zadenvlak modulus  $\bar{k}$ . Hoofdstuk 6 gaat over deze parameter. De waarde van de zadenvlak modulus bepaalt hoe gemakkelijk verbindingen tussen twee membranen kunnen ontstaan. Connectors kunnen makkelijk gevormd worden als  $\bar{k} \approx 0$  en dit zou daarom een voorwaarde kunnen zijn voor fusie tussen twee membranen. Om deze hypothese te testen is gekeken naar de invloed van fusie stimulators en remmers op  $\bar{k}$ . Het blijkt dat moleculen die fusie van vesikels stimuleren er inderdaad voor zorgen dat de zadenvlak modulus heel klein wordt, terwijl  $\bar{k}$  juist groter (negatiever) wordt als er fusie remmers worden toegevoegd. Maar ook hier is de buigingsmodulus  $k_c$  van belang; als vesikels kleiner zijn dan hun evenwichtsstraal zullen ze de neiging hebben te fuseren, terwijl vesikels die veel groter zijn dan hun stabiele straal deze neiging niet zullen hebben.

In het laatste hoofdstuk wordt de reactie van hele grote vesikels (zogenoemde reuze vesikels) op het onttrekken van water bekeken. De reuzen reageren hetzelfde als de eerder besproken cellen; ze splitsen kleine vesikels af naar de binnenkant. Experimenten waarin de bilaag stijver wordt gemaakt, laten zien dat de straal van de afgesplitste vesikels afhangt van buigingsmodulus  $k_c$ . Omdat de meeste vesikels los komen van de bilaag, kunnen ze niet meer in de bilaag opgenomen worden tijdens wateropname. De reus zal na wateropname niet zijn oorspronkelijke volume kunnen bereiken, en door een tekort aan membraan oppervlak zal het grote vesikel exploderen.

Hoewel (alle) processen in cellen geregeld worden door een complexe biochemische machinerie, vertonen lipide vesikels en celmembranen opmerkelijke overeenkomsten. Zowel reuze vesikels als celmembranen lijken veranderingen in de oppervlakte/volume verhouding tijdens dehydratatie op te vangen door vesikels aftesplitsen. Wanneer de gekropen reuze vesikels vervolgens weer water opnemen knappen ze omdat de afgesplitste vesikels niet snel genoeg kunnen worden opgenomen in de lipide bilaag. Dit tekort aan membraanmateriaal is waarschijnlijk ook de reden dat imbibitie schade optreedt in celmembranen van uitdroogtolerante organismen. De inzichten die verkregen zijn in de grootte regulatie en stabiliteit van lipide vesikels kunnen ons helpen een beter inzicht te krijgen in problemen die ontstaan wanneer biologische systemen te maken krijgen met veranderende verhoudingen tussen membraanoppervlak en celinhoud. Gebaseerd op deze inzichten kunnen nu strategieën worden ontworpen om imbibitieschade te voorkomen.



# Dankwoord

Het is alweer bijna 5 jaar geleden dan ik werd aangenomen op het project ‘Imbibitional Stress and Seed Performance’. Ondanks de opstartproblemen en tegenslagen aan het begin van het project, heb ik een leuke tijd gehad. Dit is natuurlijk mede te danken aan de enthousiaste begeleiding van mijn copromotoren Frans en Folkert.

Met Frans als begeleider kun je niet alleen experimenteel werk doen; er moet ook gerekend worden. Ik ingewijd in een deel van de geheimen van de `sfbox`. Uiteindelijk hebben de SCF berekeningen aan bilagen erg geholpen om de experimentele resultaten te begrijpen. Maar Frans heeft mij niet alleen geholpen met de berekeningen, zijn (soms wat al te wilde) ideeën voor experimenten zijn ook een grote bron van inspiratie geweest.

Hoewel het onderzoek vaak erg fysisch en weinig biologisch was, heb ik veel gehad aan de discussies met Folkert. Het enthousiasme waarmee hij kan vertellen over uitdroogtolerantie (en waarover niet) en de mogelijke betekenis van onze bevindingen heeft mij vaak geholpen. De reis die ik met de Folkerts groep naar Zuid-Afrika maakte heeft ons op het pad van membraanvesiculatie en -fusie gezet; de discussie die ik daar had met James Wesley-Smith over de EM data was daarin van doorslaggevend belang.

Zonder het enorme werk dat Jan en Jos hebben verzet met het programmeren van de `sfbox` zou een groot deel van dit proefschrift er nooit zijn geweest. Gelukkig vonden zij nog een fout in de implementatie van de elektrostatica (de beruchte factor -1). Dit maakte voorgoed een einde aan de voorkeurskromming in bilagen die ik in de computerresultaten zag voor bilagen die bestaan uit een soort lipide.

Adriaan heeft mij tijdens de eerste twee jaren van mijn promotieonderzoek veel enthousiasme voor elektronenmicroscopie bijgebracht. Ondanks het feit dat het merendeel van het proefschrift niet over EM gaat, zijn de keuzes die ik heb gemaakt gebaseerd op het werk dat we samen met Olivier hebben uitgevoerd bij Beiersdorf in Hamburg.

Ik heb veel plezier gehad in het begeleiden van afstudeerstudenten die ook geïnteresseerd waren in membranen. Maykel werkte aan het ontstaan van gaten in membranen, hem heb ik maar even begeleid. Hij werd door Frans gevangen voor het rekenwerk. Het werk van Bart aan de stabiliteit van vesikels heeft bijgedragen aan het ontstaan van hoofdstuk 2 en hoofdstuk 5. Door het werk van Bas hebben we meer geleerd over de interacties tussen geladen vesikels en

PEG.

Mijn vader heeft altijd grote belangstelling gehad voor mijn onderzoek. De discussies die ik met hem had over elasticiteit, bellen, en ballonnen hebben erg geholpen bij het schrijven van het laatste hoofdstuk. Bovendien zie ik nu in dat de verschillen tussen moleculaire wetenschappen en werktuigbouw kleiner zijn dan je op het eerste gezicht zou denken.

Mireille



# Levensloop

Mireille Claessens werd op 10 januari 1975 geboren in Asten. Het VWO diploma behaalde ze in 1993 aan het toenmalige College Asten-Someren. In dat zelfde jaar begon ze aan de studie Moleculaire Wetenschappen aan de Landbouw Universiteit te Wageningen. Het doctoraal examen werd in september 1998 behaald met als hoofdvakken Plantenfysiologie en Moleculaire Fysica. Na een aantal maanden onderzoek te hebben uitgevoerd bij de vakgroep Moleculaire Fysica, is zij in december 1998 begonnen als onderzoeker in opleiding bij de vakgroep Fysische Chemie en Kolloïdkunde. Het door STW gefinancierde samenwerkingsproject met de vakgroep Plantenfysiologie heeft tot dit proefschrift geleid.